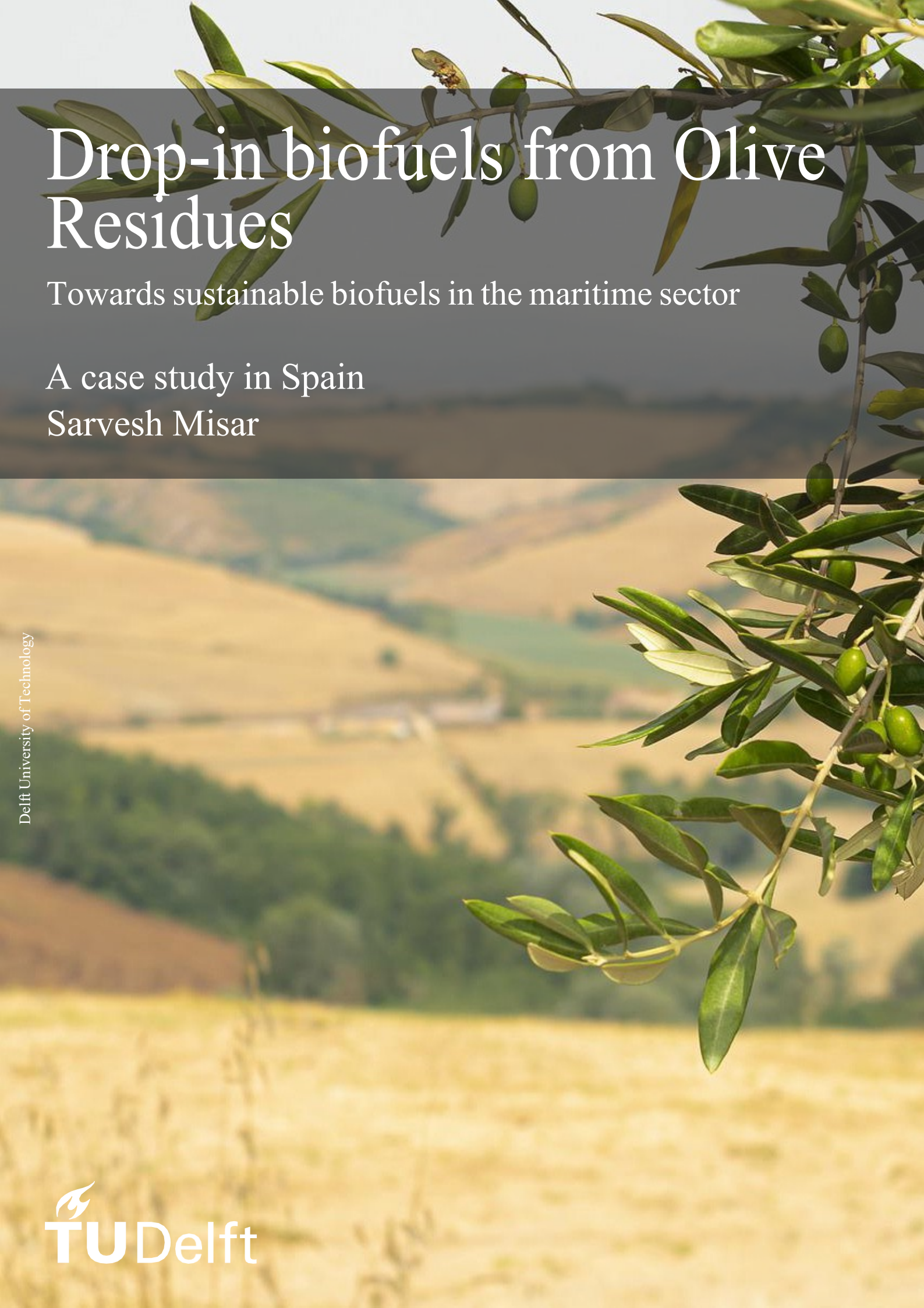

Drop-in biofuels from Olive Residues

Towards sustainable biofuels in the maritime sector

A case study in Spain

Sarvesh Misar

Delft University of Technology

TU Delft

Drop-in biofuels from Olive Residues

Towards sustainable biofuels in the maritime sector

by

Sarvesh Misar

In partial fulfillment of the requirements for the degree of

Master of Science

in Sustainable Energy Technology at the Delft University of Technology,
to be defended publicly on Monday 29 August 2022 at 10:00 AM

Student number:	5215552	
Project duration:	December 2021 – August 2022	
Supervisor:	Prof. dr. Wiebren de Jong,	TU Delft
Daily supervisor:	Dr. Luis Cutz,	TU Delft
Thesis committee:	Prof. dr. Wiebren de Jong,	TU Delft (chair)
	Dr. Burak Eral,	TU Delft
	Prof. dr. ir. Kamel Hooman,	TU Delft

Cover: Olive Plantation in Spain by Andrea Toxiri from Pixabay

TU Delft

Preface

The shipping industry, especially the merchant sector is one of the most important players to enable the world trade. This sector accounts for around 3% of the global CO_2 emissions (IEA Bioenergy, 2017). Currently, the fuel type used in shipping has a high environmental impact and this needs to be taken care of to facilitate a transition to a sustainable energy future. The main challenge with biofuels in the shipping sector is that it is not yet completely ready to incorporate them as a part of their fuel supply because this will lead to a lot of changes in the current infrastructure and also an another challenge that needs to be addressed is that the volume of biofuel required is quite large (IEA Bioenergy, 2017).

In this sense, agricultural residual flows are attractive due to the high quantities in which these are produced, and the short cycle time associated with their CO_2 cycle compared to woody biomass. To address these challenges, a case study was developed using agricultural biomass to produce "drop-in" biofuels compatible with the existing shipping infrastructure. This thesis aims to establish the most optimal way in which olive residues can be transformed via hydrothermal liquefaction (HTL) into a drop-in bio-oil and simultaneously create social and environmental benefits for the region where production will take place. Experiments will be carried out using olive residues selected from different regions in Spain. The goal will be to analyze the influence of major reactor variables such as temperature, residence time, catalyst upon the mass yield of bio-oil and other products obtained.

This research project forms a part of the graduation project for the Master's program curriculum of Sustainable Energy Technology (SET) and also the Clean Shipping Project which was a grant awarded by NWO to the Large-scale energy storage group (LSE) and other collaborators. This work was conducted at the Large-Scale Energy Storage group at Process & Energy division of the 3mE faculty under the supervision of Prof. Dr. Wiebren de Jong and daily supervision of Dr. Luis Cutz to whom I am grateful for constant direct and indirect support and guidance during the entire duration of the project.

Sarvesh Misar
Delft, August 2022

Abstract

The olive industries, especially in the Mediterranean countries are known to produce a significant amount of residues such as crude olive pomace (COP) and olive tree pruning waste (OTPW) which can lead to various environmental and societal issues if not treated or further utilized (Garcìa Martìn et al., 2020). Considering the fact that not all olive oil industries make use of these olive residues (COP and OTPW) for further processing, they seem to be a promising candidate to produce renewable energy due to their bioenergy potential and physicochemical properties. These residues could be valorized to produce liquid biofuels which would help creating a circular economy. This work aims to expand the current state-of-art of hydrothermal liquefaction (HTL) of olive residues such as COP and OTPW, which will contribute towards the profitability and sustainability of olive oil industries. This work will also serve as a basis to future studies such as development of a continuous process to support the high commercial demand of the liquid biofuel and carrying out a techno-economic assessment of the HTL process of COP and OTPW at this scale.

Due to the characteristics of the olive residues, especially their high moisture content and organic compounds (Ribeiro et al., 2020), the use of HTL has been proposed for the development of the thermochemical conversion process for bio-oil production. So far, only non-catalytic HTL processes have been investigated in batch scale laboratory setups. Thus, the main novelty of this work is that the effects of catalyst dosage (0 - 10 wt.%) along with reaction temperature (250 - 340 °C) and residence time (5 - 60 min) using a central composite design of experiments has been evaluated. The bio-oil and biochar fractions resulting from HTL were characterized by elemental analysis, bomb calorimetry, X-ray fluorescence (XRF), X-ray Diffraction (XRD), X-ray photoelectron spectroscopy (XPS), Scanning electron microscopy coupled with Energy dispersive spectroscopy (SEM-EDS), and Fourier-transform infrared spectroscopy (FTIR). From the experiments, it was proven that the production of liquid biofuels from olive residue biomass from Spain is possible under both, catalytic and non-catalytic routes. By implementing the central composite design experimental campaign, a set of mathematical models were developed for predicting the mass yields of the bio-oil, biochar, aqueous, and gas phase produced under combinations of the evaluated process variables.

The main finding of this work is that by using a catalyst, significantly higher mass yields of bio-oil were achieved with lower operational conditions when compared with the existing literature. The maximum bio-oil yield was found out to be 56.0% wt. on treating COP at 330°C for 60 minutes and 10 wt. % catalyst whereas for OTPW, the maximum bio-oil yield was found out to be 56.3% wt. at 330 °C for 30 minutes and 7.5 wt. % catalyst. The bio-oil produced under these conditions showed an average energy content of 23.21 MJ/kg. The highest high heating value (HHV) of 32.09 MJ/kg was obtained under non-catalytic HTL route at 340 °C and 15 minutes. The determination of the energy content (HHV) of the bio-oil fractions showed that there is a potential trade-off between the respective mass yield and HHV when using the catalyst.

Table of Contents

List of Figures

List of Acronyms

	Acronyms
cat	Catalyst or catalytic
COP	Crude olive pomace
d.b.	Dry basis
DCM	Dichloromethane
DoE	Design of experiments
FTIR	Fourier-transform infrared spectroscopy
HHV	High heating value
HTL	Hydrothermal liquefaction
MAWL	Maximum allowable water loading
OML	Olive mill leaves
OTPW	Olive tree pruning waste
OS	Olive stones
SEM-EDS	Scanning electron microscopy/Energy dispersive spectroscopy
XRF	X-ray fluorescence
XRD	X-ray powder diffraction
XPS	X-ray photoelectron spectroscopy

List of Symbols

P	: Pressure [Pa/bar]	T	: Temperature [°C]
t	: Residence time [min]	N	: Nitrogen
C	: Carbon	O	: Oxygen
H	: Hydrogen	Ni	: Nickel
S	: Sulfur	Cl	: Chlorine
Al	: Aluminum	K	: Potassium
Y	: Response Variable	X_i	: Process Variable

1. Introduction

Over time, fossil fuels have proven to be the most effective source for the petroleum and petrochemical industries, resulting in the creation of millions of petroleum-based products. However, due to factors such as depletion of easily accessible deposits, ever-increasing demand from emerging economies, and an increase in environmental concerns such as global warming, it is widely acknowledged that the use of renewable energy sources is essential for the long-term sustainability of our society. In comparison to current levels, global energy demand is expected to increase from 580 million terajoules by nearly 47% by 2050 mainly because of the growth in population and economy especially in countries like India and China (British Petroleum, 2021; Gordon & Weber, 2021). The increase in energy demand requires the replacement of a large portion of the fuel used in transport with renewable energy sources, as well as technological advancements in this area. Biomass can be considered as the most important source of renewable energy, contributing to the energy used to drive transportation, heat buildings and industry, and produce electricity. Among the various renewable energy sources such as solar and wind, biomass plays a significant role as it accounts for about one-tenth of the total primary energy supply today (IEA, 2022). Due to its ubiquity, biomass is found almost everywhere in the world and is distributed much more evenly than conventional fossil fuels and could therefore substitute fossil crude oil in the manufacturing of liquid fuels and petrochemicals (Castello et al., 2018).

Biomass encompasses a diverse range of materials such as forestry and agricultural residues, energy crops, as well as organic wastes such as sewage sludge, food, and sorted organic waste (Castello et al., 2018). Large amounts of waste and by-products are also produced by agriculture and agri-food processing industries (Evcil et al., 2021). In this context, the olive industry produces significant amounts of residues throughout its supply chain (Garcìa Martìn et al., 2020). The Mediterranean and European countries account for nearly all of the world's olive-growing region and contributes to production of almost 20 million tons of olives in a year (Garcìa Martìn et al., 2020). Although the majority of this production is used for the manufacturing of olive oil, a large amount of by-products are still generated during the entire process of harvesting and production of olive oil. For example, olive oil residues such as crude olive pomace (COP), generated during the extraction of olive oil, contain a high moisture content (46-54 wt.%), high energy content (16.5 MJ/kg), low pH, and large amount of polyphenols, which makes cost-effective treatment of utmost importance to the industries (Alburquerque et al., 2004). On the other hand, olive tree pruning waste (OTPW) are generated during the pruning operation carried out by farmers and they usually contain thin branches and leaves. The energy content of these olive-pruning debris is typically between 16.7 to 19.8 MJ/kg which on utilizing to produce energy can maximize its reuse and lead to production of value-added products to supply for clean renewable energy (Garcìa Martìn et al., 2020). These residues can be used to support low-cost liquid biofuel production especially in the Mediterranean countries (Che et al., 2012; Evcil et al., 2021; Garcìa Martìn et al., 2020).

Hydrothermal Liquefaction (HTL) is one of the many thermochemical conversion processes that forms a promising technology to process biomass feedstocks with high moisture content and heterogenous nature (Anastasakis et al., 2018; De Filippis et al., 2016). This process utilizes water at sub-critical conditions to convert biomass into a liquid fuel (bio-oil) and other valuable products. The bio-oil obtained from this process has similar properties to that of petroleum crude and can be used as a drop-in fuel (gasoline, diesel, kerosene, heavy fuel oil) on further upgradation (Anastasakis et al., 2018; Elliott et al., 2015). When compared with

other thermochemical technologies, HTL has the advantage of processing feedstocks with high moisture content and a heterogeneous nature such as COP, thus avoiding the necessary step of feedstock drying (Anastasakis et al., 2018). So far, only a few studies are available for the use of HTL for processing olive residues, such as COP and OTPW. To the best of our knowledge, most of the studies for HTL of COP and OTPW have only been conducted with a traditional approach of changing one variable (residence time or temperature) at a time. This has hindered the optimization of operational variables such as temperature, residence time, and catalyst loading, being evaluated at the same time. Here we use a Design of Experiment (DoE) approach to evaluate the interaction between the different process variables and develop robust mathematical models to determine the optimum conditions for maximizing the bio-oil production. Additionally, use of catalyst will be thoroughly examined to enhance the yield of the liquid biofuel produced and lower the energy requirements of the process to obtain similar yields as that of non-catalytic routes.

1.1. Project Scope

The experimental work of this study was divided into three campaigns: screening of COP, central composite design (CCD) campaign of COP and CCD campaign of OTPW. These experiments are aimed to understand the influence of temperature, residence time, and catalyst loading on the mass yields of the products obtained through HTL of COP and OTPW. The screening campaign focuses on a preliminary set of experiments at two levels, different temperatures, and a fixed residence time, based on literature to validate the production process and form a base to the full experimental CCD campaigns. The objective of the CCD campaigns of COP and OTPW was to understand the influence and interaction between the different reactor variables on the bio-oil yield. In addition, a thorough characterization for examining the physicochemical properties of bio-oil and biochar was carried out using various techniques such as: elemental analysis, bomb calorimetry, scanning electron microscopy and energy dispersive x-ray spectroscopy (SEM-EDS), x-ray diffraction (XRD), x-ray fluoresce (XRF) analysis, fourier-transform infrared spectroscopy (FTIR), and x-ray photoelectron spectroscopy (XPS).

1.2. Research Question

This thesis aims to provide a deeper understanding regarding the potential of COP and OTPW as a source for the production of biofuels and to expand the current state-of-art of HTL of olive residues, which will contribute towards increasing the sustainability and circularity of olive oil industries. This work will also serve as a basis to future studies such as development of a continuous process to support the high commercial demand of the liquid biofuel and carrying out a techno-economic assessment of the HTL process of COP and OTPW at this scale.

This works analyzes experimentally the effect of major process variables such as temperature, residence time, and catalyst loading on the bio-oil yield. To develop this case study, the following research questions were considered:

Is it experimentally possible to produce bio-oil and other value-added products from crude olive pomace and olive tree pruning biomass via hydrothermal liquefaction process, and if so, what are the effects of temperature, residence time, and catalyst loading on the yield of the products obtained?

To answer the main research question, following sub-research questions were considered to form a base for the development of the case study. These questions are:

- *What are the optimum operation conditions for maximizing the yield of bio-oil?*
- *What are the physicochemical properties of the bio-oil and biochar obtained from HTL of COP and OTPW?*
- *What could be the potential applications of the various value-added products from HTL of COP and OTPW, considering their properties?*

1.3. Report Outline

Chapter 2 focusses on the literature regarding the feedstocks chosen for developing this case study, COP and OPTW, various available thermochemical conversion technologies for the production of liquid biofuels, and justification of the choice of HTL for this study. This is followed by a brief overview on the products obtained by HTL process with their potential characteristics and applications, influence of major reactor variables on the yield of products obtained, a discussion on batch and continuous processes, and various challenges of the HTL process. Chapter 3 provides a detailed methodology for developing the experimental work with an introduction to the design of experiments (DoE) theory to carry out the experimental campaign, from sample preparation to the characterization of the products obtained. The results after analyzing the experimental data are presented and discussed in Chapter 4. The conclusions of this study will be presented in Chapter 5. Finally, Chapter 6 will provide various recommendations and future perspectives to be considered for the further development of this study and technology.

2. Literature Review

This chapter provides the basic review of the context and underlying principles that are relevant for the report and building of the case study. First, a general description of olive residues as a feedstock is discussed. This is followed by the olive oil extraction techniques, various thermochemical conversion processes, and the chosen process for the development of this case study with a brief overview on the prior work carried out on HTL of olive residues. Then a discussion on various products of HTL process and major reactor variables are provided with a distinction between batch and continuous process.

2.1. Feedstock: Olive residues

The Mediterranean region contributes to about 95% of the world's olive production with Spain being one of the greatest producers of olive oil (Alburquerque et al., 2004). It is estimated that Spain accounts for providing 25% of the world's olive tree cultivation. The southern region of Spain has a high density of agricultural wastes, producing more than 70% of olive waste generated throughout the country. In the Andalusia region in Spain, Jaén is the region that produces the most olives (Cardoza et al., 2021). Cardoza et al. 2021 investigated potential locations in the province of Jaen for a bio-refinery based on biomass from olives. These locations correspond to low environmental fragility zones with high olive biomass availability (>300.000 t/year) within a 30 km radius, which would ensure a reliable supply and reasonable prices. The following map in Figure 1, presents the areas A, B, and C in the southern region of Spain, which have been chosen as the most suitable locations. There is at least 1 large olive oil extracting industry with >65,000-ton olive pomace generated annually and several small and medium-sized mills with capacity of around 5000 tons of olive mill leaves (OML) (Cardoza et al., 2021).

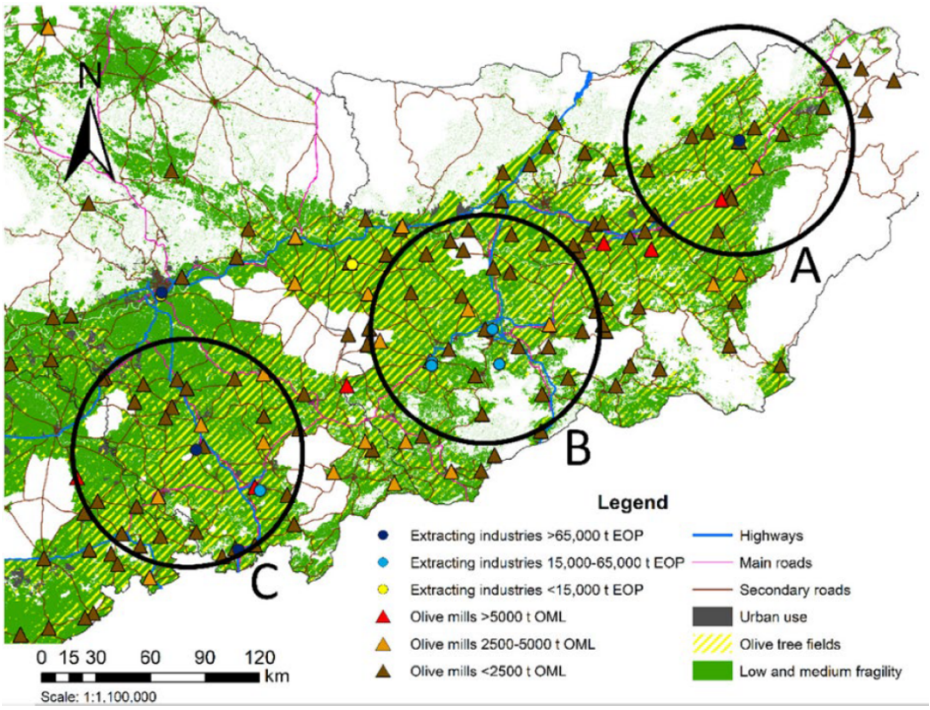

Figure 1: A map for the choice of most suitable locations for the development of biorefinery as per the availability of olive mills (Cardoza et al., 2021)

The olive wastes can be categorized as OTPW, olive pomace also known as COP (alperujo), exhausted olive pomace (EOP/orujillo), olive mill leaves (OML), and olive stones (OS) which can be noticed in the waste distribution schematic of olive residues in Figure 2. OTPW is generated by carrying out a pruning operation after the fruit has been harvested and they usually consist of varying percentages of thin and thick branches (usually <5cm diameter), woods, and leaves. On the other hand, olive oil industries generate a major by-product called as olive pomace along with olive mill leaves (OML) and olive stones (OS) which can be considered as lignocellulosic biomass feedstock (Alburquerque et al., 2004). Olive residues which are generated from the olive oil extraction stage can be categorized into two types of pomaces: the first referred to as "Crude Olive Pomace" (COP) and the second referred to as "Extracted Olive Pomace" (EOP) which is a result of further processing of COP in pomace extraction plants (Garcìa Martìn et al., 2020). The produced olive pomaces are delivered to the pomace extraction facilities where the remaining oil is extracted from them. In these facilities, residual oil is extracted using a solid-liquid extraction method, with the most popular solvent technically being hexane (a mixture of alkanes). COP oil and an EOP byproduct are the results of this process. To make olive pomace oil, crude pomace oils are sent to oil refineries. The extracted olive pomace, on the other hand, is a by-product of the extraction process and is a very intriguing solid biofuel with an HHV of 13.8 to 15.8 MJ/kg.

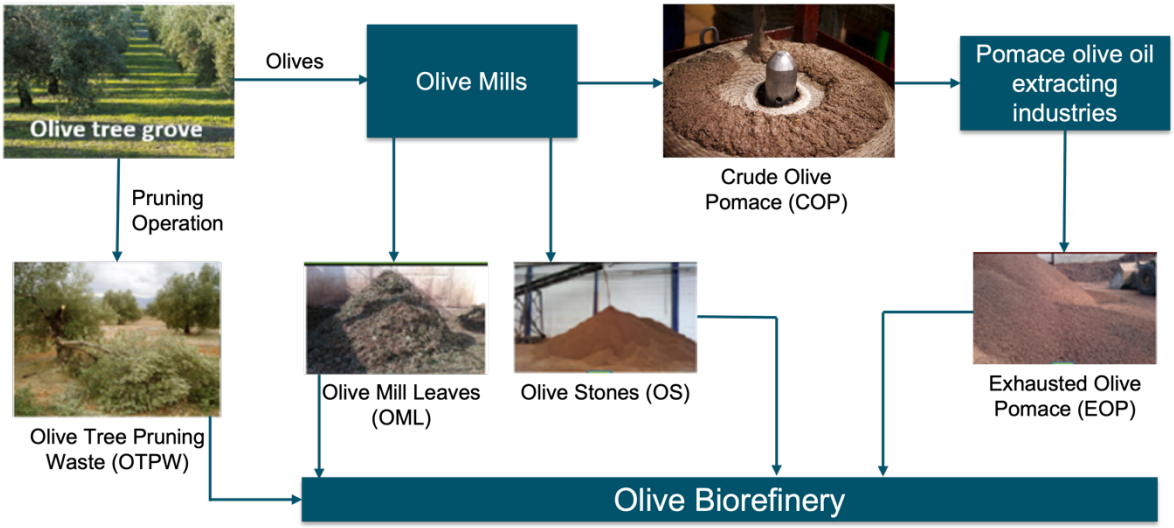

Figure 2: A schematic of olive residue waste distribution (own elaboration)

Some of the properties of these by-products which make them a suitable candidate for thermochemical conversion can be seen in Table 1:

Table 1: Properties of olive residues (Alburquerque et al., 2004; Garcìa Martìn et al., 2020)

By-product	Moisture content (%)	Energy Content (MJ/kg)
Olive Mill Leaves	37	9.88
Olive Stones	13	16
Olive Tree Pruning Waste	10	16.7 – 19.8
Crude Olive Pomace	46-54	16.5

Furthermore, only the Andalusia region of Spain accounts for about 60% of total olive tree crops whereas the region of Jaén is identified as the main producer of OML and OS due to the presence of high number of mills (Cardoza et al., 2021). COP is a blend made of water, oil, cellulose, lignin, proteins, soluble carbohydrates, small portions of active phenol compounds and other derivatives (Alburquerque et al., 2004). COP is a dark compound with an intense smell, highly organically charged, a moderately acid pH and a high conductivity (Hernández et al., 2014). On the other hand, the main components of olive tree pruning, which is a lignocellulose material, are cellulose, hemicellulose, and lignin (Garcìa Martìn et al., 2020). The debris from olive pruning is typically either ground and plowed into the ground or left on the land to be burned, which not only pollutes the air (CO_2 emissions), but also mineralizes the soil and raises the danger of pest infestation and fire mishaps (Garcìa Martìn et al., 2020). If the pruning-debris from olive trees were used to generate energy, it would not only maximize the use and exploitation of byproducts with value-added, but it would also address environmental pollution and provide clean, renewable energy. This makes OTPW an appealing material to produce pellets and other solid or liquid biofuels.

2.2. Olive oil extraction process

The system to extract olive oil, known as the three-phase centrifugation has been around since the beginning of 1970s and by means of this system, the oil, vegetation water and solid phase of the olive can be separated in a continuous process (Alburquerque et al., 2004). The main inconvenience of the three-phase system is that it generates large quantities of olive mill wastewater (OMW), which is a very polluting liquid due to the presence of phenol, organic and fatty acid contents during a short period of the year (November–February). OMW is made of the olive vegetation water plus the water added in the different steps of oil production (Alburquerque et al., 2004). To lessen the environmental impact of OMW, different methods have been experimented to make the best use of this stream; these include storage in evaporation ponds and its direct application to agricultural soils as fertilizers. However, these methods have gradually become less viable for OMW disposal, and so a new two-phase centrifugation system for oil extraction was developed during the early 90s to greatly reduce wastewater generation, energy required, and the contaminant load (Alburquerque et al., 2004). Although this system tackles the issues of the three-phase system, it still produces a solid and very humid by-product called COP (in Spanish ‘‘alperujo’’). This new centrifugation system is estimated to be used roughly by 90% of olive-mills (Alburquerque et al., 2004). The COP is further extracted with a second centrifugation system to get a residual oil which is further dried and extracted with hexane to obtain an additional oil yield (in Spanish ‘‘orujillo’’). A detailed comparison between the three-phase and two-phase centrifugation systems can be seen in Figure 3.

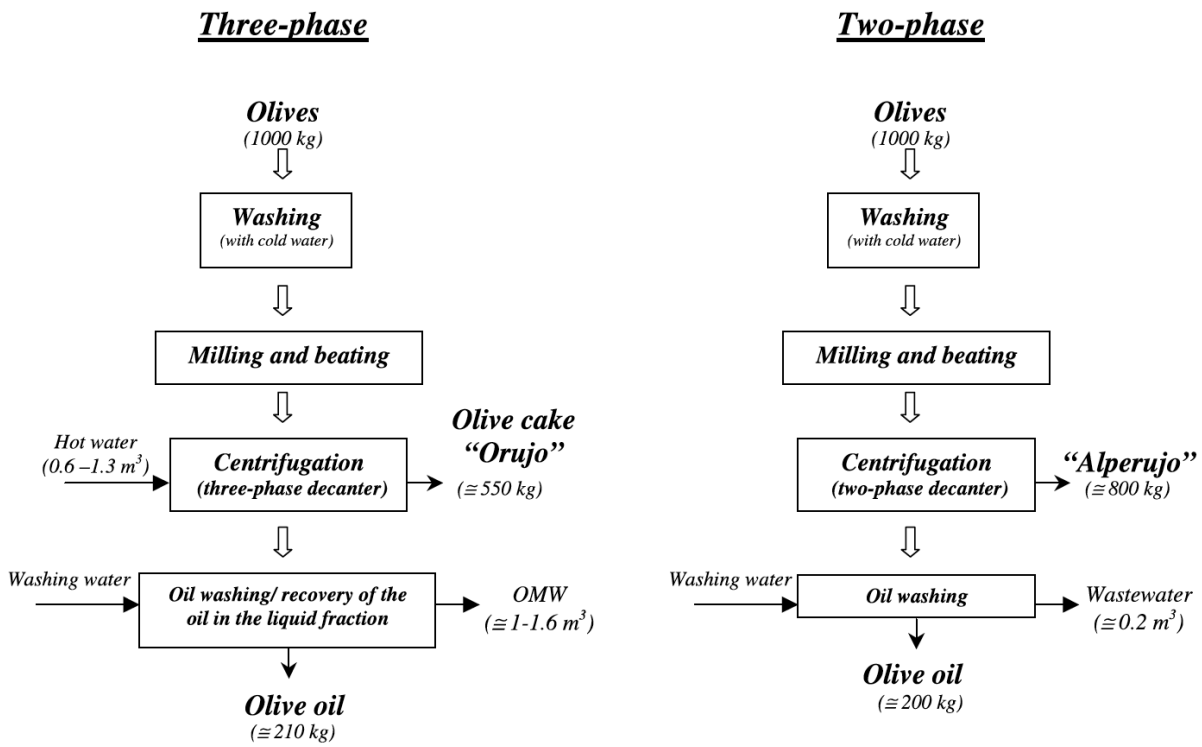

Figure 3: Comparison of the three phase and two-phase centrifugation systems for olive oil extraction (Alburquerque et al., 2004)

2.3. Thermochemical Conversion Technologies: Biomass to Biofuel

Biomass conversion to solid, liquid, and gaseous forms is frequently viewed as a cost-effective and environmentally friendly energy source for a variety of industries, including heat, power, and transportation (Osman et al., 2021). Thermochemical methods use biomass in the presence of a heat source and a controllable oxygen atmosphere to convert biomass to different energy forms (Verma et al., 2012). Some of the common thermochemical conversion techniques which are used to process agricultural residues or industrial/domestic waste to produce liquid fuels are fast pyrolysis, hydrothermal liquefaction, and gasification. A brief explanation of each technology can be found below:

1. **Fast/Flash Pyrolysis:** Due to its potential to transform virtually all types of biomasses into marketable biofuels and valuable chemical feedstocks for the industrial sector, the pyrolysis process is currently receiving a lot of attention from the forestry, municipalities, and agricultural sectors (Verma et al., 2012). However, in theory, pyrolysis can be defined as any high temperature heating of organic matter in the absence of oxygen (Osman et al., 2021). The term "fast/flash pyrolysis" refers to pyrolysis processes with a very brief residence time of intense thermal treatment, which typically lasts from 0.5 to 3 s at 400 to 600°C (Osman et al., 2021; Verma et al., 2012). Fast/flash pyrolysis processes increase the significance of heat and mass transfer, phase transition, and chemical reaction kinetics due to the organic matter's (e.g., biomass) shorter heat exposure time. According to literature, fast pyrolysis requires several pre-requisites, including dry biomass (10% moisture), small particle size (3 mm), short

residence times, and moderate-to-high temperatures (Verma et al., 2012). To obtain a liquid biofuel with improved physicochemical properties, catalytic pyrolysis could also be employed in which catalysts such as natural zeolite, Cu/Al2O3, Co/Mo, Z are used to increase the selectivity towards the desired products (Osman et al., 2021). This process can be utilized for upgrading the bio-oil quality by removing oxygen from the biomass and increasing the production of aromatics and olefins (Osman et al., 2021).

2. **Hydrothermal Liquefaction:** HTL process is a thermochemical process where a lignocellulosic feedstock, whether wet or dry, is broken down into renewable liquid fuel (Verma et al., 2012). The process of HTL and fast pyrolysis can usually be differentiated by the need of a pre-treatment step for the feedstock and their operating parameters (Verma et al., 2012). At temperatures and pressures between 250 and 350°C and 4 and 22 MPa, HTL primarily produces liquid, solid, aqueous and gaseous phase (Osman et al., 2021; Verma et al., 2012). Some of the advantages associated with this process which makes it suitable for agricultural residues are its ability to process feedstocks with high moisture content and produce liquid fuels in line with the petroleum products (Verma et al., 2012).

3. **Gasification:** Gasification is the thermochemical process of turning biomass into useful gases, also known as synthesis gases, at temperatures above 800°C in the presence of a gasifying agent like air, oxygen, steam, CO_2, or a combination of them (Osman et al., 2021). The products of gasification consist of the synthesis gas (which is usually a mixture of CO and H_2), CO_2, NO_x, SO_x, and ash depending on the type of biomass used. The syngas can find applications in fuel cells, as a synthetic fuel, and as a feedstock for various chemical processes (Verma et al., 2012). Supercritical water gasification is a type of gasification that is typically done in the presence of a significant amount of water to produce H_2 and CH_4. The process yield is extremely high and is primarily influenced by variables like temperature, catalyst, and the biomass/water ratio (Osman et al., 2021).

2.4. Choice of Hydrothermal Liquefaction Process

HTL is a method of producing clean biofuel from biomass in the presence of a solvent (mostly water) at a moderate to high temperature (250–370 °C) and pressure (4–22 MPa) (Toor et al., 2011). At these conditions, water changes its properties and acts as a catalyst for decomposing the biomacromolecules into smaller compounds under the conditions reached in hydrothermal reactors (Toor et al., 2011). COP can be processed using thermochemical conversion techniques such as pyrolysis, combustion, gasification, and hydrothermal processing (Evcil et al., 2021). One of the most significant advantages of HTL is that it eliminates the need for the energy-intensive biomass-drying step that is required in all thermochemical processes, allowing the use of biomass with high moisture content, such as COP, microalgae, olive residue, and grape mark (De Filippis et al., 2016). The crude bio-oil is an energy dense product that can potentially be used as a substitute for petroleum crudes (Toor et al., 2011). Liquefaction also produces gases, solids, and water-soluble compounds that can be converted to obtain valuable chemical species or can be used as energy vectors (Toor et al., 2011).

This process is a technique that uses subcritical water (below the critical point of water at 374 ◦C and 22 MPa) for converting biomasses into valuable products (Evcil et al., 2021). In this process, cracking and formation of partially de-oxygenated products occur (Hernández et al.,

2014). This method has several advantages associated with it, including suitability for any type of biomass (wet or dry waste biomasses, sludge, food wastes, lignocelluloses, and algal biomasses), high deoxygenation capacity, and the ability to operate at relatively low temperatures (Akhtar & Amin, 2011; Evcil et al., 2021). Product yields, as well as composition of bio-oils from the HTL process, are related by feedstock type and operating conditions so several feedstocks (municipal sewage sludge, food waste, and agricultural residues) have been used for the HTL of biomass to produce bio-oils under various operating conditions (Evcil et al., 2021) A schematic of the HTL process for COP can be seen in Figure 4.

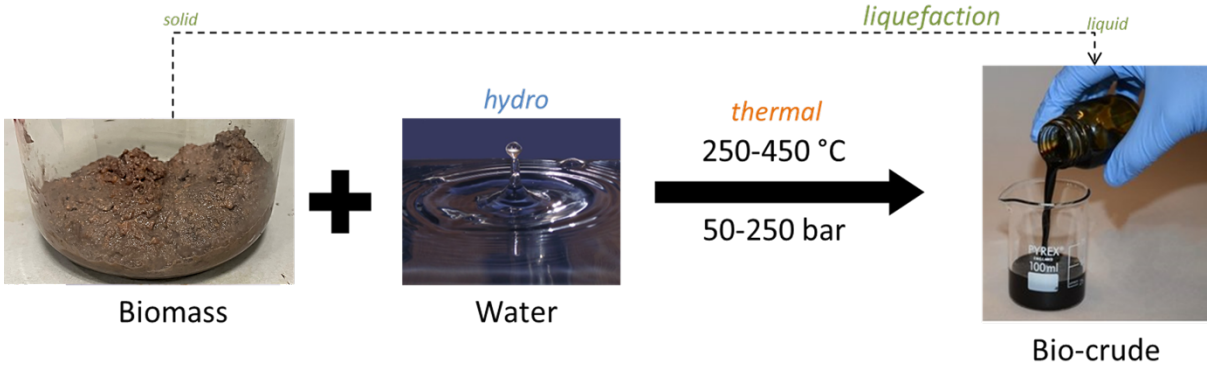

Figure 4: A schematic of the HTL process of biomass (COP)(Own elaboration based on the works of Toor et al. 2011)

This thermochemical processing technology has been extensively investigated by Cao et al. 2017 and Castello et al. 2018 for bio-oil production from agricultural and forestry wastes and was found to be superior over other techniques due to the several advantages it offers such as its suitability to process wet biomass feedstocks, high deoxygenation capacity, and ability to operate at low operating temperatures. Moreover, HTL can be labelled as an environmentally friendlier technique when compared with other alternatives due to the fact that other chemicals are unnecessary for the processing of biomass; there's no formation of harmful/hazardous byproducts such as the products of combustion; and is also less corrosive to equipment than other alternatives (Akhtar & Amin, 2011). The bio-oil obtained from the HTL process can be purified and be used as fuels for burners, stationary diesel engines, turbines, and boilers. Bio-oils can also be further upgraded into transportation fuels (diesel and gasoline) and products, including aromatics, polymers, asphalt, and lubricants (Cao et al., 2017).

Some of the drawbacks associated with this technology is that it hasn't been demonstrated at a large scale as it has only been developed at a laboratory scale. Several attempts have been made for building commercial scale/continuous systems for HTL of lignocellulosic biomass (Elliott et al., 2015). The major disadvantages associated with the HTL process are that of the feeding system, solvent recovery and reuse, and separation of solid residues. The feeding system must be able to handle the feedstock and operate at a higher pressure than the reactor and provide a large throughput in order to feed the feedstock into pressurized reactors. The cost associated with the solvent might be high even when wastewater treatment is not considered. Hence, the reuse/recycle of the solvent is receiving significant attention considering the benefits of using the recovered solvent in the process (Elliott et al., 2015). The separation of solids is more difficult in HTL process than in pyrolysis or gasification due to the small density difference between the solvent and solids. This will result in the plugging of filters, screens, or hydrocyclones at continuous operation (Haverly et al., 2020).

2.5. Prior work on HTL/treatment of olive residues

Previous studies have proved that olive residues as feedstocks can be converted to liquid biofuel and other value-added products through HTL process. Prior work included the conversion of these residues through both catalytic and non-catalytic pathways. The main studies that proved to form a foundation to this study were:

• Evcil et al. 2021, conducted an experimental study on HTL of olive residues obtained from Turkey, at various operating condition ranges with temperature varying from 250°C to 330°C and a residence time of 5, 15, 30, and 60 minutes. The effect of different catalysts such as $AlCl_3$ and $SnCl_2$ was also explored to study its effects on product yields and composition. A maximum bio-oil yield of 30.75% wt. was reported at 300°C and 15 min residence time with absence of catalyst. The energy content of such bio-oil was reported to be 29.78 MJ/kg. A maximum HHV of 32.19 MJ/kg was obtained for bio-oil processed at 300°C and 5 min residence time.

• Madsen & Glasius 2019 investigated the effects of temperature, residence time, and catalyst loading on the HTL process. More importantly, a response surface methodology was utilized to study the maxima/minima for the yields of the products while the coefficients were used to determine the flux of the different product fractions. This work adapts a similar approach by developing a response surface for determining an optimal response to produce bio-oil.

• De Filippis et al. 2016 also conducted a similar study as that of Evcil et al. 2021 to investigate the feasibility of HTL process under sub-critical conditions to obtain bio-oil from olive residues. The experimental tests in this work were carried out at 320°C and 13MPa, using a biomass to water weight ratio of 1:5. The bio-oil yield obtained at this condition was reported to be 32.40% wt. This study also focused on the influence of two major catalysts CaO and Zeolite on bio-oil yield and properties. De Filippis et al. 2016, reported a maximum bio-oil yield of 38.05% wt. when CaO was used as a catalyst for the HTL process.

2.6. Products of HTL

During HTL, the physical properties of water are changed, and it acts as a catalyst for biomass decomposition reaction according to the conditions reached in the reactor. During HTL, the lignocellulosic materials undergo several depolymerization reactions to form water-soluble intermediates which is the aqueous phase and repolymerization reactions to form water-soluble intermediates such as the bio-oil and biochar (Gollakota et al., 2018). The products of this process and their description can be seen below, and a detailed product map can be noticed in Figure 5:

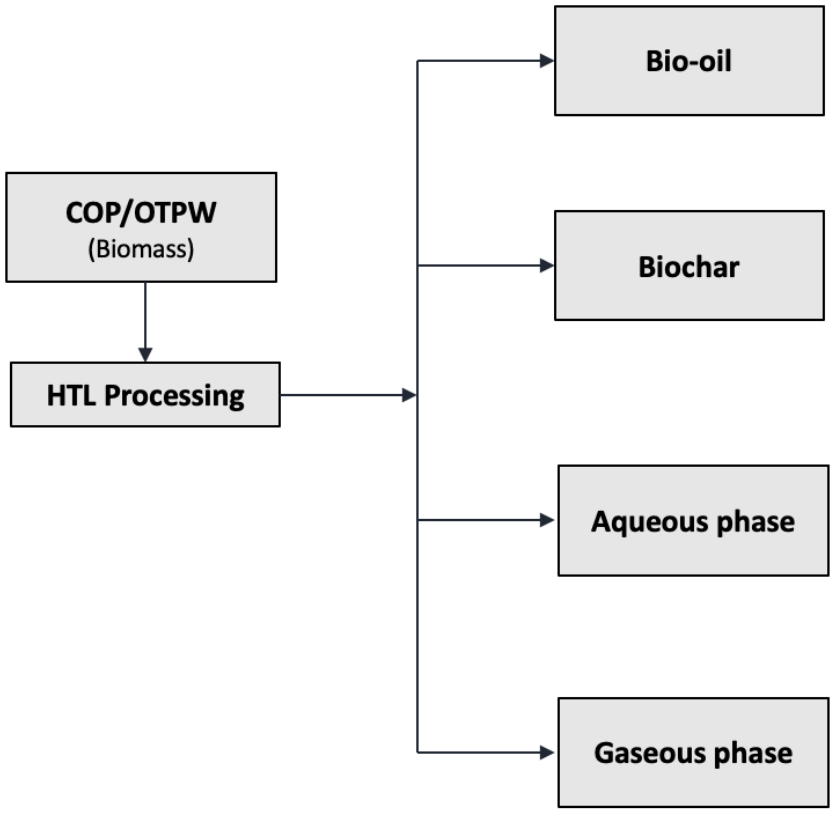

Figure 5: Summary of products/phases obtained from HTL of COP

2.6.1. Bio-oil

According to the findings of Mathanker et al. 2021, Evcil et al. 2021, and Cao et al. 2017, HTL derived bio-oil is a dark, viscous, and energy-dense liquid. Its high heating value (HHV) ranges from 25 to 40 MJ/kg, and its energy content is between 70 and 95 percent that of petroleum fuel oil (Cao et al., 2017; Mathanker et al., 2021). The complex chemical compounds that make up bio-oil include alcohols, polyols, unsaturated and saturated hydrocarbons, ketones, aldehydes, phenolics, phenyl derivatives, fatty acids, esters, fatty acid alky esters, and a small amount of nitrogenous compounds like amine and amides (Mathanker et al., 2021). The factors that usually affect the bio-oil yield and its physicochemical properties are the feedstock, chosen process conditions, and route of conversion (Cao et al., 2017; Mathanker et al., 2021).

2.6.2. Aqueous Phase

HTL produces a significant amount of aqueous phase as a byproduct which is often formed as a secondary product in the batch HTL process (Mathanker et al., 2021). Depending on the temperature, pressure, residence time, catalyst, and type of biomass, the typical yields of the aqueous phase products can range from 20% to 50% of the raw biomass (Cao et al., 2017). In a study conducted by Mathanker et al. 2021, it was reported that the aqueous phase consists of low molecular weight compounds such as organic acids and polyols, with the presence of small amounts of sugar, a medium percentage of phenolic compounds, and ketones. With a significant amount of aqueous phase being generated from the process, it could be utilized in a

better way by recirculating it (Mathanker et al., 2021). This could lead to an increase in the efficiency of process contributing towards better yield and quality of bio-oil and biochar. This is mainly due to the presence of organics in the aqueous phase which facilitates the decomposition of biomass and also by limiting the consumption of fresh water (Mathanker et al., 2021). From the investigations carried out by Zhu et al. 2018 and Biller et al. 2011 for different kinds of biomass, it was evident that the overall increase in the yield of bio-oil was quite significant.

2.6.3. Gaseous Phase

According to the investigations performed by Cao et al. 2017 and Mathanker et al. 2021 for HTL processing, the fraction of gas obtained was found to be around 5-15 wt% of the total product distribution. The fraction of CO_2 and CO in the gaseous phase produced by HTL were dominating, followed by H_2 and CH_4 (Cao et al., 2017; Mathanker et al., 2021). The main source of CO_2 and CO was found to be the decomposition of oxygen-containing groups in lignocellulosic biomass through decarboxylation and decarbonation reactions that take place in hydrothermal processing (Cao et al., 2017). There is still a need for more research to quantify the detailed composition of the gaseous phase, effective ways of sampling, and exploring its applicability to obtain a better understanding of the reaction mechanisms in the HTL process.

2.6.4. Biochar

The second product of interest in HTL is the solid residue referred as biochar. Typically, the yield of biochar has been found to be in the range of 5-60 wt% depending mainly on the type of the feedstock, its composition, catalyst loading, and process conditions (Mathanker et al., 2021). Biochar produced by liquefying agricultural and forestry wastes has a high weight percentage of carbon, hydrogen, and nitrogen but little oxygen present which in turn contributes towards a higher heating value (HHV) (Mathanker et al., 2021).

Due to its promising qualities, biochar can find various applications in the enhancement of soil, as an adsorbent, and for use in the energy applications due to the high calorific value (Mathanker et al., 2021). Evcil et al. 2021 reported an increase in the fixed carbon content of the biochar obtained after the HTL process which further justified its use in coal combustion, direct combustion, or the preparation of energy storage materials like bio-batteries, fuel cells, and bio-capacitors. Additionally, literature also suggests the use of biochar as an adsorbent to filter pollutants like heavy metals and organic substances out of wastewater, water, and flue gas (Cao et al., 2017; Mathanker et al., 2021). These properties and applications indicate the biochar to be a better solid fuel than biomass.

2.7. Major Reactor Variables

For the bio-oil yield and quality of the product, processing conditions such as final liquefaction temperature, residence times, rate of biomass heating, biomass particle size, type of solvent media, and hydrogen donor solvents are critical. This section will go over the potential impact of these variables on the yield and composition of liquid products.

2.7.1. Effect of Temperature

The yield and quality of bio-oil are directly influenced by reaction temperature, which is a critical component of the HTL of biomass (Cabrera & Labatut, 2021). The chemical bonds between each component of the biomass gradually breaks down into small molecules with an increase in reaction temperature when the temperature is below the subcritical point of water. The likelihood of the polycondensation of small molecules rises as the concentration of free radicals does as well, increasing the yield of bio-oil (Cao et al., 2017). Temperature has a synergetic effect on liquid yield due to extended biomass fragmentation as temperature rises. Extensive biomass depolymerization occurs when the temperature is sufficiently higher than the activation energies for bond cessation. Because the properties of water change rapidly in near supercritical conditions, determining the optimum temperature can be difficult (Cao et al., 2017).

Initially, a rise in temperature enhances the production of bio-oil. Further increases in temperature inhibit biomass liquefaction after the oil yield reaches a maximum as can be seen in Figure 6. In terms of both operational cost and liquid oil yield, very high temperatures are not usually suitable for the production of liquid oils. There are two reasons for this behavior in general. At high temperatures, secondary decompositions and Boudouard gas reactions become active, resulting in the formation of gases (Cao et al., 2017). Second, due to their high concentrations, the recombination of free radical reactions results in the formation of char. At high temperatures, these two mechanisms become dominant, reducing the amount of oil produced from biomass. At >250 °C, lignin and cellulose fragment rapidly under hydrothermal conditions. As a result, Cao et al. 2017 and Cabrera & Labatut 2021 concluded that it's reasonable to assume that a temperature range of 250-350°C would be effective for decomposition of biomass in subcritical conditions with the most optimal point being around 300-330°C.

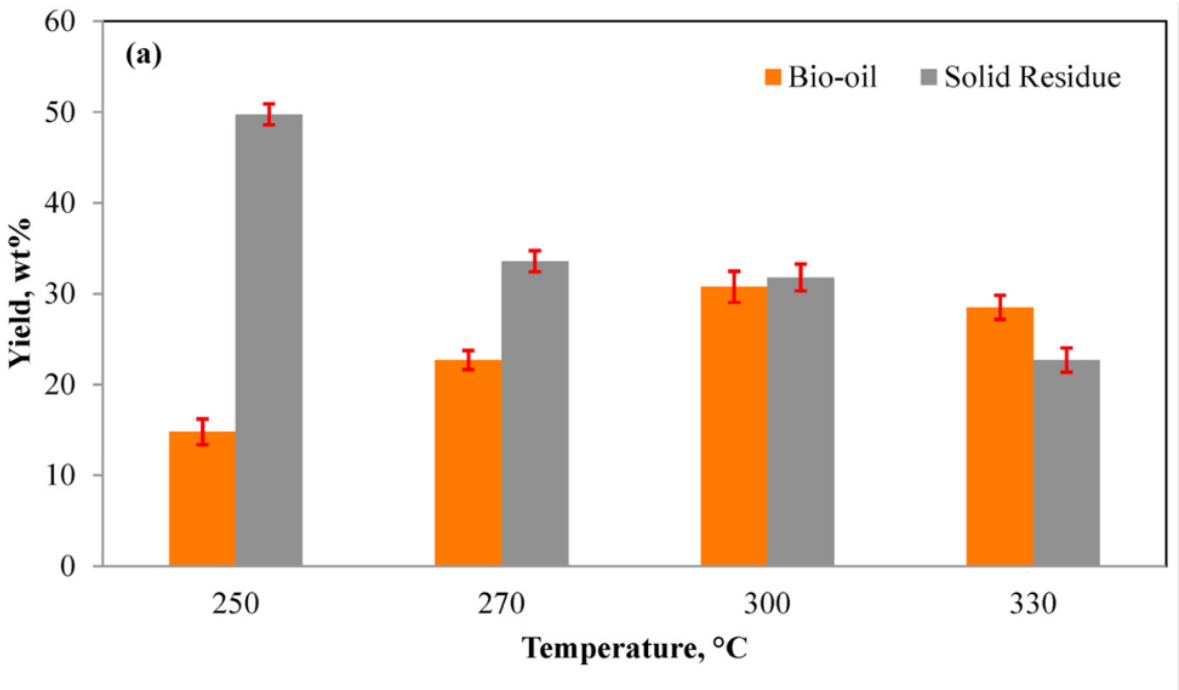

Figure 6: Effect of temperature on the yield of bio-oil (Evcil et al., 2021)

2.7.2. Effect of Residence Time

The HTL reaction time at the target temperature, excluding the time for heating and cooling, is referred to as the residence time. The amount of time directly affects the bio-oil yield level: too little time results in incomplete polymerization and degradation reactions, while too much time results in intermediate polymerization reactions and lowers bio-oil yield (Cao et al., 2017).

According to Ragauskas & Jindal n.d. and Cao et al. 2017, short residence times are preferred during HTL and shorter residence times at high temperatures result in higher oil yields, whereas longer residence times at high temperatures result in higher yields of solid residue. For HTL of olive residues, Evcil et al. 2021 found the most optimum bio-oil yield at a residence time of 15 mins as can be witnessed from Figure 7. However, factors such as the presence of catalyst could influence obtaining the optimal residence time hence further research in this domain is necessary.

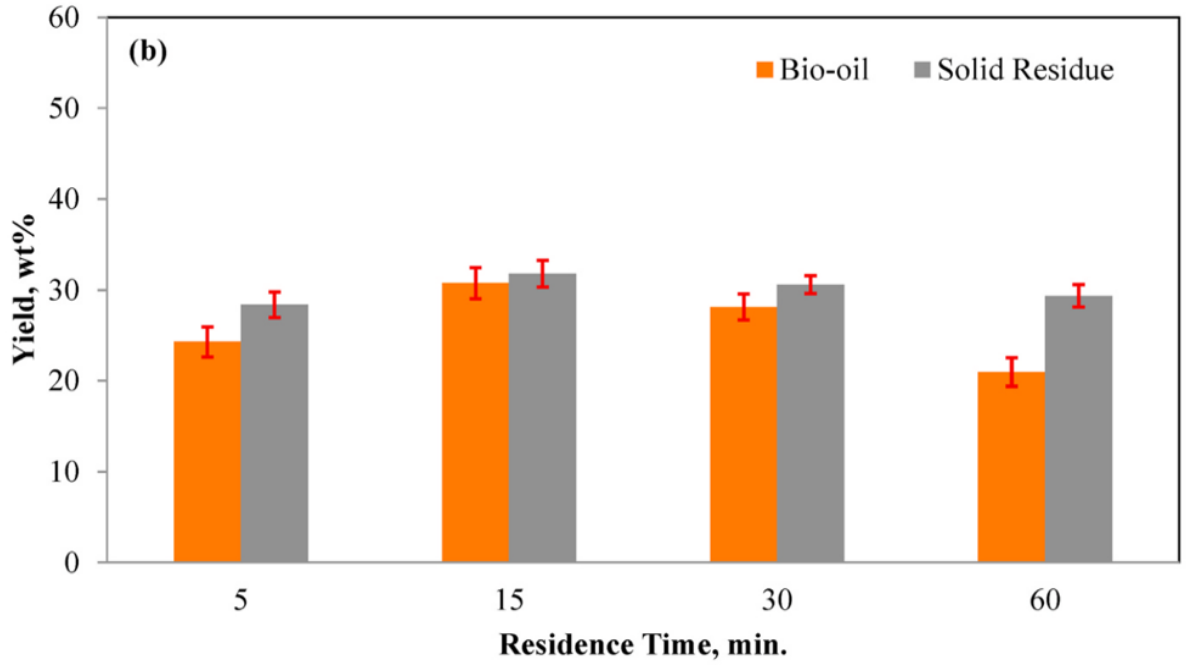

Figure 7: Effect of residence time on the yield of bio-oil (Evcil et al., 2021)

2.7.3. Effect of Catalyst

It has been found in the literature that the addition of catalysts can improve the yield and quality of bio-oil in the HTL process for biomass by inhibiting side reactions, lowering reaction pressure and temperature, speeding up the reaction, and decreasing the formation of solid residues (Cao et al., 2017; Evcil et al., 2021). Both homogeneous and heterogeneous catalysts can be employed for this purpose.

The use of homogeneous catalysts such as acid and alkali catalysts in the HTL of biomass has shown effective results according to the study conducted by Tekin & Karagöz 2013. Acid catalysts that are frequently used include sulfuric acid, phosphoric acid, formic acid, acetic acid, perchloric acid, and hydrochloric acid. According to the study of Cao et al. 2017, these acids played more of a solvent role during the HTL process, but the bio-oil obtained had a higher oxygen content. Although strong acids have an impressive catalytic effect, their potent corrosive effect prevented their widespread industrial use. Alkali catalysts, on the other hand, have been applied more frequently in various studies. Among other alkali catalysts, there are Na_2CO_3, K_2CO_3, NaOH, and KOH. Based on biomass conversion and liquid yield analysis by Cao et al. 2017 and Tekin & Karagöz 2013 it was found that the order of reactivity for alkalis was K_2CO_3 > KOH > Na_2CO_3 > NaOH.

Heterogeneous catalysts can be subdivided into two main categories namely supported catalysts and metal catalysts. Pd, Pt, Ru, Co, Mo, Ni, and Pt, as well as extensively researched catalysts like SiO_2, Al_2O_3, and zeolites, have all been studied in recent years. Studies by Biller et al. 2011 and Cao et al. 2017 have found that heterogeneous catalysts may also be crucial in lowering the liquid product's nitrogen and sulfur content and enhancing the quality of the bio-oil. Biller et al. 2011 investigated the use of Ni/Al_2O_3 catalyst and observed that the de-oxygenation was highest for biomass containing lipids. The elemental analysis of the bio-oil obtained from HTL of soya oil with the use of Ni/Al_2O_3 catalyst showed an increase in the

carbon content and the high heating value (HHV) (Biller et al., 2011). This suggests that the use of heterogeneous catalysts especially Ni/Al_2O_3 could favor de-oxygenation of biomass.

The yield and composition of bio-oil can change when different catalysts are used. The feedstocks, however, determine the catalyst to use. The decision is important because it may have a favorable or unfavorable impact on the necessary decomposition/depolymerization reactions. Therefore, additional research is required to choose appropriate catalysts to produce the desired compounds selectively, thereby promoting the industrialization of HTL (Cao et al., 2017).

2.8. Batch and Continuous Process

2.8.1. Batch/Laboratory Scale Process

Due to their relatively straightforward operation, batch/laboratory scale activities in the field of HTL are frequently discussed in the literature (Mathanker et al., 2021; Toor et al., 2011). The batch approach entails adding a mixture of biomass and water to an autoclave, possibly along with a catalyst. A typical batch reactor assembly includes a mechanical stirrer, inlet and outlet tubes, gas pressurization and depressurization valves, a heating and cooling system, a temperature detector, a pressure gauge, and a controller. The heating system can be a sand bath heater, coil heater, or external electric furnace. In addition, a gas cylinder is attached to the reactor to supply an initial pressure (inert gas) to prevent a phase change from occurring while the process is running. The reactor is pressurized with either an inert gas or a process gas after it has been loaded with feedstock and solvent. After reaching the desired temperature in the autoclave and the chosen reaction time, the system is cooled down, the products are collected, and an analysis is performed on them.

A wide range of operating conditions and process variations can be tested, and virtually any kind of material can be screened in an autoclave (Castello et al., 2018). However Toor et al. 2011, Castello et al. 2018, and Mathanker et al. 2021 highlight several drawbacks associated with the batch processing of HTL as follows:

1. As the system must transition from ambient conditions to the desired temperature and pressure, and back again, during batch operations, process conditions are not constant. It is challenging to distinguish the effects of temperature and time because of this transience.
2. Another common issue with conventional batch reactors is the long time needed to reach the final process temperature and the long time needed for its cooling, which significantly lengthens the total amount of time that products spend in the relatively high subcritical temperature regime. The issue with the prolonged heating time is that it causes adverse side effects that reduce the overall oil yield.
3. Another issue with the batch reactor is the ineffective mixing of the biomass-water slurry, which causes dead zones to form at the bottom corners. The accumulation of biomass in these dead zones causes incomplete conversion and the formation of char.

2.8.2. Continuous Process

To address the challenges associated with the batch process as highlighted in the previous subsection, a review on the development of a continuous HTL process will be discussed. In a study conducted by Castello et al. 2018, various reports of continuous HTL for the production of biofuel from biomass are reviewed. Batch type reactors are typically only used industrially to produce high added-value products, which are frequently produced in small quantities. The production of fuel, which frequently accounts for production volumes in the range of thousands of barrels per day, is most definitely not the case. Additionally, HTL needs to be thoroughly optimized to lower the process's energy consumption, which can only be done in a continuous configuration (Castello et al., 2018). Even though HTL is still a relatively new technology, there are already some businesses involved in its commercialization and some of which have even constructed demonstration units.

A company in Australia, Licella Pty Ltd., has created a patented catalytic hydrothermal process (Cat-HTR) having the primary target of this process is non-edible biomass, particularly agricultural and industrial wastes and residues like pulp, paper, and plastics (Licella Pty Ltd., 2022). The central component of this technology is a catalytic reactor for HTL that makes use of a cheap catalyst. Since 2009, the company has developed a process, moving from a small pilot plant with an annual capacity of 100 t of slurry to the current development, which will result in a commercial plant with an annual capacity of 125,000 t. The end results of the process will be used to make chemicals like resins, adhesives, and aromatics as well as biofuels.

2.9. Challenges of HTL

The most typical reaction medium in HTL is water. Water serves as a catalyst and a solvent during hydrothermal processes. Water has a lower viscosity and a higher solubility of organic compounds as it approaches the critical point. The yield and quality of bio-crude are directly increased by this behavior (Beims et al., 2020). However, the use of only water as a solvent has the disadvantage that some of the produced organic compounds may migrate to the aqueous phase or solid residues, lowering the yield of bio-crude and results in higher material corrosion. To overcome this, Beims et al. 2020 investigated the use of organic solvents such as methanol, ethanol, acetone, and glycerol. It was found out that pure alcohol such as ethanol as a solvent usually promotes higher bio-oil yield at milder conditions, also contributing to higher HHV of the bio-oil. Also, the use of pure alcohol as a solvent result in a single phase of liquid fraction from HTL and the bio-oil can be separated easily by rotary evaporation. But this is often associated with a higher operational cost. When using water as a reaction medium, material corrosion is a major concern. Subcritical water has polar properties and a relatively high density, which creates an environment that is even more harshly acidic and oxidizing. One drawback of using water is that it is susceptible to corrosion. To guarantee reactor longevity in HTL systems, research on new reactor materials and ongoing monitoring are required (Beims et al., 2020).

Although the aqueous phase is not the primary target of HTL, it is still produced in large quantities during the reaction and must be treated before being released into the environment. Reusing the aqueous phase in a new HTL operation is one alternative. Recycling alone could cut down on water use and eliminate the need for wastewater treatment (Beims et al., 2020). Cabrera & Labatut 2021 explores and suggests the benefits associated with re-using the aqueous phase as a reaction medium in HTL. The yields of biocrude are increased by the

recirculation of the aqueous phase because it gives unreacted dissolved organics like acetic acids, alcohols, and amino compounds more time to form esters and amides. Additionally, the concentration of organic solutes in the aqueous phase rises after repeated uses (i.e., recycling), which may reduce the solubility of the organic acids present and lead to the formation of oil (Beims et al., 2020; Cabrera & Labatut, 2021). From a techno-economic standpoint, reusing the aqueous phase can increase biocrude yields while also lowering treatment costs for the aqueous product and avoiding the use of freshwater. Reusing the aqueous phase for feedstocks with high moisture content, however, might not be advised because it could result in increased dilution and lower biocrude yields and hence further research in this direction could prove quite useful (Cabrera & Labatut, 2021).

3. Methodology

In the following sections, a description on the design of experiments is provided with material preparation. This is followed by the experimental procedure of HTL to liquefy COP & OTPW into a bio-oil, including separation, purification, and characterization of the products obtained.

3.1. Design of Experiments

Design of experiments (DoE) is a branch of applied statistics concerned with the planning, execution, analysis, and interpretation of controlled tests to determine the factors that influence the value of a parameter or group of parameters (Bower, 2022). It allows for the manipulation of multiple input factors to determine their impact on a desired output (response). DoE can identify important interactions that might be missed when experimenting with one factor at a time by manipulating multiple inputs at the same time. This eventually allows us to learn about these interactions at a great extent from as few experiments as possible while achieving better and reliable results. There are numerous experimental designs available and each one serves a specific function. Some typical designs are the two-level factorial design, central composite design, optimal design, and mixture designs (Bower, 2022). In this report, a special focus to the central composite design of experiments is given.

To reduce the number of experiments while still being able to achieve an accurate response, a Response Surface Methodology (RSM) is typically adopted for the design of experiments. RSM is a quick technique for process development, improvement, and optimization based on the data obtained from experiments carried out at a number of input variables at various levels (Zhu et al., 2018). It enables the determination of the importance of each parameter as well as the importance of parameter interactions. It has the advantage of optimizing nonlinear systems, allowing for a more accurate computation of the main and interaction effects through regression fitting, when compared to other experimental design methods (Zhu et al., 2018).

Central Composite Design (CCD) is the most used design in the response surface model. It is basically a fractional factorial design wherein the center points are augmented with a group of star points as can be seen in Figure 8 used to build a second order (quadratic) model for the response variable that allows the estimation of the curvature (in this case being the bio-oil yield) without needing to use a complete/full factorial design (Bhattacharya, 2021; Minitab, 2022). And, after all the data points for the response are obtained, a linear regression approach is used to obtain the desired results by determining the first and second order terms (Bhattacharya, 2021). The quadratic polynomial equation that will be developed to study the effects of linear, square, and interacting terms of the independent process variables can be seen in Equation 1.

$$Y = a_o + \sum_{i=1}^{3} a_i X_i + \sum_{i=1}^{3} a_{ii} X_i^2 + \sum_{i=1}^{3} \sum_{i<j} a_{ij} X_i X_j \quad (1)$$

Where Y is the response function, X_1, X_2 and X_3 are the reaction temperature, residence time, and catalyst loading respectively: a_o represents the intercept of the model, a_i, a_{ii} and a_{ij} represent the coefficients of linear, quadratic, and interaction terms respectively.

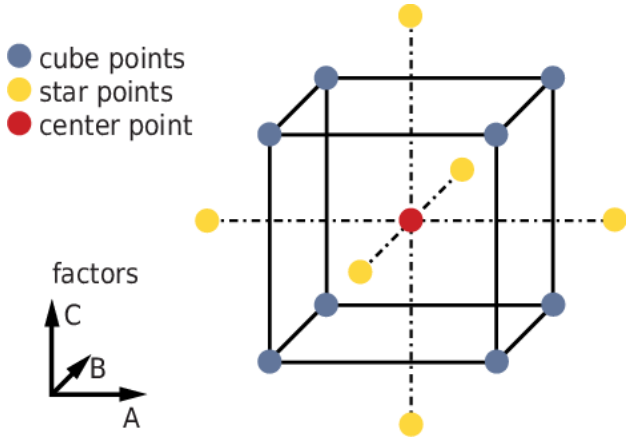

Figure 8: A schematic of DoE approach using Central Composite Design methodology

3.1.1. Components of Experimental Design

Considering the HTL batch process to produce bio-oil, there are three aspects of the process that will be analyzed by the designed experiment as shown in Figure 9.

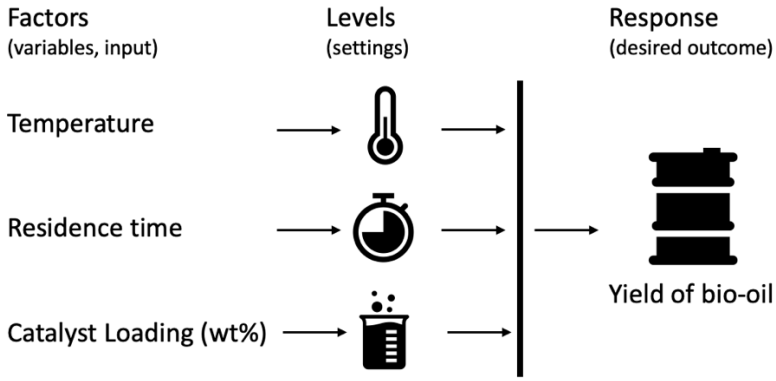

Figure 9: Factors and levels considered for the design of experiments

- **Factors, also known as process inputs**. These can be categorized as process variables which are to be tested for their influence/interactions on the response which in this case is the yield of bio-oil and other products of HTL. The temperature, residence time, and catalyst loading (wt%) are the variables to be considered in this case.
- **Levels,** or the settings of each chosen factor in the study. Examples include the different temperature settings, residence time levels, and particular amount of catalyst.
- **Response,** or the desired output of the experiment. In this case, the yield of bio-oil and other value-added products such as biochar, aqueous phase, and gas is the desired response potentially influenced by the factors and their respective levels.

3.1.2. Experiment Design Process: Screening Campaign

For the preliminary campaign, the process temperature was varied between 250°C and 340°C at a fixed residence time of 15 mins. These parameters were chosen as per the optimum conditions for bio-oil production based on the prior work carried out for the HTL of olive residues by De Filippis et al. 2016 and Evcil et al. 2021. It was found out that the bio-oil production was maximized at a residence time of 15 mins. The main objective of carrying out the preliminary campaign was to perform a screening/proof of concept and validation of the bio-oil production process using COP as a feedstock and HTL. The catalyst loading was set to 0% (non-catalytic). In Table 2, we can observe the chosen parameters for the screening campaign.

Table 2: Chosen parameters for the screening campaign for the production of bio-oil

Temperature	250°C, 270°C, 300°C, 330°C, 340°C
Residence time	15 min
Catalyst Loading (wt%)	0

For this screening campaign, a full-factorial design of experiments was considered and the total number of HTL experiments that were conducted were 10 including the duplicates to ensure the accuracy of the results

3.1.3. Experiment Design Process: Central Composite Design

The objective of this campaign was to obtain a response surface to understand the significance of major reactor variables on the yield of bio-oil and the interaction between various parameters. Based on the results of the screening campaign, an experimental design with 3 factors namely temperature (A), residence time (B), and catalyst loading (C). The DoE for HTL of COP and OTPW were built using Design expert Software® trial version 7 (Design Expert, 2022). Table 3 shows the factors and their levels chosen for the full experimental design from the results obtained in the preliminary campaign:

Table 3: Chosen factors and levels for the design of experiments for full experimental campaign

Factors	**Levels of Factors**				
	-1.633	**-1**	**0**	**1**	**1.633**
Temperature (°C)	250	270	300	330	340
Residence Time (mins)	5	10	15	30	60
Catalyst Loading (wt%)	0	2.5	5	7.5	10

Using the RSM-CCD design approach with the help of Design expert Software® trial version 7 (Design Expert, 2022), a design framework was generated with 20 experiments containing 14 axial points and 1 center point with 6 replicates to ensure the accuracy of the model and experiments. The purpose of the factorial design in this case was to estimate the model's curvature. The center point provided a method for estimating experimental errors and determining whether there was a lack of fit.

3.2. Materials/Samples of COP and OTPW

The samples of COP and OTPW were brought in from an olive mill in Jaén, Spain and shipped to The Netherlands. Prior shipment, the samples of COP were stored in N2-flushed 5L plastic containers. No conditioning or pre-treatment was required for COP samples prior the HTL process due to process' capability of handling wet feedstocks. The samples of OTPW were brought in from stored in plastic bags in dry conditions to avoid the change in its moisture content.

3.2.1. Preparation of slurry

Prior to running the HTL process, the moisture content of the COP and OTPW sample was determined according to the analytical procedures of National Renewable Energy Laboratory (NREL), namely TP-510-42621. Then, slurries of 150 g were prepared in the autoclave vessel, using Milli-Q water as a solvent such that the solid content of biomass was about 15 wt.%. This in agreement with previous research of Zhu et al. 2018 and Evcil et al. 2021. In case of catalytic runs, the Nickel on silica-alumina catalyst dosage was set to different loading according to the design developed in section 3.1.3. with respect to the biomass content on a dry basis (d.b.). A maximum allowable water loading (MAWL) was defined to prevent any damages to the sealed pressure autoclave vessel due to the rise in pressure. According to Parr (Parr Instument Company, 2015), a vessel must not be filled more than three-fourths of its available free space, especially for water and water solutions. For the preliminary campaign, the reactor vessel was loaded with 53 grams of COP and 97 grams of Milli-Q water regardless of the operating condition (as the catalyst loading was fixed at 0%) based on the total solid content of the biomass and MAWL of the autoclave vessel. Whereas for the full experimental campaign, the weight of the COP/OTPW and water varied depending on the catalyst loading as per the design of experiments. The catalyst used for the full experimental campaign was Nickel on silica-alumina.

3.3. HTL Experimental Procedure

The experimental phase of this study was divided into three campaigns. The HTL process was conducted in a 300 mL batch stainless steel autoclave outfitted with a manometer, a K-Type thermocouple, an overhead mechanical stirrer, and a valve for the gas inlet-outlet. The autoclave used was a benchtop mini-reactor provided by Parr Instrument Co. (Parr 4560 – Mini Bench Top Reactor). The reactor was also equipped with a built-in electric jacket to provide the necessary heating as can be seen in Figure 10.

Figure 10: Parr 4560 - Mini Bench Top Reactor schematic (Parr Instument Company, 2015)

After the reactor was loaded with the COP/OTPW sample and Milli-Q water, the reactor was sealed and purged with N_2 gas to remove any remaining air from the headspace. Before the heating was switched on, the reactor was pressurized to 1.4 bar (g) to attain the sub-critical conditions to facilitate the HTL process. A continuous stirring speed of 150 rpm was used for all the HTL experiments. The set points for the operating temperature and the stirring speed were set using the reactor controller via the SpecView® software. After the reactor reached the predetermined temperature, the start time of the experiment start time was noted along with the pressure attained at that point. The reaction was then allowed to run for the pre-determined residence time according to the design of experiments. An online controller and data logger were used to monitor the temperature and pressure (Parr 4848 Reactor controller). After the completion of the reaction, the heating jacket was removed, and the reactor was cooled to room temperature using an ice bath and the gas products were released. The autoclave was then opened, and the reaction mixture was meticulously removed for analysis in accordance with the steps outlined in the next section.

3.4. Product Collection and Extraction

Figure 11 summarizes the whole experimental procedure including the product collection & extraction using a batch HTL process to obtain bio-oil, biochar, and water-soluble organics. The gaseous phase was not collected.

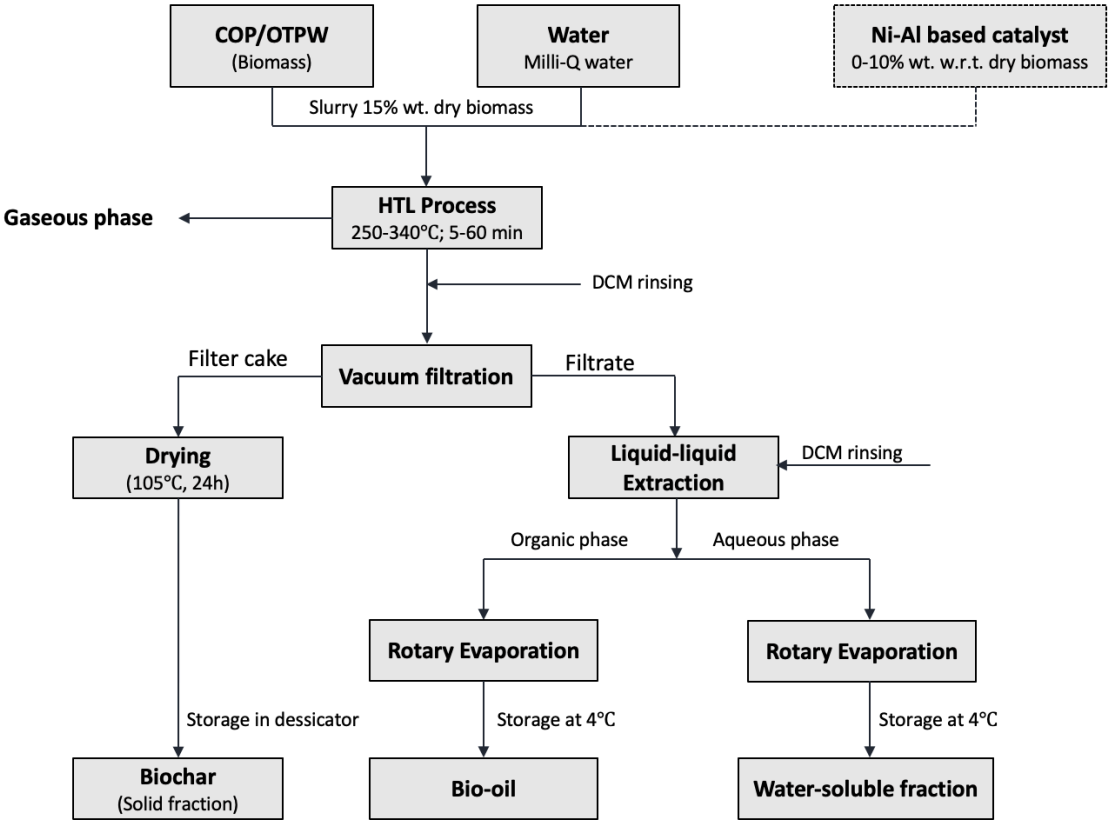

Figure 11: Schematic of the experimental procedure of HTL with product collection and extraction (Own elaboration)

The products/contents of the HTL were collected from the reactor vessel into pre-weighed beakers to fulfill the mass balance. The product slurry which is the aqueous rich phase was carefully transferred into a beaker. After this step, the walls of the reactor vessel and the stirrer were rinsed with dichloromethane (CH_2Cl_2) (DCM, Sigma-Aldrich 99.8% purity) to extract the maximum amount of products as possible. The volume of the solvent used at this stage ranged from 35 mL (for the preliminary campaign) to 70 mL (for the full experimental campaign with catalyst). On obtaining the maximum amount of oil from the vessel, this phase namely the organic rich phase was transferred to another pre-weighed beaker along with the bio-char.

After collecting the products of HTL, they were taken to the laboratory for further separation and extraction processes (Figure 11). The slurry usually contains solid particles and was subjected to vacuum filtration to separate the liquid and solid phase using a Büchner funnel with a 2.5-µm pore size filter paper (Whatman Grade 5). Subsequently, the organic rich phase is also subjected to vacuum filtration using the same filter paper to separate the oil rich phase and the solid phase. The beaker containing the oil phase was rinsed with approximately 15 mL of DCM. The filter cake is further washed with 20 mL of DCM until a change in color from

dark brown to light yellow was noticed which indicated that filtration was complete. The filter cake was then renamed to “biochar” and dried for 24 hours in an oven at 105 °C. After drying, the biochar was weighed and kept in a desiccator for further analysis which will be discussed in detail in the next section.

The step of vacuum filtration was followed by liquid-liquid extraction of the filtrate obtained to extract bio-oil using DCM as extraction solvent. The amount of DCM used for this step was 15 mL and the extraction is repeated until the organic rich phase (DCM & bio-oil) are collected in a pre-weighed Erlenmeyer flask. This step is followed by rotary evaporation to remove the DCM from the bio-oil (Heidolph-VAP® Precision, Heildoph Instruments). The steps of liquid-liquid extraction and rotary evaporation can be witnessed in Figure 12. The aqueous phase is also subjected to rotary evaporation to remove the water. The final products obtained, namely the bio-oil and aqueous phase are stored in pre-weighed bottles in a fridge which is maintained at 4°C to ensure there’s no degradation in the quality of the products obtained.

Figure 12: Representation of the process of liquid-liquid extraction and rotary evaporation

3.5. Characterization of the Products Obtained

3.5.1. High Heating Value/Calorific Value of Bio-oil & Biochar

The higher heating value (HHV) also referred to as the gross calorific value is the quantity of heat released by that fuel after combustion and after the products have returned to a temperature of 25 °C allowing the water to condensate (Chem Europe, 2022). HHV is helpful in calculating heating values for fuels where condensation of the reaction products is practical because it accounts for the latent heat of vaporization of water in the combustion products (Chem Europe, 2022). By concealing a stoichiometric mixture of fuel and oxidizer in a steel container at 25 °C, the higher heating value is experimentally determined in a bomb calorimeter. An ignition source then starts the exothermic reaction, which is followed by the completion of the combustion reactions. Water vapor is produced during combustion when hydrogen and oxygen react. HHV is then calculated as the heat released between identical initial and final temperatures after the vessel and its contents have been cooled to the original 25 °C (Chem Europe, 2022).

The HHV of COP sample, bio-oil, and biochar for this study was determined by employing an adiabatic Parr 6772 Bomb Calorimeter according to ASTM standard D2015-00. Enough oxygen was supplied (up to 27 bar(g)) into the pressurized vessel containing samples of about 1.0 g of biochar and 0.5 g of bio-oil. All the measurements for HHV were carried out in duplicates to ensure the accuracy of the results.

3.5.2. Proximate and Ultimate Analysis of COP, bio-oil, and biochar

Proximate analysis is a procedure used to determine the following: (a) moisture content; (b) ash content; (c) volatile matter and; (d) fixed carbon (Arisanti, 2018). The proximate analysis of the COP sample and biochar was carried out according to the analytical procedures of National Renewable Energy Laboratory (NREL), namely TP-510-42621 and TP-510-42622/ASTM D3174-12 and ASTM D3175-20 for total solids, ash, and volatile matter (VM) respectively.

For the estimation of the amount of solids or moisture present in the COP sample and biochar, a conventional oven drying process at 105ºC was adapted (Furnace Nabertherm 30 – 3000 °C) and weighed after cooling using a desiccator. This was also cross checked with an automatic infrared moisture analyzer. Whereas for the determination of ash content, a dry oxidation technique was adapted at 575°C using a Muffle Furnace (FisherThermo Scientific F6030CM-33-AVL) and all the findings were expressed in terms of the sample's dry weight at 105 °C in the oven. The volatile matter of the samples was determined using a thermogravimetric analyzer (TGA Q600).

The ultimate analysis also known as the elemental analysis is an investigation performed to examine the levels of carbon, hydrogen, oxygen, nitrogen, and sulfur (CHNS) in the sample. The CHNS elemental analysis of COP sample, bio-oil and biochar was carried out using an EuroVector EA3400 Series CHN-O analyzer using acetanilide as reference.

3.5.3. Surface and Chemical Composition analyses

The surface's chemical composition affects the properties and traits of solid surfaces. The surface and chemical composition analyses on the COP sample and biochar were conducted using the following techniques:

- **Scanning electron microscopy/Energy dispersive spectroscopy (SEM-EDS)** is a technique in which the sample material is exposed to electron radiation, which causes the emission of x-rays specific to the elements present (The University of Melbourne, 2022). The various elements present in the sample are identified by a spectrum profile, which is produced by translating the energy emissions into spectral peaks of varying intensity (i.e., lead, iron, copper, zinc etc.)(The University of Melbourne, 2022). A JEOL IT100 scanning electron microscope (SEM) with an energy dispersive X-ray spectroscopy (EDS) detector was used to conduct SEM-EDS in low vacuum mode. Using a backscattered electron detector in compositional mode with an accelerated voltage of 10 kV and a beam current of 65 pA, SEM images were captured. To ensure a fair description of the COP and biochar, two regions of interest (ROI) for each sample were examined.

- **Fourier-transform infrared spectroscopy (FTIR)** was used to identify the functional groups at the surface of the biochar. The FTIR spectra of COP and biochar obtained at the best conditions for the bio-oil yield were recorded between 4000 cm-1 and 700 cm-1 using a Perkin Elmer Spectrum 100 spectrometer with an attenuated total reflectance (ATR) configuration. All spectra were reported as absorbance [%].

- **X-ray photoelectron spectroscopy (XPS)** was used to determine the biochar atomic state, chemical composition, and electronic state. When a solid surface is exposed to an X-ray beam, XPS spectra are produced by measuring the kinetic energy of the electrons that are emitted from the top 1 to 10 nm of the material. The number of ejected electrons over a range of kinetic energies is used to create a photoelectron spectrum. Identification and measurement of all surface elements are made possible by the energies and intensities of the photoelectron peaks (except hydrogen) (ThermoFisher Scientific, 2022).

- **X-ray powder diffraction (XRD)** is an analytical method that mainly determines the phase of crystalline materials and can give details on unit cell dimensions. The material under analysis is finely ground, homogenized, and the bulk composition is calculated on average. COP and biochar measurements were made using a Bruker D8 Advance diffractometer with Bragg-Brentano geometry, a Lynxeye position-sensitive detector, and a Cu K radiation source.

- **X-ray fluorescence (XRF)** Panalytical Axios Max WD-XRF spectrometer was used for the XRF analysis of COP and biochar, and SuperQ5.0i/Omnian software was used for data analysis. The energy resolution used to collect the XRF spectra was 4kW with the main focus on quantification of oxides.

4. Results & Discussion

In this chapter, we will discuss and analyze the various results obtained from the three experimental campaigns conducted for the development of the thermochemical conversion process to produce bio-oil.

4.1. Screening Campaign

The focus of the screening campaign was to identify the range of temperatures that have the highest influence on the COP bio-yield at a fixed residence time of 15 mins in the absence of a catalyst. This subsection will focus on the results obtained through a total number of 10 experiments including duplicates to ensure the accuracy of the results.

4.1.1. Product Yields

The average mass yields for each product obtained from HTL of COP along with their standard deviations for the screening campaign are summarized in Table A.1 of Appendix 1. Figure 13 highlights the distribution of the products obtained from the HTL of COP at different temperatures in terms of mass yield (wt.%).

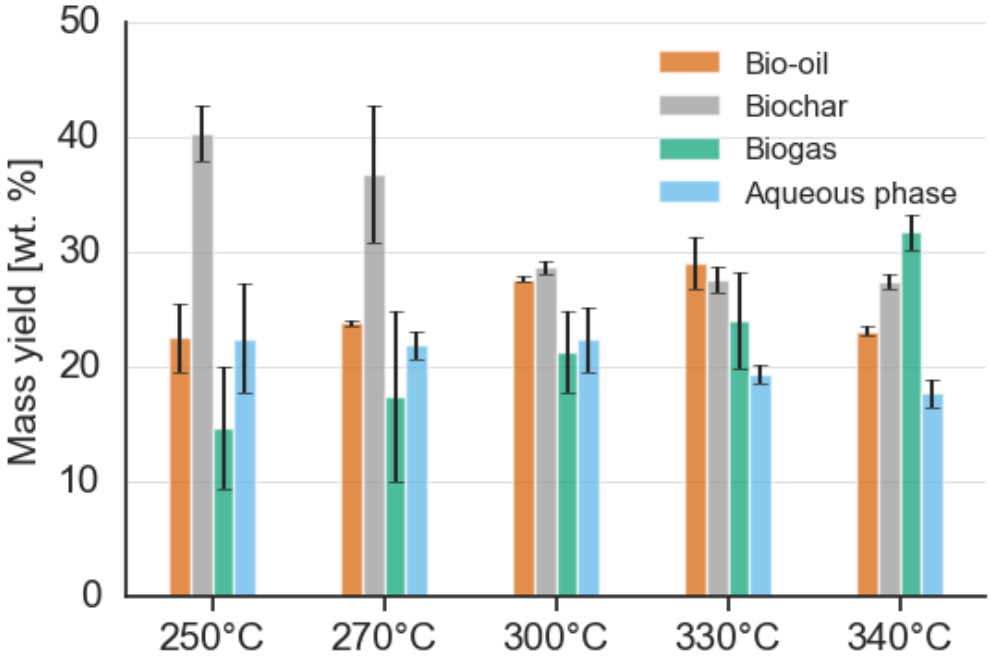

Figure 13: Product distribution for HTL of COP for the screening campaign

As can be seen in Figure 13, the bio-oil yield (production) is increased with the increase in temperature until an optimum average yield of 29 wt.% is reached. After this temperature, a decreasing trend can be witnessed for the same. At 340°C, a decrease of 20% can be seen in the average yield of bio-oil. Whereas the yield of biochar decreased with the increase in temperature. The average biochar yield at the optimum temperature (330°C) was found out to be 27.63 wt.% with a decrease in 0.5% at 340°C. This could be attributed to the formation of more gaseous products at higher temperatures and repolymerization of lignin (Evcil et al., 2021).

The trend obtained in the screening campaign is in accordance with the results obtained by the study conducted by Evcil et al. 2021 and they indicate the presence of a curvature in the response surface. This validates the findings of the study conducted by Evcil et al. 2021 except for the optimum bio-oil yield (30.75 wt.%) which was reported to be at 300°C. A constant increasing trend in the yield biogas can also be seen and this can be attributed to a higher decomposition of unreacted compounds into gaseous products.

This trend for the mass yields of bio-oil and biochar were isolated from the overall product distribution and can be better witnessed in Figure 14 and Figure 15:

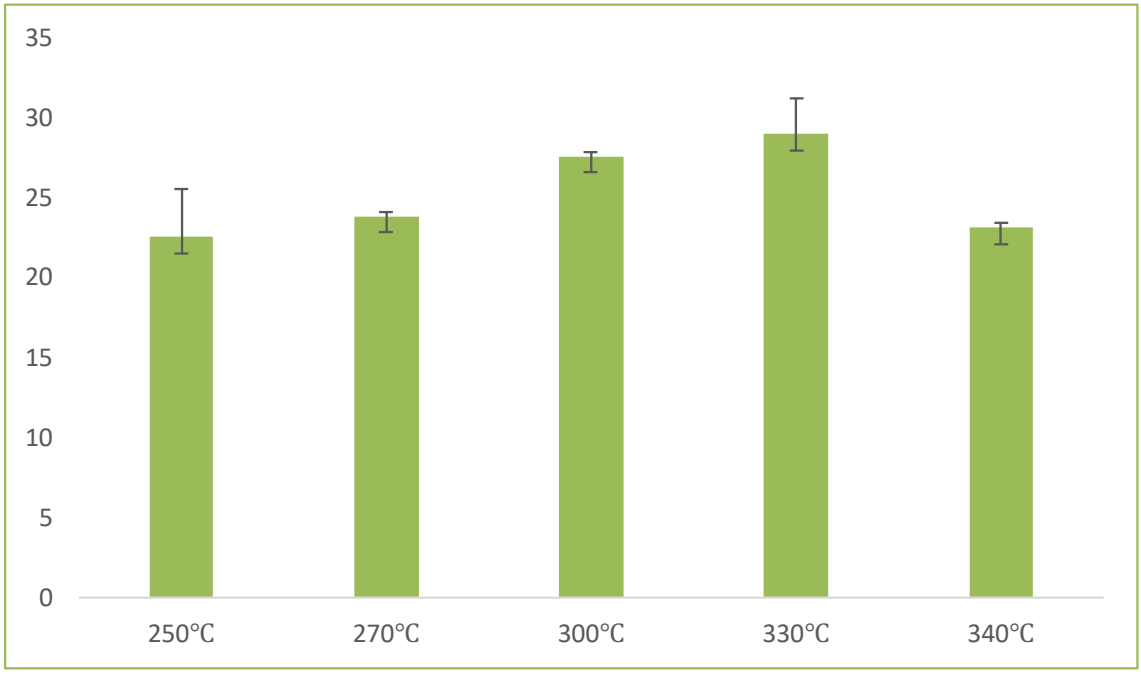

Figure 14: Mass yield of bio-oil obtained from the screening campaign

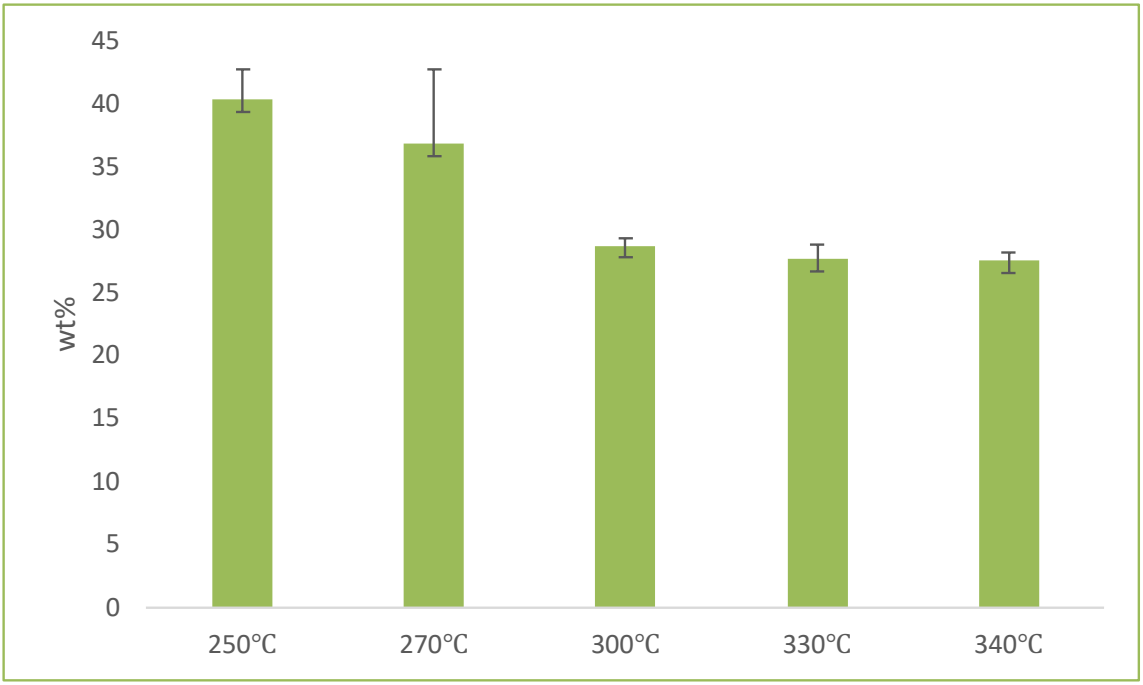

Figure 15: Mass yield of biochar obtained from the screening campaign

4.1.2. Ultimate and proximate analysis

The elemental (ultimate) and proximate analysis of the raw feedstock (COP), biochar, and bio-oil obtained at different temperatures are presented in Table 4. From the proximate analysis, the moisture content of raw COP was found out to be 57.2% which proves it to be a suitable candidate to be processed by HTL. The ash content of the raw COP was found out to be slightly higher than reported in Evcil et al. 2021 which could be attributed to difference in the nature of feedstock used. The ash content of the biochar samples at different temperatures was found to be higher than in raw COP. The volatile matter for biochar showed a decreasing trend with an increase in temperature until 330°C with a slight increase at 340°C. An increase in the fixed carbon content of the biochar was also noticed with the increase in temperature, which indicates an increase in the quality of the biochar.

It can be seen that after the HTL conversion, the bio-oil and biochar fractions exhibit a higher C-content when compared to the raw feedstock. The carbon content of the bio-oil and biochar increased with an increase in temperature. As the carbon content of the biochar samples were above 50%, they are compliant with the "European Biochar Certificate" (EBC, 2012). Contrary with the results reported in Evcil et al. 2021, the hydrogen content of bio-oil decreased with increase in temperature, which indicates the formation of more aromatic compounds (Akalin et al., 2012). The overall sulfur content was found to be the highest for bio-oil and biochar at lower temperatures and the lowest at highest temperatures. With respect to the N and S contents, these elements were never higher than the ones detected in raw COP. Notably, the oxygen content levels in bio-oil and biochar samples decreased with the increase in temperature which are mainly due to the decarboxylation and dehydration reactions occurring during the HTL processing (Evcil et al., 2021).

Table 4: Proximate and ultimate analysis of COP, bio-oil, and biochar at different temperatures

	Proximate analysis				Ultimate analysis (wt.%)				
	Moisture (%)	**VM (%)**	**FC (%)**	**Ash (%)**	**C**	**H**	**N**	**S**	**O**[1]
COP	57.2			3.6	27.78	8.23	0.08	0.02	72.12
Bio-oil									
250°C	-	-	-	-	62.50	10.48	0.00	0.18	26.84
270°C	-	-	-	-	63.99	9.72	0.10	0.11	26.08
300°C	-	-	-	-	66.26	9.23	0.24	0.06	24.21
330°C	-	-	-	-	67.79	9.04	0.36	0.03	22.78
340°C	-	-	-	-	69.48	8.70	0.42	0.03	21.37
Biochar									
250°C	-	52.5	45.5	2.0	64.63	5.56	1.02	0.40	28.39
270°C	-	46.5	47.3	6.2	69.93	5.73	0.99	0.18	23.17
300°C	-	39.5	53.9	6.6	72.45	5.41	1.09	0.06	20.99
330°C	-	36.1	58.6	5.3	73.20	5.35	1.17	0.09	20.19
340°C	-	39.2	55.4	5.4	75.41	5.51	1.18	0.06	17.84

Table 5: Atomic ratios (O/C, H/C, and C/N) for dry COP, biochar, and bio-oil obtained at different operating conditions

Sample	**Atomic Ratios**		
	O/C	**H/C**	**C/N**
COP	1.95	3.55	405.13
Bio-oil			
250°C	0.32	2.01	-
270°C	0.31	1.82	746.55
300°C	0.27	1.67	322.10
330°C	0.25	1.60	219.69
340°C	0.23	1.50	193.00
Biochar			
250°C	0.33	1.03	73.92
270°C	0.25	0.98	82.41
300°C	0.22	0.90	77.55
330°C	0.21	0.88	72.99
340°C	0.18	0.88	74.56

Table 5 shows the atomic ratios (O/C, H/C, and C/N) of dry COP, biochar and bio-oil obtained at different operating conditions for the screening campaign. It can be noticed that the O/C and H/C rations show a decrease with the increase in temperature for both bio-oil and biochar which shows the occurrence of dehydration, decarboxylation, deoxygenation, and decarbonylation reactions during the HTL process (Evcil et al., 2021; Kim et al., 2011). The C/N ratio is a useful parameter to predict N-immobilization or N-mineralization upon decomposition. As the C/N

[1] Calculated as O = 100 – C – H – N – S

ratio of all the biochar samples at different temperatures is more than 30, it indicates that the biochar might lead to N-immobilization if used as a soil amendment, thus becoming unavailable to the crops by microbial consumption (F.J. Stevenson & M.A. Cole, 1999). Further research would be needed to identify the biochar-soil interactions as N-immobilization is also known to be dependent on the C/N ratio of soil (Cayuela et al., 2013).

The influence of operating conditions on the elemental composition of the bio-oil and biochar obtained at different temperatures of the screening campaign is presented in the Van Krevelen diagram to estimate the fuel quality (Figure 16). The diagram presents H/C atomic ratio as a function of O/C atomic ratio of the bio-oil and biochar with other fossil derived fuels. The H/C and O/C ratios of biochar samples obtained at different temperatures were clustered in the range of lignite (at lower temperatures) and bituminous coal as the temperature increased. The biochar obtained at 330°C was in the class of bituminous coal which indicates a higher heating value (de Jong, 2015). This finding was similar to that reported by Evcil et al. 2021. On the other hand, the bio-oil produced were identified in the range of kerosene and diesel fuel with the bio-oil at 330°C showing H/C and O/C ratios almost closer to that of diesel fuel and with an increase in HHV with the increase in temperature.

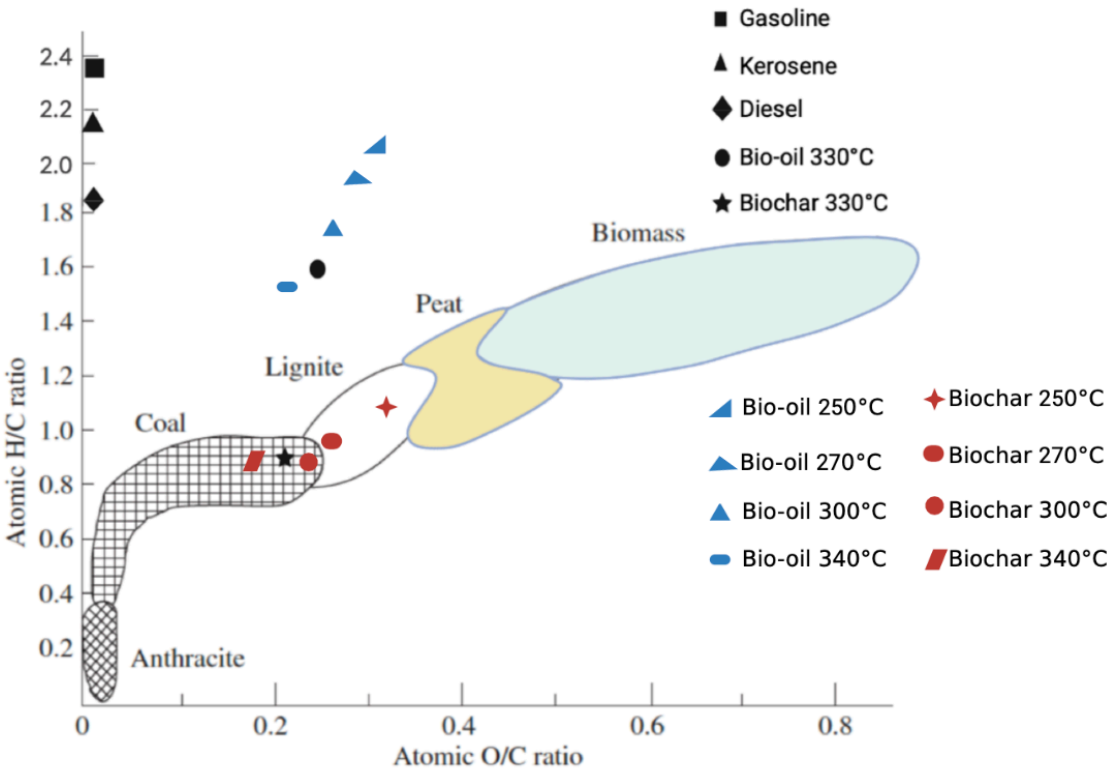

Figure 16: Van Krevelen diagram of the bio-oil and biochar obtained at different temperatures – based on de Jong, 2015

4.1.3. Effect of Temperature on HHV of bio-oil and biochar

The effect of temperature on HHV of bio-oil and biochar for the conditions of the screening campaign can be seen in Figure 17 and Figure 18. This can help to eventually identify if the bio-oil and biochar obtained have the potential to be used as biofuels. The trend for the HHV of bio-oil indicates an increase in the HHV with an increase in temperature, which reaches to a maximum of 32.1 MJ/kg for 340°C as can be seen in Figure 17. This trend obtained matches to that of the study conducted by Evcil et al. 2021 (25.95 MJ/kg – 31.76 MJ/kg), and indicates the increase in carbon content of the bio-oil obtained at higher temperatures (lower O/C ratios) which will be further confirmed by the CHNS analysis.

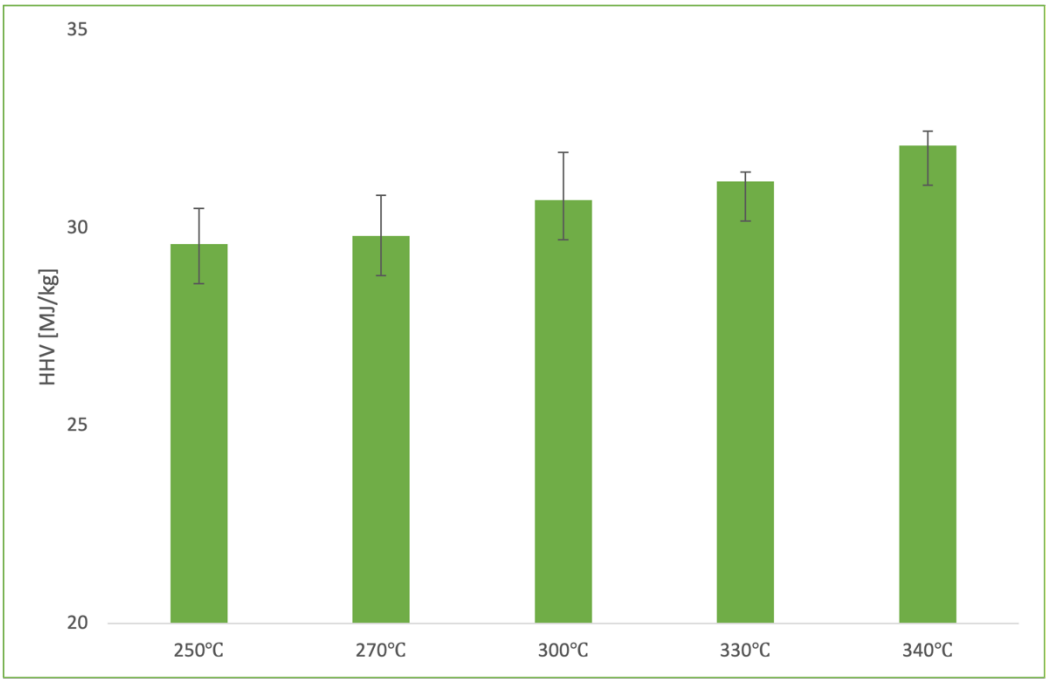

Figure 17: HHV of bio-oil obtained from the screening campaign

The HHV of biochar (Figure 18) also shows an increase with the rise in temperature except for the point at 300°C. The maximum HHV for the biochar obtained at 340°C is 29.2 MJ/kg. This is observed mainly due to the increase in the fixed carbon content with the rise in temperatures (Table *4*).

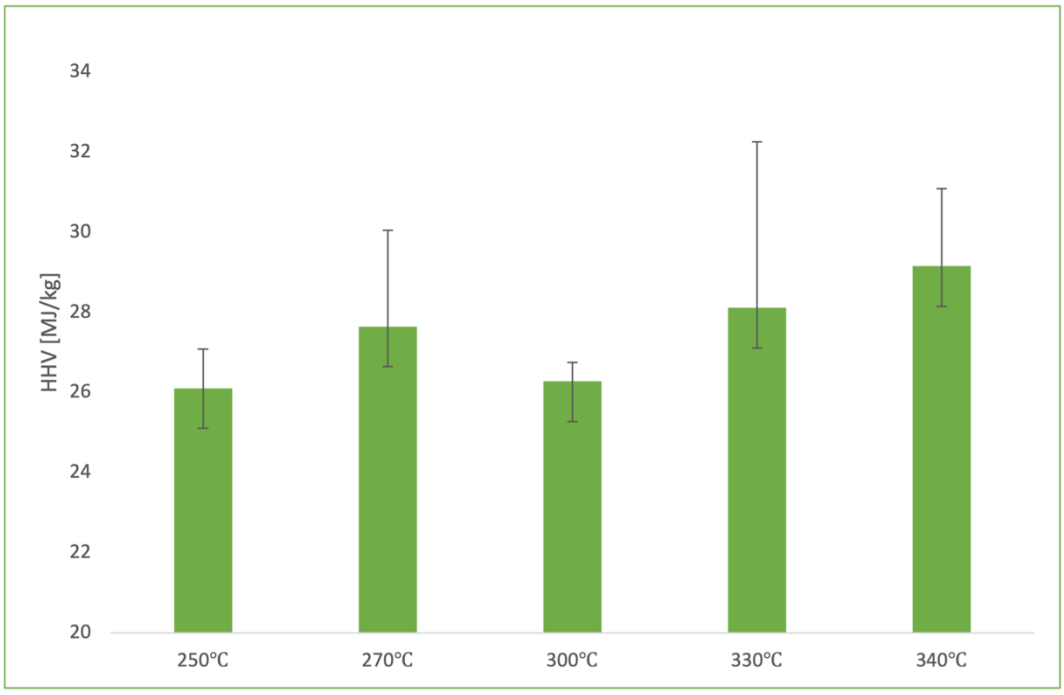

Figure 18: HHV of biochar obtained from the screening campaign

4.1.4. XRF of COP and biochar

The XRF analysis/oxide composition for raw COP and biochar at 250°C-15min (minimum point), 330°C-15min (optimum point), and 340°C (maximum point) is reported in Figure 19. This analysis was carried out to identify and report the changes in chemical composition of the raw COP on HTL processing.

As can be seen from Figure 19, CaO, P_2O_5, SO_3, Al_2O_3 and Fe_2O_3 follow the same trend of the bio-oil yield, having a peak at 330°C (see Figure 13). This indicates the enrichment of these minerals as the temperature increases from 250°C to 330°C and a decrease at 340°C. Minerals such as calcium, potassium, and phosphorous are expected to increase and get accumulated on the biochar surface as ash (Gaskin et al., 2008). This phenomenon can be observed due to the devolatilization of the biochar phase. As COP is found to be alkaline in nature (Evcil et al., 2021), the solubility of the elements such as Si, Cl, and K are fostered and because of this property they are more likely to be transferred to the aqueous phase.

Compounds like Ni and Mo were also noticed in all the biochar samples, and they are mainly attributed to the material of the autoclave vessel (Hassel alloy B2/B3), which is known to be rich in Ni and Mo. The occurrence of these compounds was due to the scraping of the walls of the vessel to extract the product with a tool which in the future can be avoided by using a tool made of plastic. Compounds having a wt.% less than 0.1% can be found in Supplementary Information.

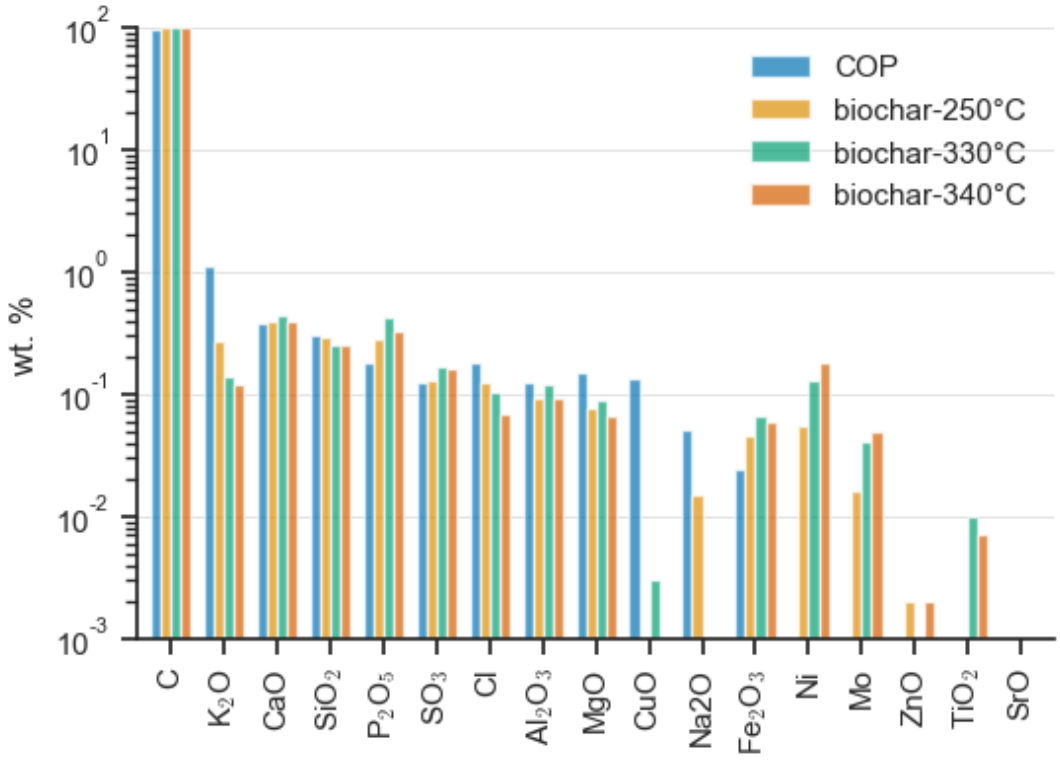

Figure 19: XRF analysis for raw COP and biochar obtained at minimum (250°C - 15min), optimum (330°C - 15min) and maximum (340°C - 15min) operation conditions.

4.1.5. XRD of COP and biochar

XRD measurements were performed to evaluate the influence of the operating conditions on the crystallinity of the biochar compared with the parent biomass. In the XRD pattern (Figure 20) a hump is observed in the 16-20-degree 2θ range due to organic carbon (Clemente et al., 2018).

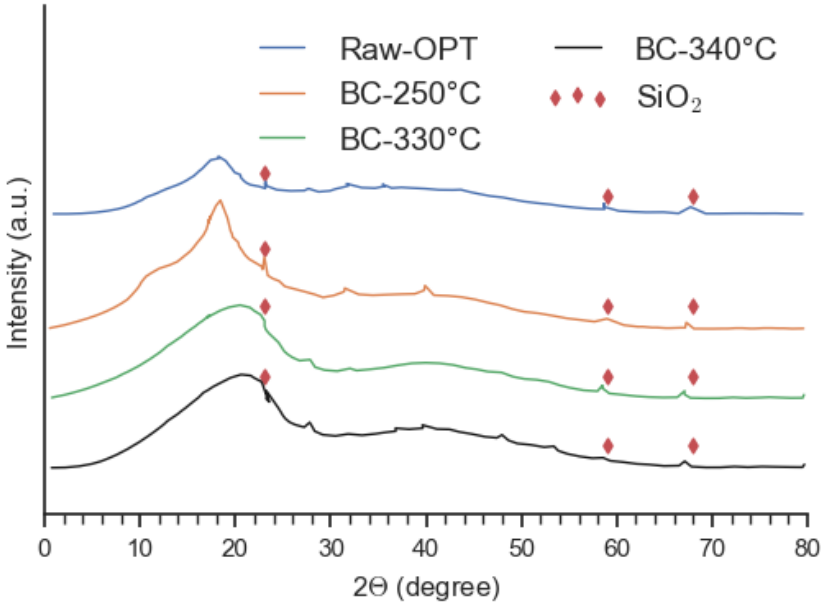

Figure 20. XRD pattern for raw COP and biochar obtained at minimum (250°C–15min), optimum (330°C–15min) and maximum (340°C–15min) operation conditions.

A broad peak is observed at 2θ = 17 corresponding to cellulose (Clemente et al., 2018). The highest amorphous nature compared to the parent biomass corresponds to the biochar obtained at the lowest temperature, 250°C. On the other hand, the main crystalline mineral observed in all biochar corresponds to turbostratic crystalline C (2θ = 23) and quartz (SiO_2) at 2θ = 59 and 68 degrees.

4.1.6. SEM-EDS of COP and biochar

SEM-EDS allows detailed evaluation of the biochar surface at the micro-scale with respect to morphology and elements. Figure 21 depicts the SEM-EDS images of the biochar obtained at the optimum condition of the screening campaign (330°C-15min).

Table 6: Concentrations of elements obtained by EDS analysis shown in Figure 21 at different locations on the surface of the COP biochar obtained at 330°C–15min.

	Location	C [at.%]	O [at.%]	Si [at.%]	Al [at.%]
Figure 18-a		82.5	17.3	-	0.3
Figure 18-b	Area 1	52.9	36.6	10.4	-
	Area 2	50.0	39.4	10.6	-

a) **b)**

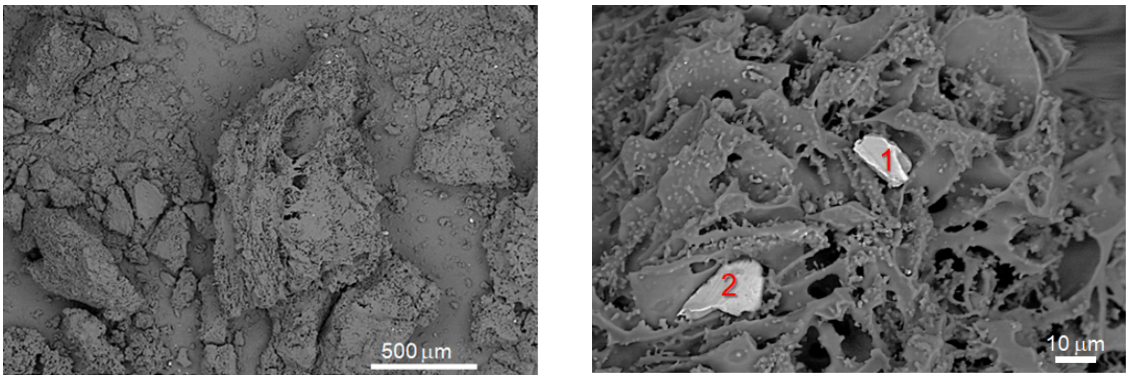

Figure 21: SEM images of the biochar obtained at optimum conditions for the bio-oil yield, 330°C-15min.

From Figure 21, it can be noticed that this biochar has an amorphous carbonaceous matrix with few visible inorganic deposits. The findings of the EDS results can be seen in Table 6, which indicate the presence of Si and O as the main minerals on the surface of biochar. These findings are also in agreement with results from XRF (Figure *19*) and XRD (Figure *20*) analysis. The silicon deposits are mainly a result of silicon oxides identified in the raw feedstock (see Figure 19).

4.1.7. XPS of biochar

In Figure 22-a, we can observe the XPS of the biochar sample obtained at the optimal condition (330°C and 15 min). The XPS spectra shows the C1s spectra deconvoluted into three peaks: C-C/C-H (286–284 eV), C-N (285–284 eV) and C=O/O=C-O (289-288 eV) (NIST, 2012; Paul van der Heide, 2011). The results show the presence of a majority of C-C/C-H bonds (72%) with a significant presence of C-N bonds (21%).

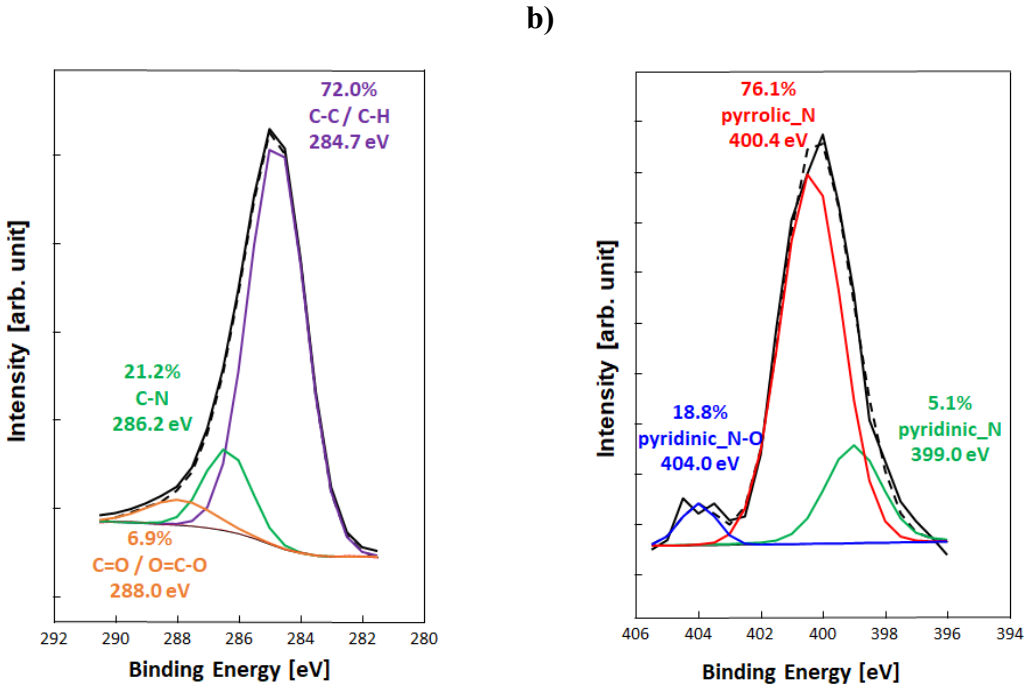

Figure 22: XPS of biochar at 330°C and 15 min

Graphitic C−C bonds are quite stable (Guo & Chen, 2014), which make this type of biochar more resistant to degradation. To further identify the type of nitrogen present in the biochar, the high-resolution N 1s spectra was recorded. Results indicate that the majority was pyrrolic nitrogen. This indicates that the COP biochar provide active sites which result in higher performance for catalysis of O_2 reduction and adsorption of CO_2 (Leng et al., 2020).

4.1.8. FTIR of biochar

The FTIR of biochar obtained at the optimum condition (330°C and 15min) was conducted and the results can be seen in Figure 23. The sharpest peak is observed between 900-1100 associated with C-C group in biochar. The FTIR showed presence of amine group at a wavelength of 3000 nm which couldn't be noticed from the results of XPS.

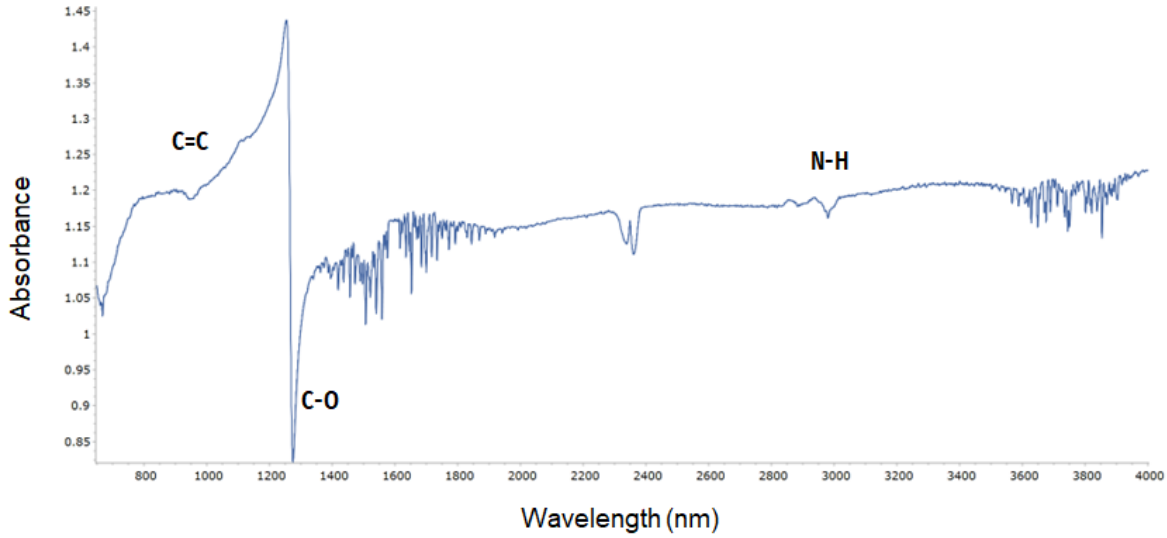

Figure 23: FTIR of biochar obtained at optimum condition (330°C and 15 min)

The presence of the Amine (N–H) group is reported to be beneficial for adsorption of Cu (II), Pb (II), SO_2 and atrazine.

4.2. CCD Campaign - COP

The CCD campaign for COP entailed conducting experiments at different design levels as discussed in Section 3.3. The design of experiments and detailed results for each experiment can be seen in Table A.2 and A.3 in Appendix A. This subsection will focus on the results obtained through a total number of 22 experiments including the validation experiments for the accuracy of the model.

4.2.1. Product Yields

The average mass yields of all the products obtained through this campaign can be seen in Appendix A (Table A.2). Figure 24 represents the yields of the various products obtained from the CCD-COP campaign at different temperatures and residence time and for this representation, the catalyst loading was fixed at 5% wt. The plot is a result of the second-degree polynomial which was generated on the completion of the experimental campaign for all the phase/products obtained. This mathematical model generated can be witnessed in the Appendix A of this report (Table A.3) and the detailed analysis of the response surface methodology can be seen in Appendix B. It can be noticed that temperature along with catalyst loading had a major effect on the mass yield of bio-oil.

The maximum mass yield of bio-oil obtained from the experimental campaign was 51.96% wt. at the condition 330°C, 30 min residence time, and 7.5% wt. catalyst loading. The mass yield of biochar was found to be maximum at lower temperatures with an overall range of 6.84-39.96 wt.% throughout the experimental campaign. The aqueous phase followed an overall decreasing trend with an increase in temperature which is likely due to a higher decomposition of unreacted compounds to gaseous phase. The mass yield of gases and losses shows that higher the temperature, the higher the yield with an effect of reaction time on it. Such effects have been reported to result from the decomposition of the bio-oil and biochar into liquid compounds

and further into non-condensable gases boosted by the Ni activity in hydrogenation and cracking reactions (Scarsella et al., 2020).

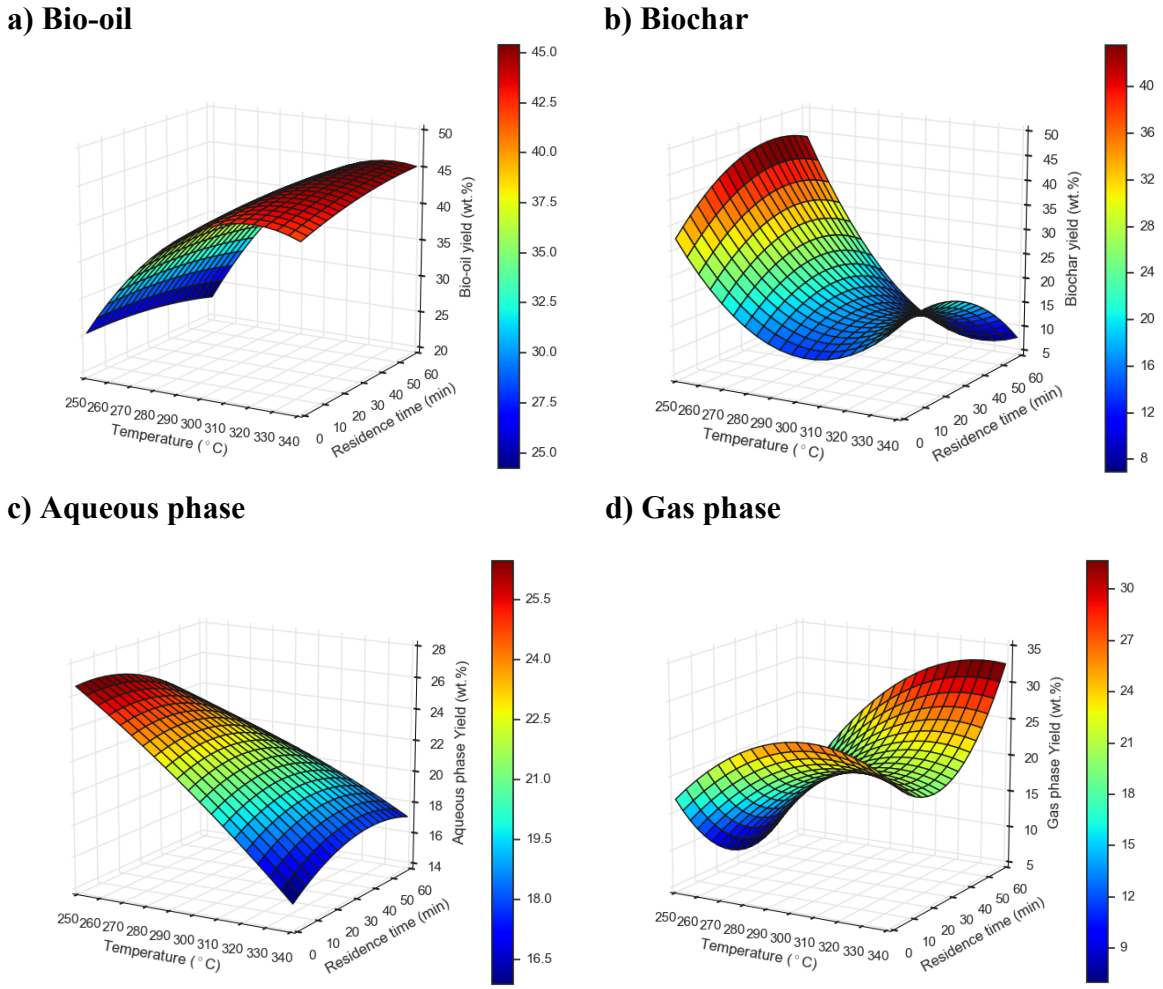

Figure 24. Product distribution for COP HTL at different temperatures and residence time for 5% catalyst.

4.2.2. Optimization and validation tests

The accuracy of the model generated was evaluated by identifying the conditions that maximized the bio-oil yield out of all the fractions of the products obtained from the HTL process. For the optimization, the following criteria (Table 7) was set in the Response Optimizer of Minitab® 21.1.1 (64-bit). This can be witnessed in further detail in Appendix B.

Table 7: Initial values and solution provided on optimization

Variable	Unit	Initial Value	Solution Provided
Temperature	°C	320	330
Residence time	min	20	60
Catalyst loading	wt.%	8	10

A set of 2 validation tests were conducted at the conditions as suggested by Minitab® 21.1.1. The results are presented in Table 8, where the model predicted a bio-oil yield of 59.01% wt. whereas on carrying the validation experiments, an average bio-oil yield of 54.23% wt. was obtained. With these values, an absolute error of 4.79% and a relative error of 8.11% was calculated for the model developed using central composite design approach.

Table 8: Responses for the bio-oil yield from the validation tests with absolute and relative error

Test: Validation CCD-COP	**Bio-oil mass yield (wt.%)**
Model prediction	59.01
Experimental Validation	54.23 (2.58)[2]
Absolute Error	-4.79%
Relative Error	-8.11%

4.2.3. Effect of Temperature on HHV of bio-oil and biochar

The effect of temperature on HHV of bio-oil and biochar for the minimum and maximum yield conditions (250°C-15mins-5% and 330°C-60mins-10% respectively) of the CCD-COP campaign can be witnessed in Figure 25 and Figure 26. This can help to eventually identify if the bio-oil and biochar obtained can be used as efficient fuels. The trend for the HHV of bio-oil indicates an increase in the HHV with an increase in temperature and catalyst loading, which reaches to a maximum of 23.2 MJ/kg for 330°C as can be seen in Figure 25. This trend obtained indicates an increase in the fixed carbon content of the bio-oil obtained at higher temperatures (lower O/C ratios) which will be further confirmed by the CHNS analysis.

[2] The figure in bracket indicates the standard deviation

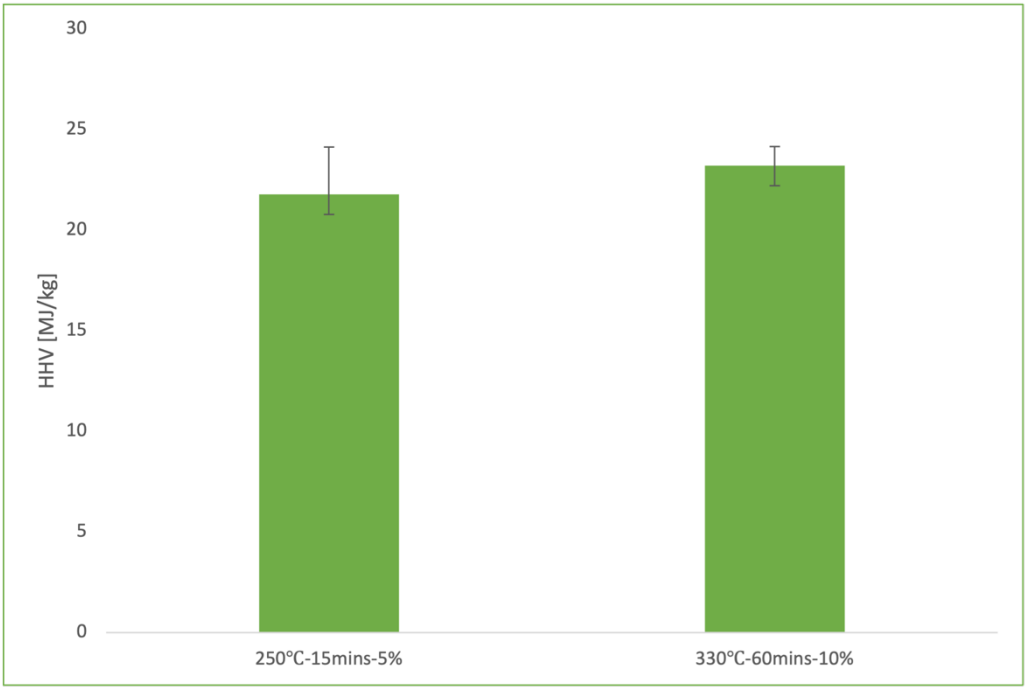

Figure 25: HHV of bio-oil at minimum and maximum condition obtained from the CCD-COP campaign

The HHV of biochar (Figure 26) shows a sharp decrease with the rise in temperature and catalyst loading. This phenomenon could be observed due to the increase in wt.% of nickel (due to increased catalyst loading) and decrease in fixed carbon content which could be further confirmed by the results of ultimate analysis (CHNS analysis).

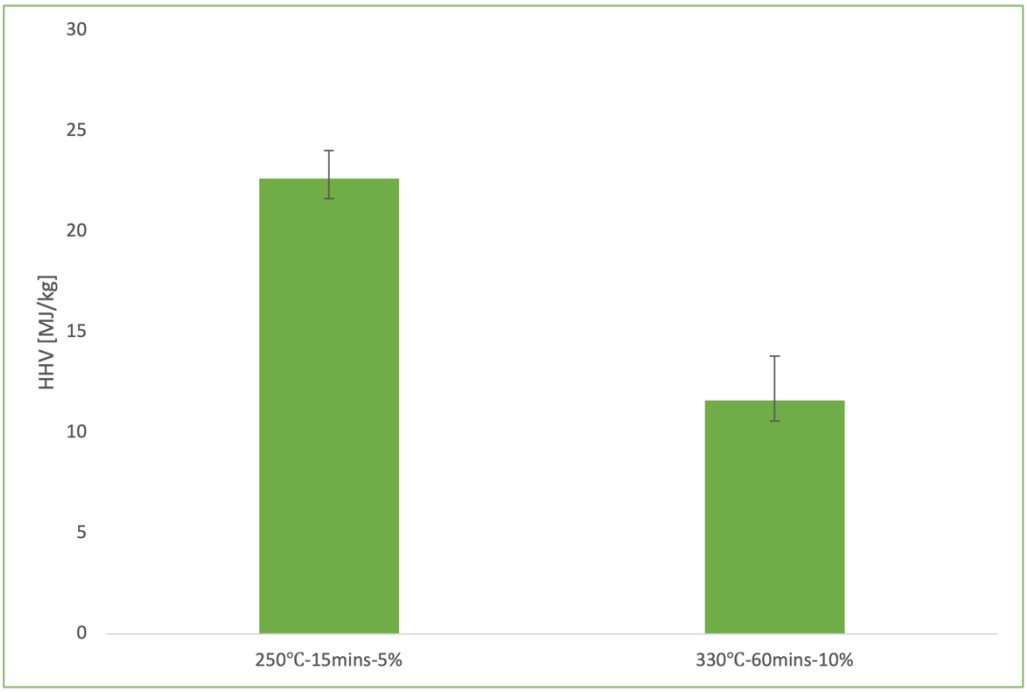

Figure 26: HHV of biochar at minimum and maximum condition obtained from the CCD-COP campaign

4.3. Full Experimental Campaign (CCD-OTPW)

The CCD campaign for OTPW entailed conducting experiments at different design levels as discussed in Section 3.3. The design of experiments and detailed results for each experiment can be seen in the Appendix A. This subsection will focus on the results obtained through 9 out of a total number of 22 experiments.

4.3.1. Product Yields

The average mass yields for each product obtained from HTL of OTPW for the screening campaign are summarized in Table 9. The highest mass yield for bio-oil obtained was 56.3% wt. at the condition of 330°C, 30 mins, and 7.5% wt. catalyst loading. The overall mass yields of bio-oil obtained by using OTPW as the feedstock is higher than that obtained on using COP. The trend obtained by this campaign indicates the potential of OTPW to produce bio-oil with higher mass yields than COP when the same Ni based catalyst is used. The trend of the mass yields of biochar, aqueous phase, and gases seem to be similar to that of the CCD-COP campaign.

Table 9: Detailed mass yield of all product fractions obtained from HTL of OTPW

Run	Operating Condition	Response 1: Bio-oil Yield (%)	Response 2: Bio-Char Yield (%)	Response 3: Aqueous phase Yield (%)	Response 4: Gas Yield (%)
1	300-15-5%	48.52	11.82	12.12	27.54
2	300-5-5%	45.28	12.11	16.64	25.97
3	270-10-7.5%	43.37	19.88	16.39	20.36
4	330-10-2.5%	47.02	11.56	22.67	18.75
5	300-15-5%	47.72	12.36	13.03	26.89
6	330-30-7.5%	56.3	9.87	4.82	29.01
7	300-15-0%	38.4	28.11	14.26	19.23
8	250-15-5%	25.76	32.47	31.09	10.68
9	270-10-2.5%	40.262	29.35	17.78	12.6

5. Conclusions

The experimental campaign for the development of this case study was divided into three phases, namely the screening campaign, CCD-COP campaign, and CCD-OTPW campaign. This section will highlight the conclusions derived from all these experimental campaigns and will lay groundwork to the future work for the further development of this thermochemical conversion technology to produce liquid biofuels.

5.1. Screening Campaign

The screening campaign focused on performing experiments at different temperatures from 250°C to 340°C at a fixed residence time of 15 mins in the absence of a catalyst. This subsection will focus on the conclusions derived through a total number of 10 experiments including duplicates to ensure the accuracy of the results. This campaign resulted in the production of bio-oil and biochar at an average mass yield of 29% wt. and 27.63% wt. respectively at an optimum condition of 330°C and 15 min residence time without the use of catalyst. An increasing trend in the yield of bio-oil was obtained until the optimum temperature of 330°C was reached and then a decrease could be witnessed, and this matched the trends obtained in the literature studies referred for the development of this case study. Similarly, a decreasing trend in the mass yield of biochar was noticed with an increase in temperature.

The energy content/calorific value of the products obtained (bio-oil and biochar) were tested. The high heating value of bio-oil and biochar obtained increased with an increase in temperature with a maximum being obtained at 340°C. The maximum HHV of bio-oil was 32.1 MJ/kg and that of biochar was 29.2 MJ/kg. This was observed due to increase in the fixed carbon content with the increase in temperature which was further confirmed by performing ultimate analysis (CHNS analysis). A Van Krevelen diagram was created for the bio-oil and biochar samples, and it indicated that the biochar samples resembled the elemental ratios of lignite and bituminous coal whereas the bio-oil samples showed elemental ratios similar to that of diesel and kerosene.

The analysis of the mineral composition and morphology of biochar showed that a slight concentration of minerals can be expected as a result of devolatilization of biomass. The minerals found were CaO, P_2O_5, SO_3, Al_2O_3 and Fe_2O_3 mainly due to the nature of olive residues. On the other hand, a significant removal of alkali elements (i.e., Cl and K) was observed indicating their transfer to the aqueous phase as the temperature increases. Heavy metals like Mo and Ni were found present in the biochar despite not being present in the feedstock, which was a result of scraping the autoclave vessel.

Finally, the findings of SEM-EDS of the biochar sample obtained at the optimum condition (330°C – 15min) showed an amorphous carbonaceous matrix with a few visible inorganic deposits. The EDS results indicated the presence of Si and O as the main minerals on the surface of biochar. The XPS results showed the presence of a majority of C-C/C-H bonds (72%) with a significant presence of C-N bonds (21%). A further XPS to identify the type of nitrogen was conducted and it was found out that the majority was pyrrolic nitrogen. This indicated that the biochar obtained has properties which provides higher performance for catalysis of O_2 reduction and adsorption of CO_2. The FTIR of biochar obtained at 330°C and 15 min indicated the presence of amine group which is beneficial for adsorption of Cu (II), Pb (II), SO_2 and atrazine.

5.2. CCD – COP Campaign

The focus of this campaign was to analyze the production of bio-oil using COP and HTL process and obtain a response surface to understand the significance of major reactor variables on the yield of bio-oil and the interaction between various parameters. This subsection will focus on the conclusions derived through a total number of 22 experiments including validation experiments which were performed to ensure the reliability of the mathematical model developed.

This campaign resulted in the production of bio-oil with a maximum mass yield of 51.96% wt. at a temperature of 330°C, 30 mins residence time, and a catalyst loading of 7.5% wt. This indicates that the use of catalyst can significantly increase the yield in favor of bio-oil production when compared to the production process without the use of catalyst. On completion of the total number of experiments as per the DoE (see Appendix A), a mathematical model was generated using Response Optimizer of Minitab® 21.1.1 (64-bit). This resulted in second-order polynomials for all the product fractions of the HTL process which helped in determining the most optimum condition for maximizing the bio-oil production. To check the accuracy of the model, a set of 2 validation experiments were carried out at the predicted condition (see Section 4.2.2.). The model predicted a bio-oil yield of 59.01% wt. whereas on carrying the validation experiments, an average bio-oil yield of 54.23% wt. was obtained. With these values, an absolute error of 4.79% and a relative error of 8.11% was calculated for the model developed and therefore proved the accuracy of the approach used to develop this thermochemical conversion process.

Finally, the energy content/calorific value of the bio-oil and biochar at the conditions which gave minimum and maximum mass yield (250°C-15mins-5% and 330°C-60mins-10% respectively) of bio-oil were tested. The HHV showed an increasing trend with increase in temperature and the catalyst loading and a maximum average HHV of 23.2 MJ/kg was found out for the 330°C-60mins-10% wt. condition. On the other hand, the HHV of biochar showed a decreasing trend with an increase in temperature and catalyst loading. The HHV of biochar obtained at 330°C-60mins-10% wt. condition was found out to be 11.6 MJ/kg which is significantly lower when compared to the non-catalytic production route. This indicates that the use of a Ni based catalyst affects the quality of the products obtained from HTL process and reduces the energy content drastically.

5.3. CCD – OTPW Campaign

The objective of this campaign was to analyze the production of bio-oil using OTPW as feedstock and HTL process and obtain a response surface to understand the significance of major reactor variables on the yield of bio-oil and the interaction between various parameters. This subsection will focus on the conclusions derived through a total number of 10 out of the 20 experiments.

This campaign resulted in the production of bio-oil with a maximum mass yield of 56.3% wt. at a temperature of 330°C, 30 mins residence time, and a catalyst loading of 7.5% wt. The trends obtained from this campaign indicate that bio-oil with higher mass yield can be obtained when compared to COP as a feedstock which indicates a high potential of OTPW to be used as a feedstock as well adding to the establishment of a circular economy for the olive industry.

6. Recommendations

From the different findings, limitations, and outcomes of this study, some challenges were identified which could be paid attention to in potential studies. Following are a few recommendations that could help in further development of this technology and enhancing the analysis of data generated during this study.

6.1. Gas capture, quantification, and characterization

The current batch reactor which was used for the production of liquid biofuel from olive residues (COP and OTPW) was not equipped with any mechanism for capturing and storing the gaseous phase which is obtained as one of the products of the HTL process. This imposes a limitation on the accuracy of the mass balance calculation and further characterization of the gaseous phase to better understand the reaction mechanisms involved during the process. It is suggested that the current laboratory setup includes necessary mechanism such as piping and sampling devices for capturing the gases and analyzing them for their physio-chemical characteristics.

6.2. Solvent recovery/Aqueous phase recycle

Reuse/recycle of the aqueous phase is one branch that could be studied in detail in future studies. As discussed previously in the report, reusing the aqueous phase in new HTL operation could offer various benefits such as eliminating the need to use fresh water, increasing the yield of the liquid biofuel, and lowering the treatment costs of wastewater. Hence future research in this domain could prove to be highly useful and lead to the development of HTL process as a whole.

6.3. Continuous HTL pilot plant

One of the major challenges of the current batch experimental setup lies on the reactor size, thus the quantity of products currently obtained hinders a complete characterization of the properties based on the industrial potential. The next step would be the development of a continuous HTL plant on a large/commercial scale. Batch type reactors are typically used industrially to produce high added-value products, which are frequently produced in small quantities. The production of fuel, which accounts for production volumes in the range of thousands of barrels per day, is most definitely not the case. Additionally, the HTL process needs to be thoroughly optimized to lower the process's energy consumption, which can only be done in a continuous configuration.

References

Akalin, M. K., Tekin, K., & Karagöz, S. (2012). Hydrothermal liquefaction of cornelian cherry stones for bio-oil production. *Bioresource Technology*, *110*, 682–687. https://doi.org/10.1016/j.biortech.2012.01.136

Akhtar, J., & Amin, N. A. S. (2011). A review on process conditions for optimum bio-oil yield in hydrothermal liquefaction of biomass. *Renewable and Sustainable Energy Reviews*, *15*(3), 1615–1624. https://doi.org/10.1016/j.rser.2010.11.054

Alburquerque, J. A., Gonzálvez, J., García, D., & Cegarra, J. (2004). Agrochemical characterisation of "alperujo", a solid by-product of the two-phase centrifugation method for olive oil extraction. *Bioresource Technology*, *91*(2), 195–200. https://doi.org/10.1016/S0960-8524(03)00177-9

Anastasakis, K., Biller, P., Madsen, R. B., Glasius, M., & Johannsen, I. (2018). Continuous Hydrothermal Liquefaction of Biomass in a Novel Pilot Plant with Heat Recovery and Hydraulic Oscillation. *Energies*, *11*(10), 1–23. https://doi.org/10.3390/en11102695

Arisanti, R. (2018). Study of the Effect of Proximate, Ultimate, and Calorific Value Analysis on Methane Gas Emission (CH4) on Combustion of Coal for Sustainable Environment. *Science and Technology Indonesia*, *3*(2), 100–106. https://doi.org/10.26554/sti.2018.3.2.100-106

Beims, R. F., Hu, Y., Shui, H., & Xu, C. (Charles). (2020). Hydrothermal liquefaction of biomass to fuels and value-added chemicals: Products applications and challenges to develop large-scale operations. *Biomass and Bioenergy*, *135*(July 2019), 105510. https://doi.org/10.1016/j.biombioe.2020.105510

Bhattacharya, S. (2021). *74955 @ www.intechopen.com*. https://www.intechopen.com/chapters/74955

Biller, P., Riley, R., & Ross, A. B. (2011). Catalytic hydrothermal processing of microalgae: Decomposition and upgrading of lipids. *Bioresource Technology*, *102*(7), 4841–4848. https://doi.org/10.1016/j.biortech.2010.12.113

Bower, K. M. (2022). *design-of-experiments @ asq.org*. https://asq.org/quality-resources/design-of-experiments

British Petroleum. (2021). *BP Statistical Review of World Energy*. https://www.bp.com/content/dam/bp/business-sites/en/global/corporate/pdfs/energy-economics/statistical-review/bp-stats-review-2019-full-report.pdf

Cabrera, D. V., & Labatut, R. A. (2021). Outlook and challenges for recovering energy and water from complex organic waste using hydrothermal liquefaction. *Sustainable Energy and Fuels*, *5*(8), 2201–2227. https://doi.org/10.1039/d0se01857k

Cao, L., Zhang, C., Chen, H., Tsang, D. C. W., Luo, G., Zhang, S., & Chen, J. (2017). Hydrothermal liquefaction of agricultural and forestry wastes: state-of-the-art review and future prospects. *Bioresource Technology*, *245*(August), 1184–1193. https://doi.org/10.1016/j.biortech.2017.08.196

Cardoza, D., Romero, I., Martínez, T., Ruiz, E., Gallego, F. J., López-Linares, J. C., Manzanares, P., & Castro, E. (2021). Location of biorefineries based on olive-derived biomass in andalusia, spain. *Energies*, *14*(11), 1–16. https://doi.org/10.3390/en14113052

Castello, D., Pedersen, T. H., & Rosendahl, L. A. (2018). Continuous hydrothermal liquefaction of biomass: A critical review. *Energies*, *11*(11). https://doi.org/10.3390/en11113165

Cayuela, M. L., Sánchez-Monedero, M. A., Roig, A., Hanley, K., Enders, A., & Lehmann, J. (2013). Biochar and denitrification in soils: when, how much and why does biochar reduce N2O emissions? *Scientific Reports*, *3*(1), 1732.

https://doi.org/10.1038/srep01732
Che, F., Sarantopoulos, I., Tsoutsos, T., & Gekas, V. (2012). Exploring a promising feedstock for biodiesel production in Mediterranean countries: A study on free fatty acid esterification of olive pomace oil. *Biomass and Bioenergy*, *36*, 427–431. https://doi.org/10.1016/j.biombioe.2011.10.005
Chem Europe. (2022). *Higher_heating_value @ www.chemeurope.com*. https://www.chemeurope.com/en/encyclopedia/Higher_heating_value.html
Clemente, J. S., Beauchemin, S., Thibault, Y., MacKinnon, T., & Smith, D. (2018). Differentiating Inorganics in Biochars Produced at Commercial Scale Using Principal Component Analysis. *ACS Omega*, *3*(6), 6931–6944. https://doi.org/10.1021/acsomega.8b00523
De Filippis, P., De Caprariis, B., Scarsella, M., Petrullo, A., & Verdone, N. (2016). Biocrude production by hydrothermal liquefaction of olive residue. *International Journal of Sustainable Development and Planning*, *11*(5), 700–707. https://doi.org/10.2495/SDP-V11-N5-700-707
de Jong, W. (2015). Biomass composition, properties, and characterization". In: Biomass as a sustainable energy source for the future. In *Syria Studies* (Vol. 7, Issue 1). https://www.researchgate.net/publication/269107473_What_is_governance/link/548173090cf22525dcb61443/download%0Ahttp://www.econ.upf.edu/~reynal/Civil wars_12December2010.pdf%0Ahttps://think-asia.org/handle/11540/8282%0Ahttps://www.jstor.org/stable/41857625
Design Expert. (2022). *Design Expert, "Version 7.0.0. Stat-Ease," Design Expert Inc., Minneapolis, 2005.*
EBC, H. (2012). European biochar certificate–guidelines for a sustainable production of biochar. *European Biochar Fondation (EBC): Arbaz, Switzerland*.
Elliott, D. C., Biller, P., Ross, A. B., Schmidt, A. J., & Jones, S. B. (2015). Hydrothermal liquefaction of biomass: Developments from batch to continuous process. *Bioresource Technology*, *178*, 147–156. https://doi.org/10.1016/j.biortech.2014.09.132
Evcil, T., Tekin, K., Ucar, S., & Karagoz, S. (2021). Hydrothermal liquefaction of olive oil residues. *Sustainable Chemistry and Pharmacy*, *22*(March). https://doi.org/10.1016/j.scp.2021.100476
F.J. Stevenson, & M.A. Cole. (1999). *Cycles of Soils: Carbon, Nitrogen, Phosphorus, Sulfur, Micronutrients*.
Garcìa Martìn, J. F., Cuevas, M., Feng, C., Mateos, P. Á., & Torres, M. (2020). Energetic Valorisation of Olive Biomass : Olive-Tree. *Processes*, *Figure 1*.
Gaskin, J. W., Steiner, C., Harris, K., Das, K. C., & Bibens, B. (2008). Effect of low-temperature pyrolysis conditions on biochar for agricultural use. *Transactions of the ASABE*, *51*(6), 2061–2069.
Gollakota, A. R. K., Kishore, N., & Gu, S. (2018). A review on hydrothermal liquefaction of biomass. *Renewable and Sustainable Energy Reviews*, *81*(June 2017), 1378–1392. https://doi.org/10.1016/j.rser.2017.05.178
Gordon, M., & Weber, M. (2021). *Global energy demand to grow 47% by 2050, with oil still top source: US EIA*. https://www.spglobal.com/commodityinsights/en/market-insights/latest-news/oil/100621-global-energy-demand-to-grow-47-by-2050-with-oil-still-top-source-us-eia
Guo, J., & Chen, B. (2014). Insights on the Molecular Mechanism for the Recalcitrance of Biochars: Interactive Effects of Carbon and Silicon Components. *Environmental Science & Technology*, *48*(16), 9103–9112. https://doi.org/10.1021/es405647e
Haverly, M. R., Ghosh, A., & Brown, R. C. (2020). The effect of moisture on hydrocarbon-based solvent liquefaction of pine, cellulose and lignin. *Journal of Analytical and*

Applied Pyrolysis, *146*(December 2019), 104758. https://doi.org/10.1016/j.jaap.2019.104758

Hernández, D., Astudillo, L., Gutiérrez, M., Tenreiro, C., Retamal, C., & Rojas, C. (2014). Biodiesel production from an industrial residue: Alperujo. *Industrial Crops and Products*, *52*, 495–498. https://doi.org/10.1016/j.indcrop.2013.10.051

IEA. (2022). *bioenergy @ www.iea.org*. https://www.iea.org/fuels-and-technologies/bioenergy

IEA Bioenergy. (2017). *Biofuels for the marine shipping sector*. 86. http://task39.sites.olt.ubc.ca/files/2013/05/Marine-biofuel-report-final-Oct-2017.pdf%0Ahttps://www.ieabioenergy.com/wp-content/uploads/2018/02/Marine-biofuel-report-final-Oct-2017.pdf

Kim, P., Johnson, A., Edmunds, C. W., Radosevich, M., Vogt, F., Rials, T. G., & Labbé, N. (2011). Surface Functionality and Carbon Structures in Lignocellulosic-Derived Biochars Produced by Fast Pyrolysis. *Energy & Fuels*, *25*(10), 4693–4703. https://doi.org/10.1021/ef200915s

Leng, L., Xu, S., Liu, R., Yu, T., Zhuo, X., Leng, S., Xiong, Q., & Huang, H. (2020). Nitrogen containing functional groups of biochar: An overview. *Bioresource Technology*, *298*, 122286. https://doi.org/https://doi.org/10.1016/j.biortech.2019.122286

Licella Pty Ltd. (2022). *22a2760bd5174b3cc2aba90e106cdf9afaa5a177 @ www.licella.com*. https://www.licella.com

Madsen, R. B., & Glasius, M. (2019). How Do Hydrothermal Liquefaction Conditions and Feedstock Type Influence Product Distribution and Elemental Composition? *Industrial and Engineering Chemistry Research*, *58*(37), 17583–17600. https://doi.org/10.1021/acs.iecr.9b02337

Mathanker, A., Das, S., Pudasainee, D., Khan, M., Kumar, A., & Gupta, R. (2021). A review of hydrothermal liquefaction of biomass for biofuels production with a special focus on the effect of process parameters, co-solvents and extraction solvents. *Energies*, *14*(16). https://doi.org/10.3390/en14164916

Minitab, L. (2022). *2d5b6d7a2d1c1acbd17103e649bb7bf1f3928e60 @ support.minitab.com*. https://support.minitab.com/en-us/minitab/18/help-and-how-to/modeling-statistics/doe/supporting-topics/response-surface-designs/response-surface-central-composite-and-box-behnken-designs/

NIST. (2012). *NIST X-ray Photoelectron Spectroscopy (XPS) Database Main Search Menu*. https://srdata.nist.gov/xps/main_search_menu.aspx

Osman, A. I., Mehta, N., Elgarahy, A. M., Al-Hinai, A., Al-Muhtaseb, A. H., & Rooney, D. W. (2021). Conversion of biomass to biofuels and life cycle assessment: a review. In *Environmental Chemistry Letters* (Vol. 19, Issue 6). Springer International Publishing. https://doi.org/10.1007/s10311-021-01273-0

Parr Instument Company. (2015). *c7058832136c7966e1d0c2c0d753b2f5032f21b8 @ www.parrinst.com*. https://www.parrinst.com

Paul van der Heide. (2011). Spectral Interpretation. In *X-Ray Photoelectron Spectroscopy: An Introduction to Principles and Practices*.

Ragauskas, A., & Jindal, M. K. (n.d.). *CONDITIONS ON HYDROTHERMAL LIQUEFACTION*. https://d1wqtxts1xzle7.cloudfront.net/47084713/ijcbs.org_79-with-cover-page-v2.pdf?Expires=1656322731&Signature=Rce2bnhas0~fzzptVAPBrG~mXgv5PI-9rr14MJy~nPXaEm6N0I6453iKtBK2WpiGcfuZ3S4g3H7GIBvnbZtLh4K~0l2WsgECDxYLNpugHWvU4JhVc5SNAAmBGkITwC9OUU462KzfQ878Yrs

Ribeiro, T. B., Oliveira, A. L., Costa, C., Nunes, J., Vicente, A. A., & Pintado, M. (2020). Total and sustainable valorisation of olive pomace using a fractionation approach.

Applied Sciences, *10*(19), 6785.
Scarsella, M., de Caprariis, B., Damizia, M., & De Filippis, P. (2020). Heterogeneous catalysts for hydrothermal liquefaction of lignocellulosic biomass: A review. *Biomass and Bioenergy*, *140*, 105662. https://doi.org/https://doi.org/10.1016/j.biombioe.2020.105662
Tekin, K., & Karagöz, S. (2013). Non-catalytic and catalytic hydrothermal liquefaction of biomass. *Research on Chemical Intermediates*, *39*(2), 485–498. https://doi.org/10.1007/s11164-012-0572-3
The University of Melbourne. (2022). *scanning-electron-microscopyenergy-dispersive-spectroscopy @ arts.unimelb.edu.au*. https://arts.unimelb.edu.au/grimwade-centre-for-cultural-materials-conservation/conservation-services/services-support/technical-analysis/scanning-electron-microscopyenergy-dispersive-spectroscopy
ThermoFisher Scientific. (2022). *xps-technology @ www.thermofisher.com*. https://www.thermofisher.com/nl/en/home/materials-science/xps-technology.html
Toor, S. S., Rosendahl, L., & Rudolf, A. (2011). Hydrothermal liquefaction of biomass: A review of subcritical water technologies. *Energy*, *36*(5), 2328–2342. https://doi.org/10.1016/j.energy.2011.03.013
Verma, M., Godbout, S., Brar, S. K., Solomatnikova, O., Lemay, S. P., & Larouche, J. P. (2012). Biofuels production from biomass by thermochemical conversion technologies. *International Journal of Chemical Engineering*, *2012*. https://doi.org/10.1155/2012/542426
Zhu, Z., Rosendahl, L., Toor, S. S., & Chen, G. (2018). Optimizing the conditions for hydrothermal liquefaction of barley straw for bio-crude oil production using response surface methodology. *Science of the Total Environment*, *630*, 560–569. https://doi.org/10.1016/j.scitotenv.2018.02.194

Supplementary Information

XRF data

	wt. %			
Compound	COP raw	COP-250°C	COP-330°C	COP-340°C
C	97.254	98.215	98.019	98.206
K2O	1.095	0.267	0.139	0.121
CaO	0.385	0.39	0.44	0.4
SiO2	0.304	0.293	0.253	0.255
P2O5	0.179	0.279	0.421	0.33
SO3	0.125	0.129	0.17	0.162
Cl	0.178	0.126	0.103	0.068
Al2O3	0.122	0.091	0.119	0.093
MgO	0.151	0.078	0.088	0.065
CuO	0.132		0.003	
Na2O	0.051	0.015		
Fe2O3	0.024	0.045	0.065	0.06
Ni		0.054	0.13	0.181
Mo		0.016	0.041	0.05
ZnO		0.002		0.002
TiO2			0.01	0.007
SrO	0.001	0.001	0.001	

Division of Tasks

This work was possible with the support from various colleagues, collaborators, and professionals at the faculty of 3mE of TU Delft, The Netherlands. In order to acknowledge their contributions, the following table containing the task division is provided.

Task	Name(s)
SEM-EDS analyses	Luis Cutz
XRD and XRF analyses	Ruud Hendrikx
Conceptualization	Sarvesh Misar and Luis Cutz
HTL experiments	Sarvesh Misar
HHV determination	Sarvesh Misar
TGA	Luis Cutz
GC-MS and Ultimate analysis	Wenze Guo University of Groningen
Proximate analysis	Sarvesh Misar and Luis Cutz
Data analysis and interpretation	Sarvesh Misar, Luis Cutz, Hector Maldonado
Final report writing	Sarvesh Misar
Final report editing	Luis Cutz and Sarvesh Misar

Appendix A: Details of the Screening & Full Experimental Campaign

In this appendix, details of the screening campaign and full experimental campaign are provided.

Table A.1 shows the average mass yields for each product obtained from HTL of COP along with their standard deviations (in the brackets) for the screening campaign.

Table A.1: Summary of results from the screening campaign

Test	Factors		Yields (wt. %)			
	Temperature (°C)	Time (min)	Bio-oil	Biochar	Aqueous Phase	Gas & Losses
1	250	15	22.54 (3.02)	40.30 (2.41)	22.52 (4.74)	14.66 (5.35)
2	270	15	23.87 (0.25)	36.74 (5.94)	21.92 (1.19)	17.49 (7.39)
3	300	15	27.63 (0.22)	28.71 (0.57)	22.36 (2.83)	21.31 (3.61)
4	330	15	29.00 (2.23)	27.63 (1.09)	19.34 (0.81)	24.04 (4.14)
5	340	15	23.12 (0.37)	27.47 (0.69)	17.69 (1.26)	31.73 (1.57)

Table A.2 shows the chosen temperature, residence time, and catalyst loading for each experiment based on the central composite design (CCD) approach used for designing the experiments.

Table A.2: Chosen design of experiments for both the CCD-COP and CCD-OTPW campaigns

Run	Factor 1: Temperature (deg C)	Factor 2: Residence time (min)	Factor 3: Catalyst (wt%)
1	300	15	5
2	300	60	5
3	300	5	5
4	270	10	7.5
5	330	10	2.5
6	300	15	5
7	270	30	2.5
8	340	15	5
9	330	30	2.5
10	300	15	10
11	300	15	5
12	330	30	7.5
13	300	15	0
14	300	15	5
15	300	15	5

16	300	15	5
17	270	30	7.5
18	250	15	5
19	270	10	2.5
20	330	10	7.5

Table A.3: Detailed results obtained from the CCD-COP experimental campaign

Run	Operating Condition	Response 1: Bio-oil Yield (%)	Response 2: Bio-Char Yield (%)	Response 3: Aqueous phase Yield (%)	Response 4: Gas Yield (%)
1	300-15-5%	42.26	6.84	21.56	28.88
2	300-60-5%	41.56	9.42	19.87	29.15
3	300-5-5%	43.51	8.62	21.73	26.13
4	270-10-7.5%	37.29	20.31	24.22	18.17
5	330-10-2.5%	37.38	26.13	18.85	17.64
6	300-15-5%	41.25	23.29	22.45	13.02
7	270-30-2.5%	31.12	31.91	26.36	10.62
8	340-15-5%	41.58	16.71	16.76	24.95
9	330-30-2.5%	38.4	19.82	19.87	21.91
10	300-15-10%	47.82	11.29	17.16	23.73
11	300-15-5%	40.58	22.36	20.89	16.17
12	330-30-7.5%	51.96	16.49	16.98	14.57
13	300-15-0%	27.78	29.11	24.36	18.75
14	300-15-5%	40.36	20.53	20.89	18.22
15	300-15-5%	42.62	8.58	20.85	27.95
16	300-15-5%	41.73	15.42	21.96	20.88
17	270-30-7.5%	38.45	26.22	22.22	13.11
18	250-15-5%	22.58	39.96	26.4	11.06
19	270-10-2.5%	32.98	30.8	24.62	11.6
20	330-10-7.5%	49.69	18.49	15.51	16.31

Table A.4: Mathematical model developed on the completion of the detailed CCD-COP experimental campaign

Bio-oil
-295.7 + 2.145*X1 - 0.353*Y1 - 4.19*Y2 - 0.003531*X1**2 - 0.00085*Y1**2- 0.1265*Y2**2 + 0.00112*X1*Y1 + 0.02372*X1*Y2 + 0.0161*Y1*Y2
Biochar
676 - 4.21*X1 +1.54*Y1 - 7.21*Y2 + 0.00686*X1**2 - 0.00681*Y1**2 + 0.215*Y2**2 - 0.00475*X1*Y1 + 0.0087*X1*Y2 + 0.0499*Y1*Y2
Aqueous phase
32.7 + 0.045*X1 - 0.192*Y1 + 0.71*Y2 - 0.000265*X1**2 - 0.001449*Y1**2 - 0.0309*Y2**2 + 0.001061*X1*Y1 - 0.00282*X1*Y2 - 0.0106*Y1*Y2
Gaseous phase
-311 + 2.01*X1 - 1.00*Y1 + 10.65*Y2 - 0.00303*X1**2 + 0.00925*Y1**2 - 0.056*Y2**2 + 0.00256*X1*Y1 - 0.0296*X1*Y2 - 0.0555*Y1*Y2

Table A.5: Detailed results obtained from the CCD-OTPW experimental campaign

Run	Operating Condition	Response 1: Bio-oil Yield (%)	Response 2: Bio-Char Yield (%)	Response 3: Aqueous phase Yield (%)	Response 4: Gas Yield (%)
1	300-15-5%	48.52	11.82	12.12	27.54
2	300-60-5%				
3	300-5-5%	45.28	12.11	16.64	25.97
4	270-10-7.5%	43.37	19.88	16.39	20.36
5	330-10-2.5%	47.02	11.56	22.67	18.75
6	300-15-5%				
7	270-30-2.5%				
8	340-15-5%				
9	330-30-2.5%				
10	300-15-10%				
11	300-15-5%	47.72	12.36	13.03	26.89
12	330-30-7.5%	56.3	9.87	4.82	29.01
13	300-15-0%	38.4	28.11	14.26	19.23
14	300-15-5%				
15	300-15-5%				
16	300-15-5%				
17	270-30-7.5%				
18	250-15-5%	25.76	32.47	31.09	10.68
19	270-10-2.5%	40.262	29.35	17.78	12.6
20	330-10-7.5%				

Appendix B: Analysis of Response Surface Methodology

Response Surface Regression: Response 1: Bio-oil Yield (%) versus Factor 1: Temperature (deg C), Factor 2: Residence time (min), Factor 3: Catalyst (wt%)

Coded Coefficients

Term	Coef	SE Coef	T-Value
Constant	41.68	1.19	34.99
Factor 1: Temperature (deg C)	9.75	1.73	5.64
Factor 2: Residence time (min)	0.11	1.12	0.10
Factor 3: Catalyst (wt%)	10.32	2.28	4.52
Factor 1: Temperature (deg C)*Factor 1: Temperature (deg C)	-7.15	1.47	-4.88
Factor 2: Residence time (min)*Factor 2: Residence time (min)	-0.64	1.71	-0.37
Factor 3: Catalyst (wt%)*Factor 3: Catalyst (wt%)	-3.16	1.61	-1.97
Factor 1: Temperature (deg C)*Factor 2: Residence time (min)	1.39	2.84	0.49
Factor 1: Temperature (deg C)*Factor 3: Catalyst (wt%)	5.34	2.15	2.48
Factor 2: Residence time (min)*Factor 3: Catalyst (wt%)	2.22	3.72	0.60

Term	P-Value	VIF
Constant	0.000	
Factor 1: Temperature (deg C)	0.000	4.05
Factor 2: Residence time (min)	0.924	1.14
Factor 3: Catalyst (wt%)	0.001	5.06
Factor 1: Temperature (deg C)*Factor 1: Temperature (deg C)	0.001	1.14
Factor 2: Residence time (min)*Factor 2: Residence time (min)	0.717	1.14
Factor 3: Catalyst (wt%)*Factor 3: Catalyst (wt%)	0.078	1.07
Factor 1: Temperature (deg C)*Factor 2: Residence time (min)	0.636	4.05
Factor 1: Temperature (deg C)*Factor 3: Catalyst (wt%)	0.033	1.06
Factor 2: Residence time (min)*Factor 3: Catalyst (wt%)	0.565	5.00

Model Summary

S	R-sq	R-sq(adj)	R-sq(pred)
2.02946	95.57%	91.59%	0.00%

Analysis of Variance

Source	DF	Adj SS	Adj MS
Model	9	888.887	98.765
Linear	3	226.109	75.370
Factor 1: Temperature (deg C)	1	131.147	131.147
Factor 2: Residence time (min)	1	0.039	0.039
Factor 3: Catalyst (wt%)	1	84.184	84.184
Square	3	109.166	36.389
Factor 1: Temperature (deg C)*Factor 1: Temperature (deg C)	1	97.978	97.978
Factor 2: Residence time (min)*Factor 2: Residence time (min)	1	0.574	0.574
Factor 3: Catalyst (wt%)*Factor 3: Catalyst (wt%)	1	15.917	15.917
2-Way Interaction	3	27.757	9.252
Factor 1: Temperature (deg C)*Factor 2: Residence time (min)	1	0.984	0.984
Factor 1: Temperature (deg C)*Factor 3: Catalyst (wt%)	1	25.312	25.312
Factor 2: Residence time (min)*Factor 3: Catalyst (wt%)	1	1.462	1.462
Error	10	41.187	4.119
Lack-of-Fit	5	37.100	7.420
Pure Error	5	4.087	0.817
Total	19	930.074	

Source	F-Value	P-Value
Model	23.98	0.000
Linear	18.30	0.000
Factor 1: Temperature (deg C)	31.84	0.000
Factor 2: Residence time (min)	0.01	0.924
Factor 3: Catalyst (wt%)	20.44	0.001
Square	8.83	0.004
Factor 1: Temperature (deg C)*Factor 1: Temperature (deg C)	23.79	0.001
Factor 2: Residence time (min)*Factor 2: Residence time (min)	0.14	0.717
Factor 3: Catalyst (wt%)*Factor 3: Catalyst (wt%)	3.86	0.078
2-Way Interaction	2.25	0.145
Factor 1: Temperature (deg C)*Factor 2: Residence time (min)	0.24	0.636
Factor 1: Temperature (deg C)*Factor 3: Catalyst (wt%)	6.15	0.033
Factor 2: Residence time (min)*Factor 3: Catalyst (wt%)	0.35	0.565
Error		
Lack-of-Fit	9.08	0.015
Pure Error		
Total		

Regression Equation in Uncoded Units

Response 1: Bio-oil Yield (%) = -295.7 + 2.145 Factor 1: Temperature (deg C)
- 0.353 Factor 2: Residence time (min)
- 4.19 Factor 3: Catalyst (wt%)
- 0.003531 Factor 1: Temperature (deg C)*Factor 1: Temperature (deg C)
- 0.00085 Factor 2: Residence time (min)*Factor 2: Residence time (min)
- 0.1265 Factor 3: Catalyst (wt%)*Factor 3: Catalyst (wt%)
+ 0.00112 Factor 1: Temperature (deg C)*Factor 2: Residence time (min)
+ 0.02372 Factor 1: Temperature (deg C)*Factor 3: Catalyst (wt%)
+ 0.0161 Factor 2: Residence time (min)*Factor 3: Catalyst (wt%)

Fits and Diagnostics for Unusual Observations

Obs	Response 1: Bio-oil Yield (%)	Fit	Resid	Std Resid	
2	41.56	42.30	-0.74	-2.60	R
18	22.58	25.33	-2.75	-2.24	R

R Large residual

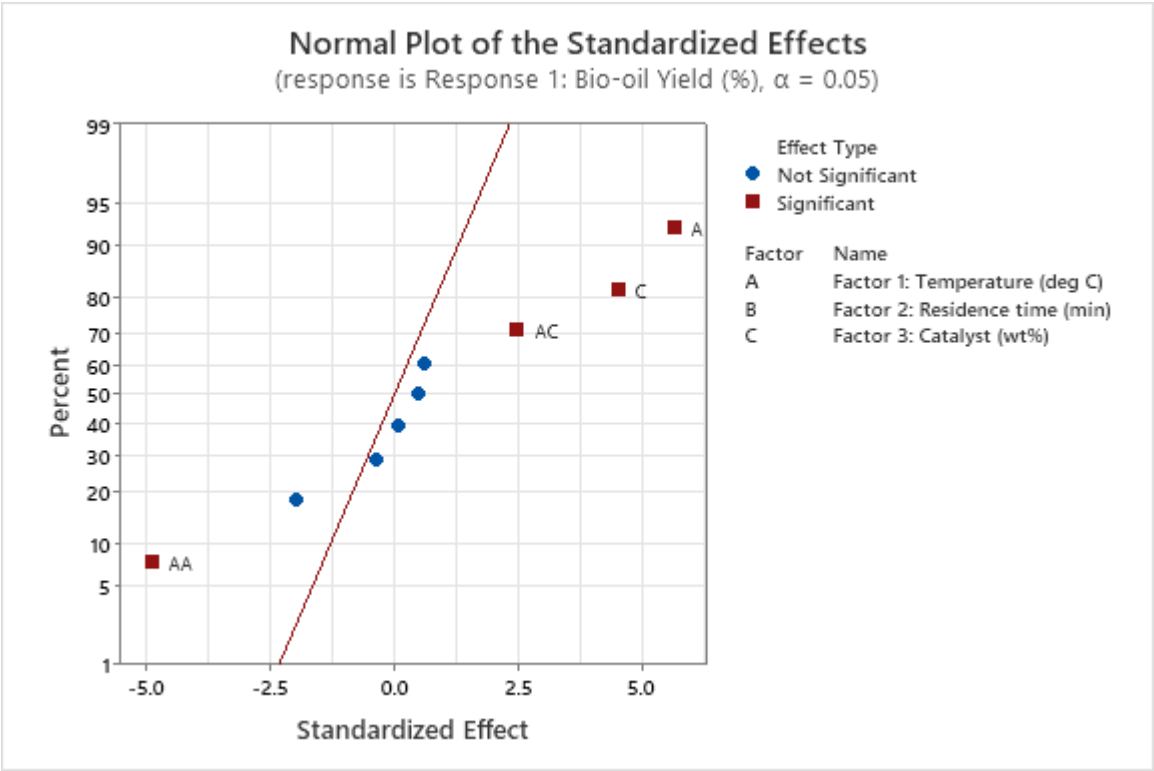
Normal Plot of the Standardized Effects
(response is Response 1: Bio-oil Yield (%), α = 0.05)
Percent
99
95
90
80
70
60
50
40
30
20
10
5
1
-5.0
-2.5
0.0
2.5
5.0
Standardized Effect
A
C
AC
AA
Effect Type
Not Significant
Significant
Factor Name
A Factor 1: Temperature (deg C)
B Factor 2: Residence time (min)
C Factor 3: Catalyst (wt%)

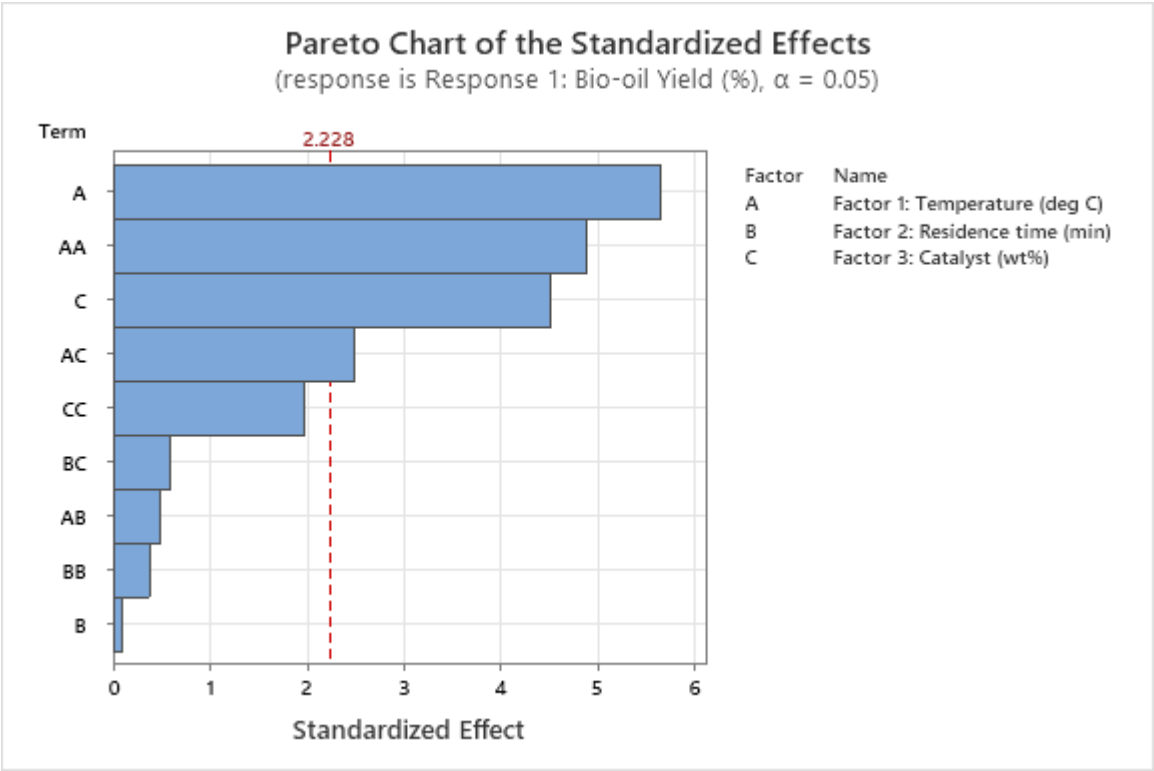
Pareto Chart of the Standardized Effects
(response is Response 1: Bio-oil Yield (%), α = 0.05)
Term
2.228
A
AA
C
AC
CC
BC
AB
BB
B
0
1
2
3
4
5
6
Standardized Effect
Factor Name
A Factor 1: Temperature (deg C)
B Factor 2: Residence time (min)
C Factor 3: Catalyst (wt%)

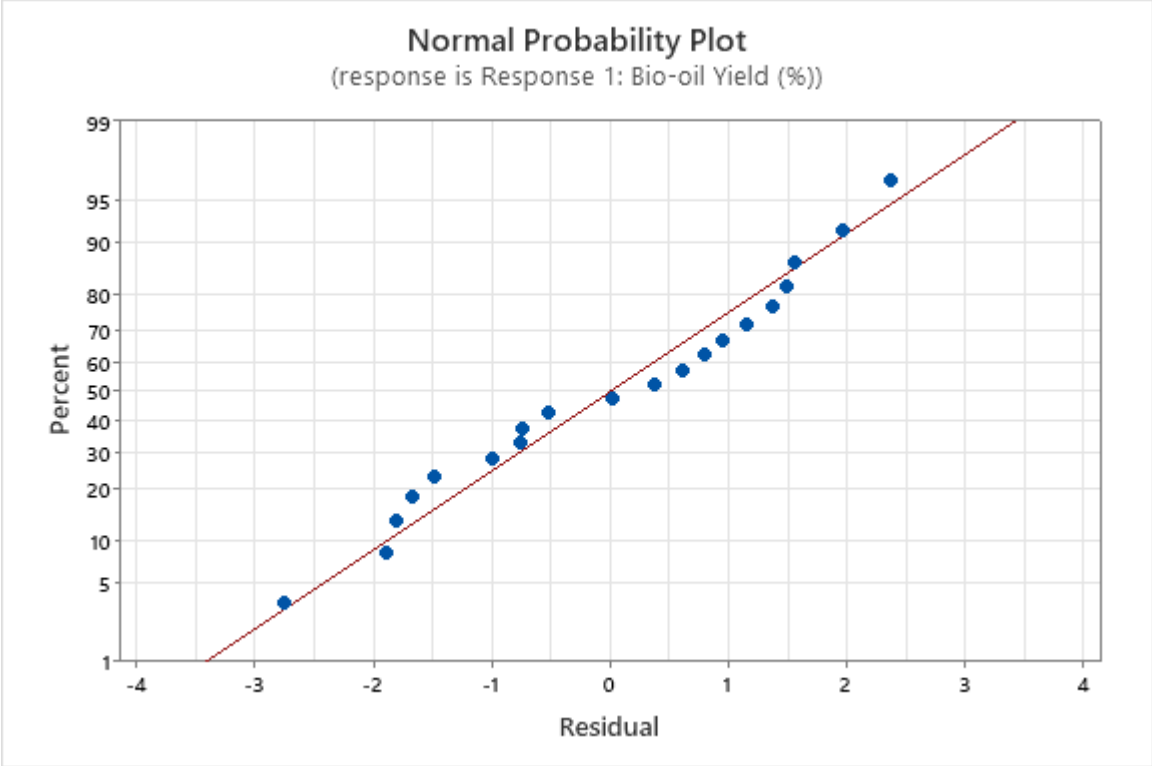
Normal Probability Plot
(response is Response 1: Bio-oil Yield (%))
Percent
99
95
90
80
70
60
50
40
30
20
10
5
1
-4
-3
-2
-1
0
1
2
3
4
Residual

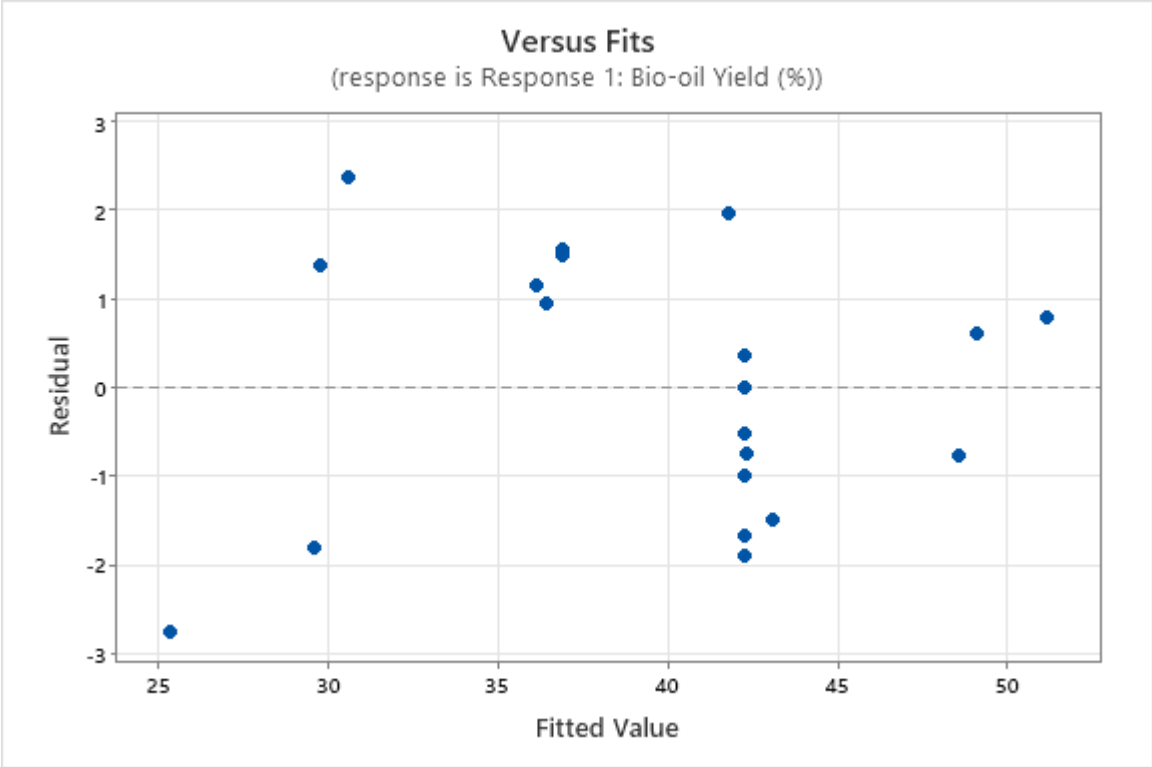
Versus Fits
(response is Response 1: Bio-oil Yield (%))
Residual
3
2
1
0
-1
-2
-3
25
30
35
40
45
50
Fitted Value

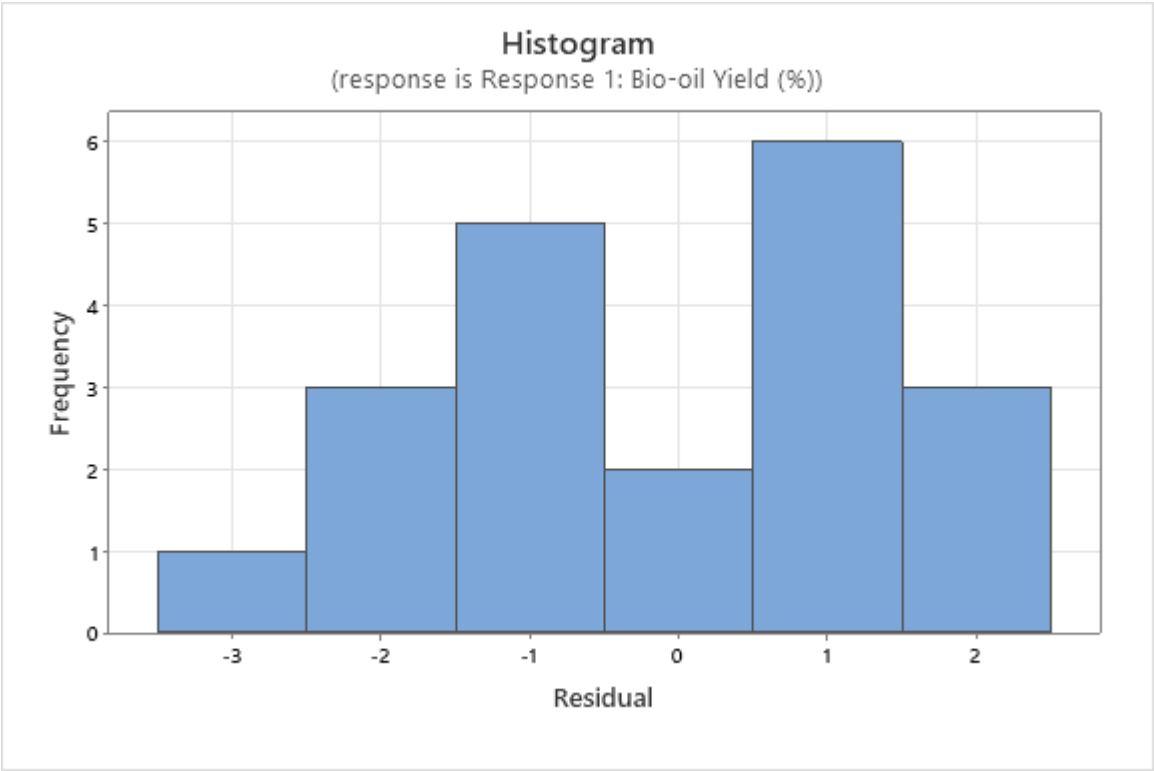
Histogram
(response is Response 1: Bio-oil Yield (%))
Frequency
0
1
2
3
4
5
6
-3
-2
-1
0
1
2
Residual

Contour Plots of Response 1: Bio-oil Yield (%)

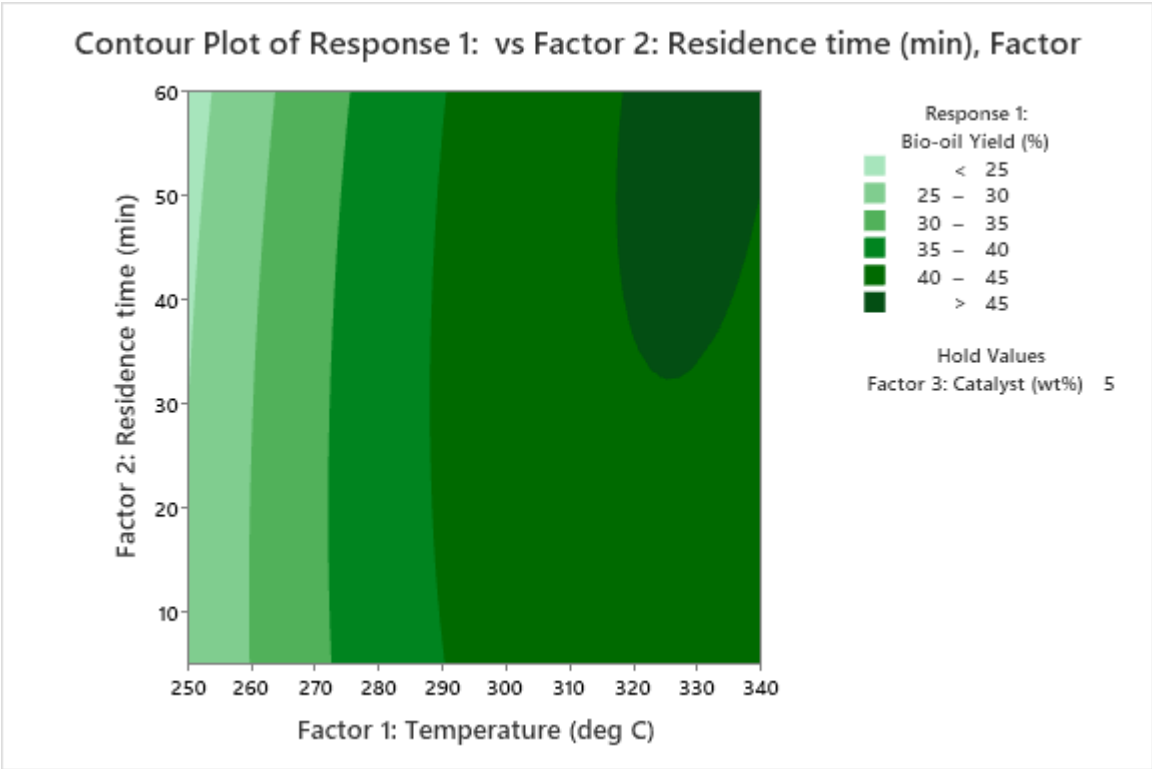

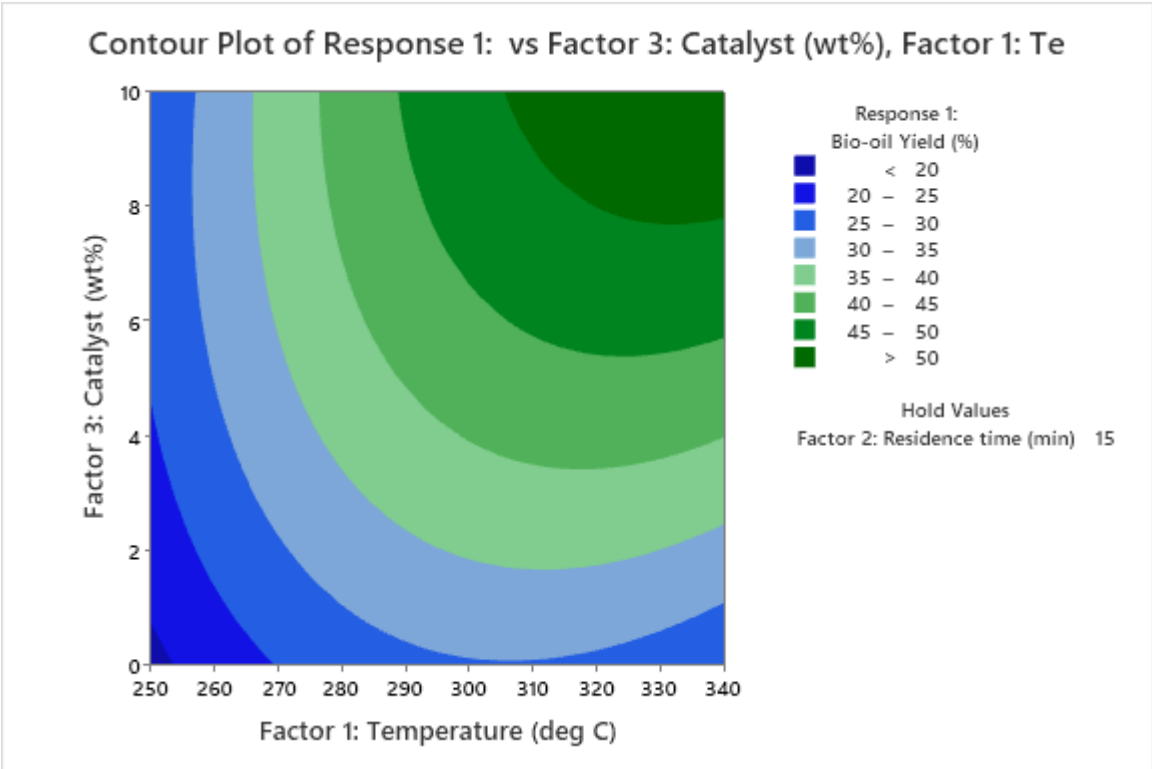

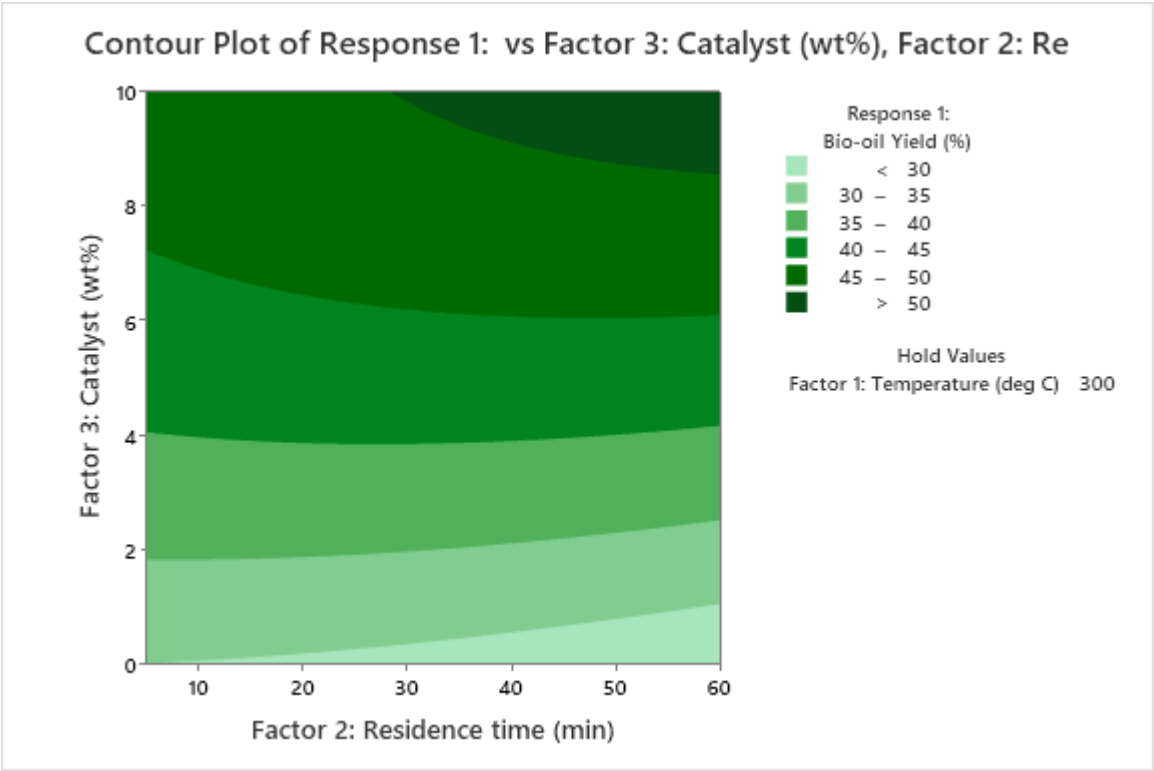
Contour Plot of Response 1: vs Factor 3: Catalyst (wt%), Factor 2: Re
Factor 3: Catalyst (wt%)
0
2
4
6
8
10
10
20
30
40
50
60
Factor 2: Residence time (min)
Response 1:
Bio-oil Yield (%)
< 30
30 – 35
35 – 40
40 – 45
45 – 50
> 50
Hold Values
Factor 1: Temperature (deg C) 300

WORKSHEET 6

Surface Plots of Response 1: Bio-oil Yield (%)

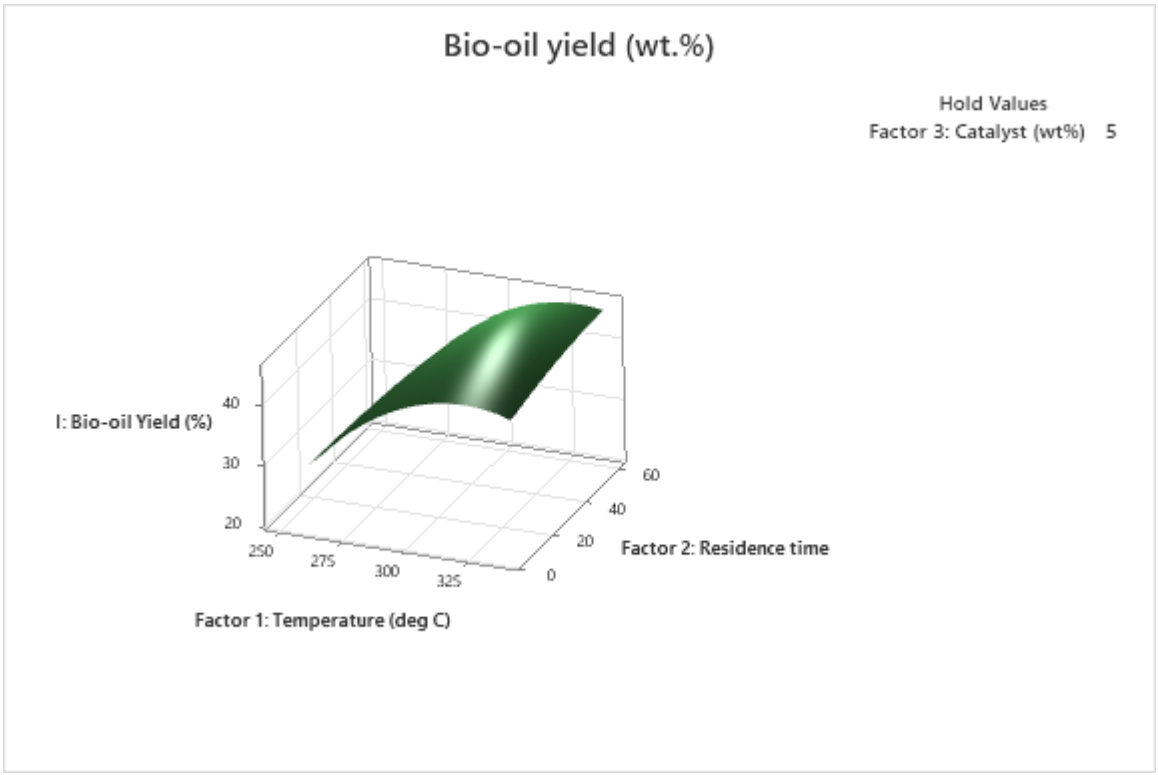

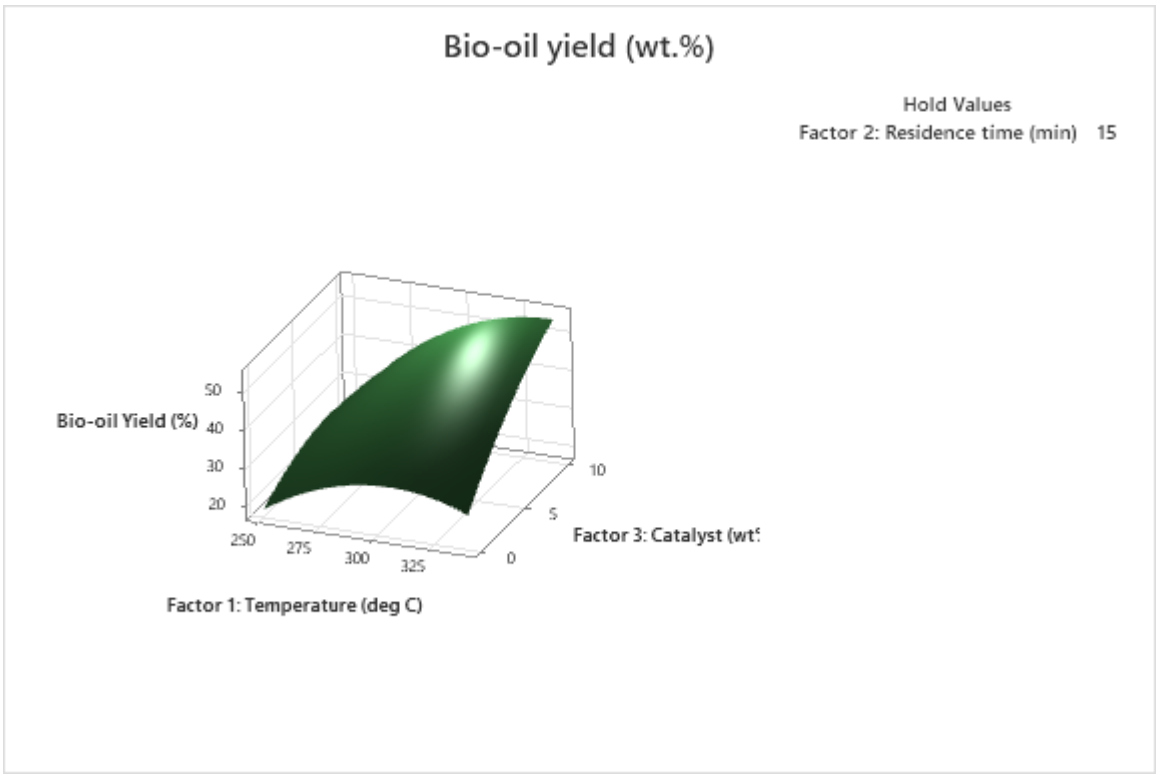

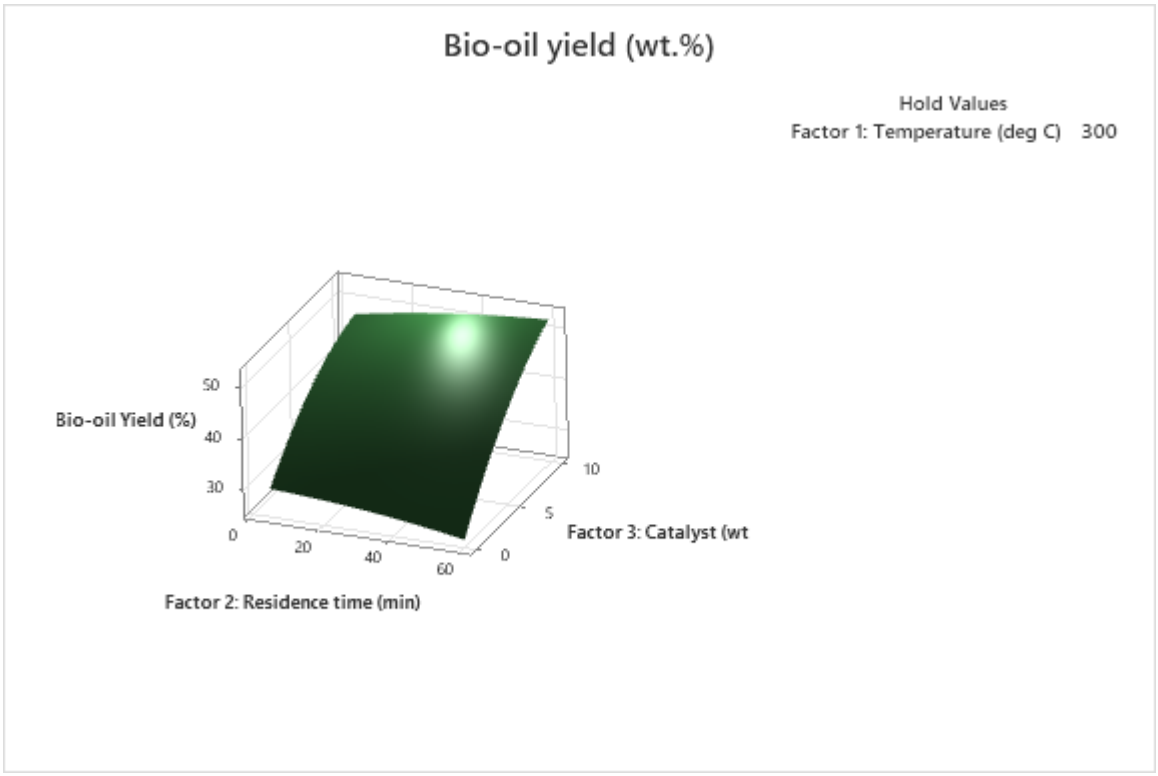

WORKSHEET 6

Surface_optimum

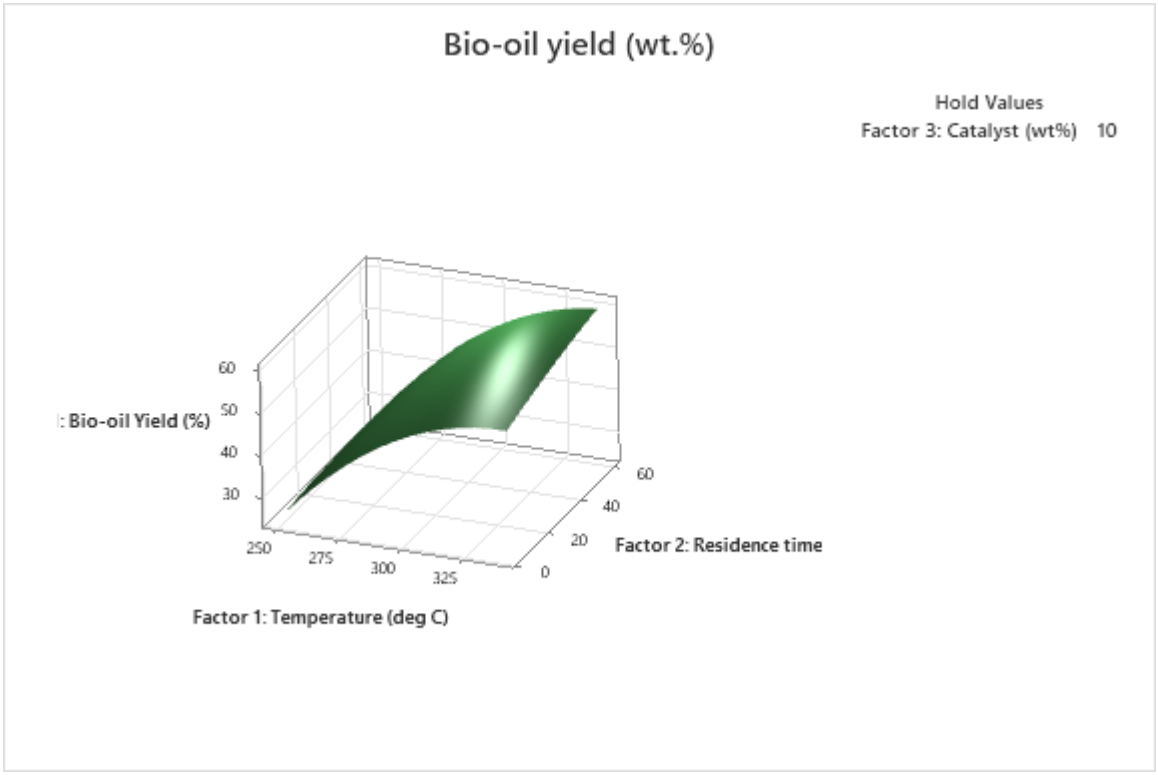

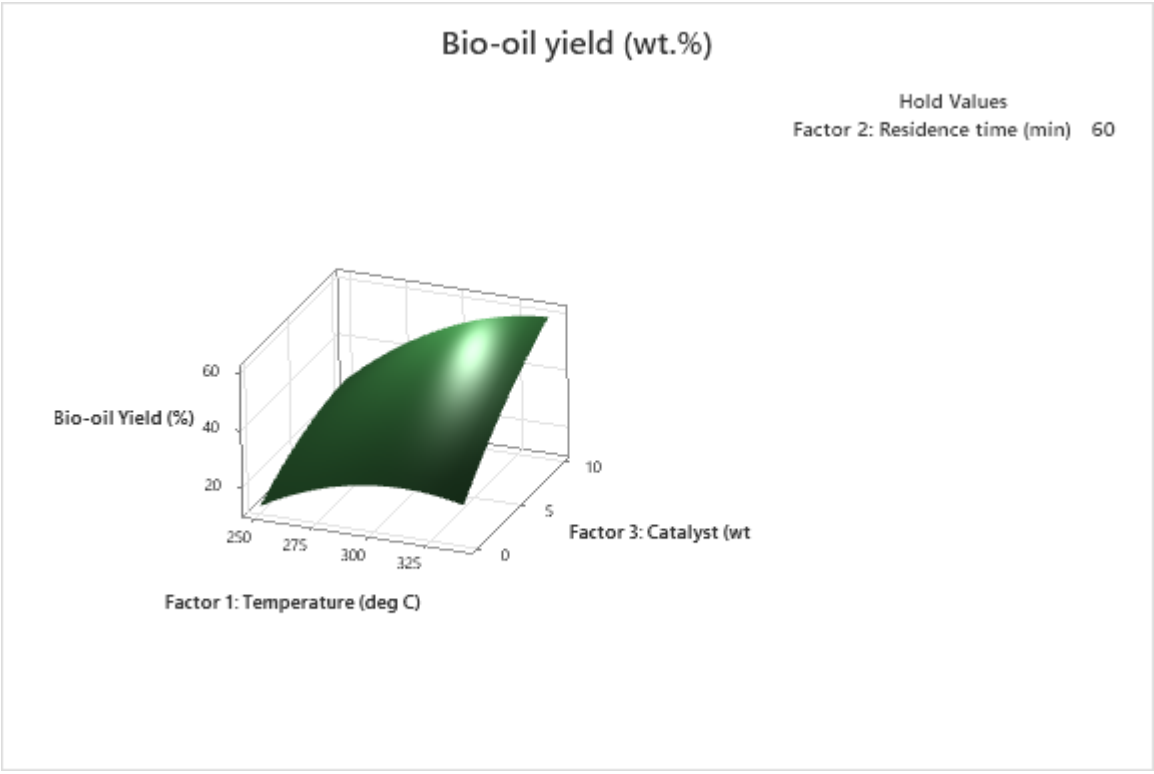
Bio-oil yield (wt.%)
Hold Values
Factor 2: Residence time (min) 60
Bio-oil Yield (%)
60
40
20
250
275
300
325
Factor 1: Temperature (deg C)
10
5
0
Factor 3: Catalyst (wt

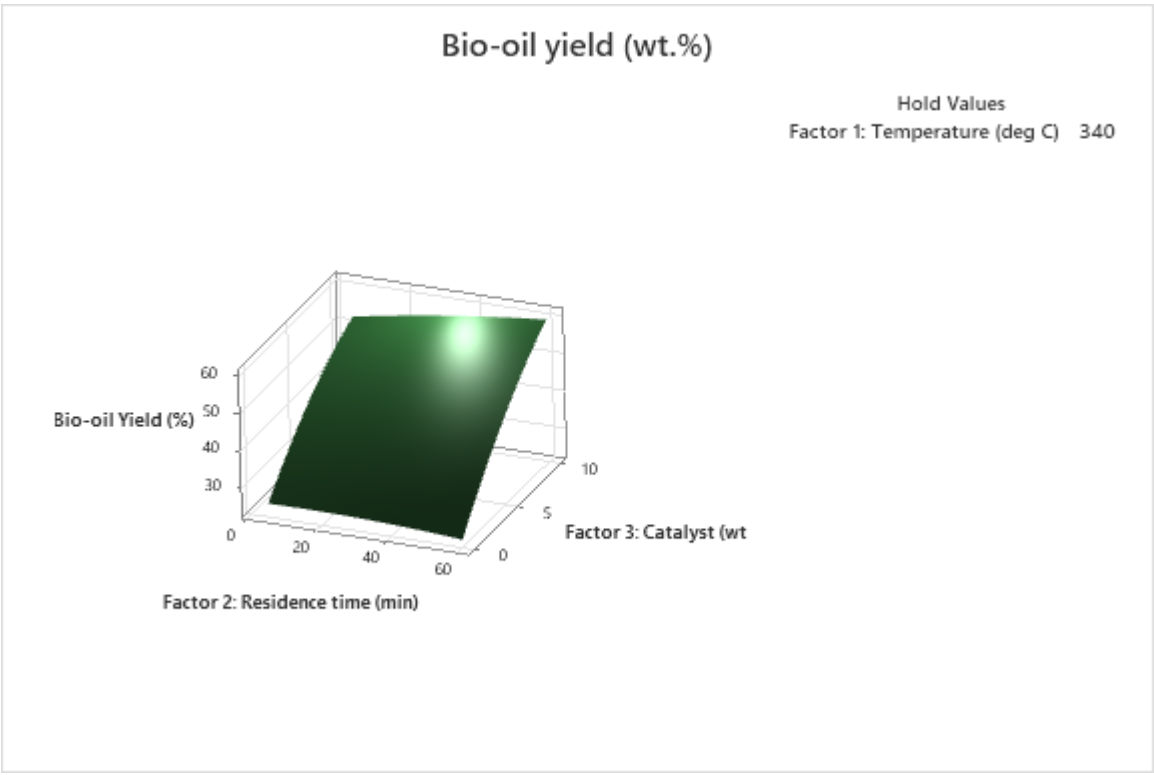
Bio-oil yield (wt.%)
Hold Values
Factor 1: Temperature (deg C) 340
Bio-oil Yield (%)
60
50
40
30
0
20
40
60
Factor 2: Residence time (min)
10
5
0
Factor 3: Catalyst (wt

WORKSHEET 6

Contour_plot_Tmax: 340 °C

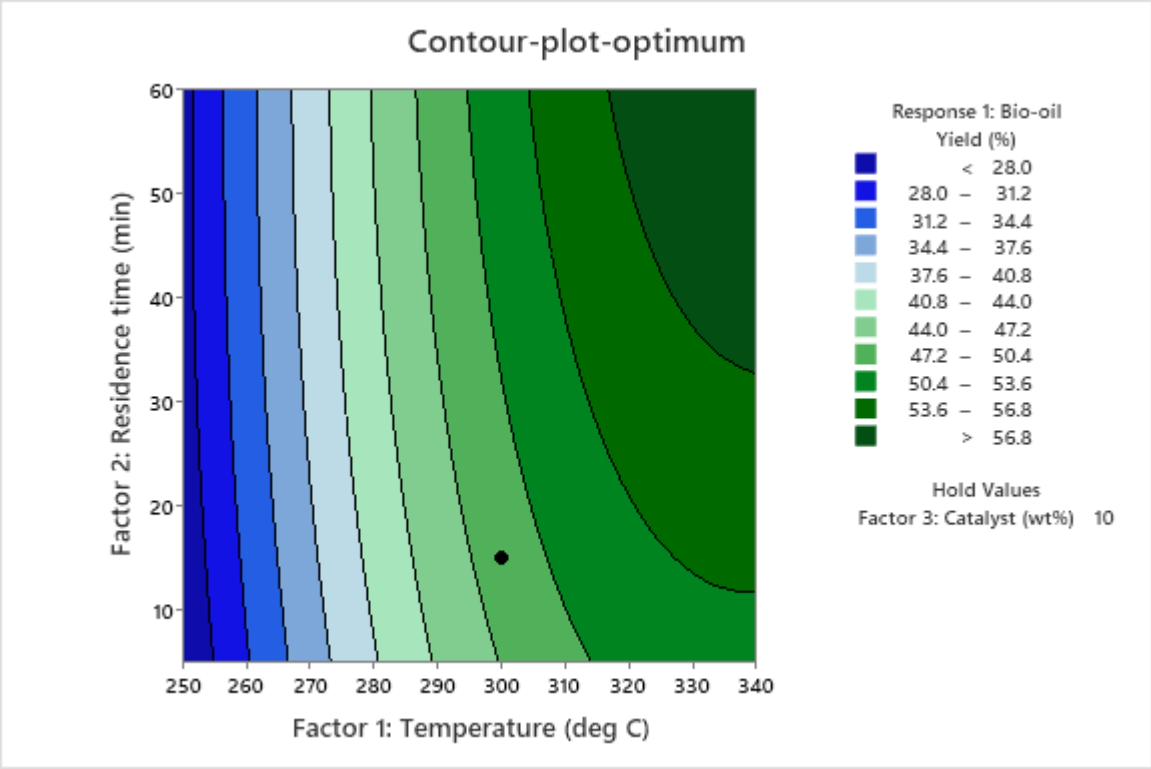

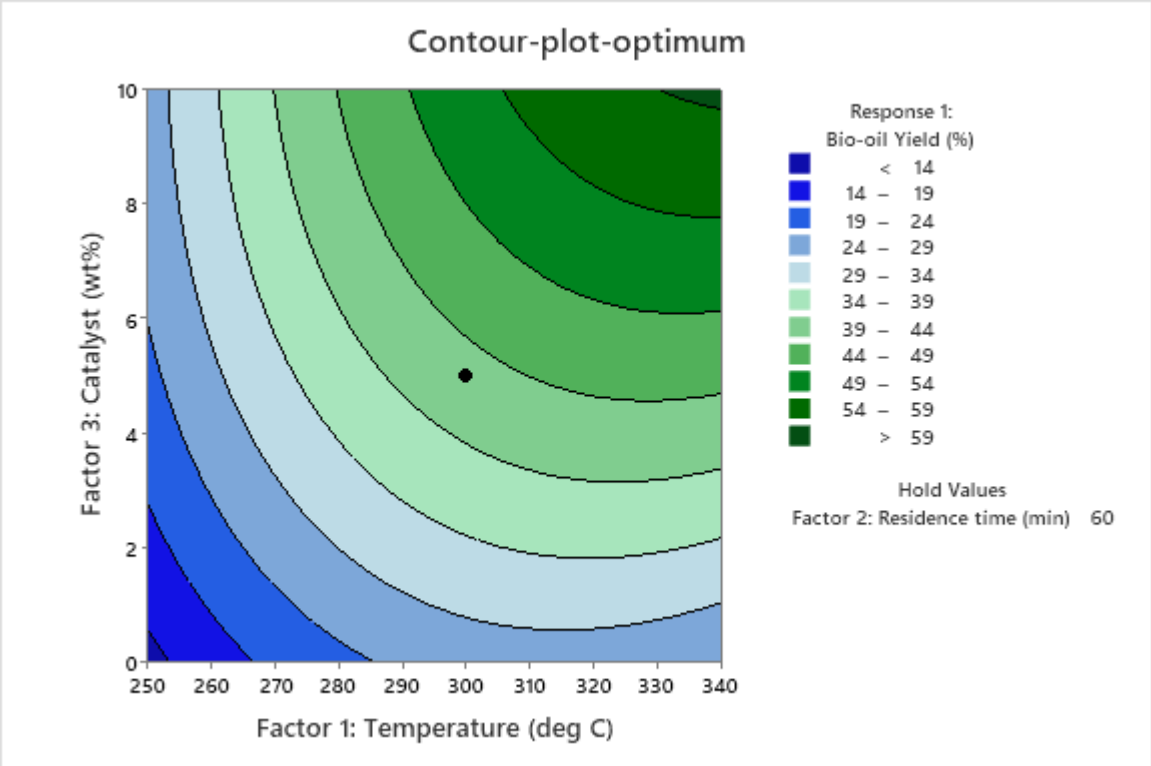

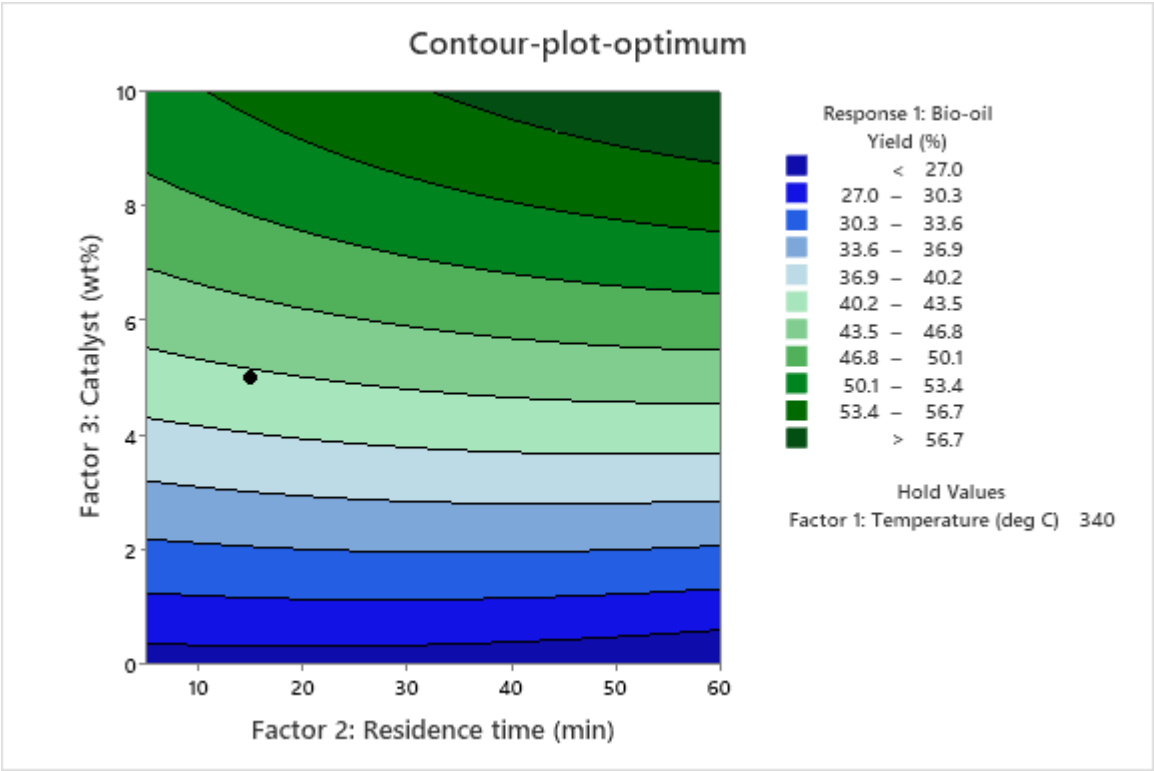
Contour-plot-optimum
Factor 3: Catalyst (wt%)
Factor 2: Residence time (min)
10
8
6
4
2
0
10
20
30
40
50
60
Response 1: Bio-oil Yield (%)
< 27.0
27.0 – 30.3
30.3 – 33.6
33.6 – 36.9
36.9 – 40.2
40.2 – 43.5
43.5 – 46.8
46.8 – 50.1
50.1 – 53.4
53.4 – 56.7
> 56.7
Hold Values
Factor 1: Temperature (deg C) 340

WORKSHEET 6

Response_optimization_T_330°C

Parameters

Response	Goal	Lower	Target	Upper	Weight	Importance
Response 1: Bio-oil Yield (%)	Maximum	22.58	51.96		5	1

Variable Ranges

Variable	Values
Factor 1: Temperature (deg C)	(250, 330)
Factor 2: Residence time (min)	(5, 60)
Factor 3: Catalyst (wt%)	(0, 10)

Starting Values

Variable	Setting
Factor 1: Temperature (deg C)	320
Factor 2: Residence time (min)	25
Factor 3: Catalyst (wt%)	8

Solution

Solution	Factor 1: Temperature (deg C)	Factor 2: Residence time (min)	Factor 3: Catalyst (wt%)	Response 1: Bio-oil Yield (%) Fit	Composite Desirability
1	330	60	10	59.0108	1

Multiple Response Prediction

Variable	Setting
Factor 1: Temperature (deg C)	330
Factor 2: Residence time (min)	60
Factor 3: Catalyst (wt%)	10

Response	Fit	SE Fit	95% CI	95% PI
Response 1: Bio-oil Yield (%)	59.01	7.21	(42.95, 75.07)	(42.33, 75.69)

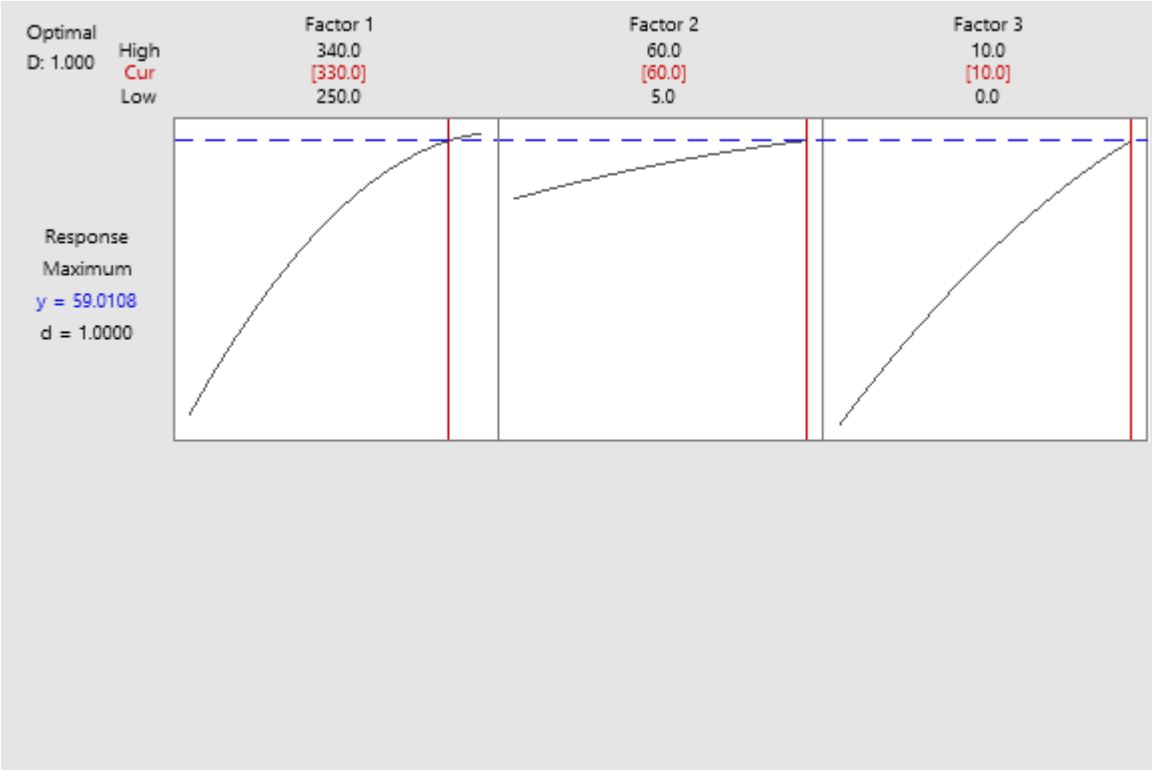

WORKSHEET 6

Factorial Plots for Response 1: Bio-oil Yield (%)